



**USAID**  
FROM THE AMERICAN PEOPLE

U.S.-Pakistan

**Centers for Advanced Studies in Water**



# Climate Change: Assessing Impact of Seawater Intrusion on Soil, Water and Environment on Indus Delta Using GIS and Remote Sensing Tools

## Final Report 2018



**Principal Investigator:**

**Prof. Dr. Altaf Ali Siyal, U.S.-Pakistan Centers for Advanced Studies in Water,  
Mehran University of Engineering and Technology Jamshoro, Pakistan**



**MEHRAN UNIVERSITY**  
of Engineering & Technology  
Jamshoro, Sindh, Pakistan



## **Citation**

Siyal, A.A. (2018). Climate change: Assessing impact of seawater intrusion on soil, water and environment on Indus delta using GIS & remote sensing tools. US. Pakistan Center for Advanced Studies in Water (USPCAS-W), MUET, Jamshoro, Pakistan

© All rights reserved by USPCAS-W. The author encourages fair use of this material for non-commercial purposes with proper citation.

## **Author**

Prof. Dr. Altaf Ali Siyal, US. Pakistan Center for Advanced Studies in Water (USPCAS-W), Mehran University of Engineering & Technology (MUET), Jamshoro, Pakistan.

## **ISBN**

978-969-23238-2-6

---

## **Acknowledgment**

This work was made possible by the support of the United States Government and the American people through the United States Agency for International Development (USAID).

## **Disclaimer**

The contents of the report are the sole responsibility of the author and do not necessarily reflect the views of USAID, the United States Government and the institution.

# TABLE OF CONTENTS

ACKNOWLEDGMENT .....	x
ACRONYMS AND SYMBOLS .....	xi
EXECUTIVE SUMMARY .....	xiv
1. INTRODUCTION .....	1
1.1 River Delta .....	1
1.2 Indus Delta .....	1
1.3 Location and Climate .....	2
1.4 Issues of the Delta .....	3
1.4.1 Shrinking delta .....	3
1.4.2 Seawater intrusion .....	5
1.4.3 Degradation of water and vegetation .....	5
1.4.4 Climate change .....	6
1.5 Objectives .....	7
2. MATERIALS AND METHODS .....	8
2.1 Delineation of Indus Delta .....	8
2.2 Spatial and Temporal Change in Vegetation of the Indus Delta .....	10
2.2.1 Satellite data .....	10
2.2.2 Ground truthing .....	12
2.2.3 Image classification .....	14
2.2.4 NDVI .....	14
2.2.5 Temporal variation in mangroves .....	15
2.3 Temporal Variation in Land Surface Temperature (LST) and its Effect on the Flora of the Delta .....	16
2.3.1 Satellite data for land surface temperature .....	16
2.3.2 Meteorological data .....	17
2.3.3 Flow below Kotri Barrage .....	17
2.4 Spatial and Temporal Variation in Soil Salinity of the Delta .....	18
2.4.1 Soil sampling .....	18
2.4.2 Physicochemical analysis of soil samples .....	18

2.4.3	Mapping of soil salinity . . . . .	20
2.4.4	Salinity indices . . . . .	20
2.5	Spatial Variation in Surface and Groundwater Quality in the Delta. . . . .	21
2.5.1	Surface water quality . . . . .	21
2.5.1.1	Water sample collection . . . . .	21
2.5.1.2	Water quality indices . . . . .	23
2.5.2	Groundwater quality . . . . .	23
2.5.2.1	Groundwater sampling . . . . .	23
2.5.2.2	Physicochemical analysis . . . . .	24
2.5.2.3	Geospatial analysis and mapping . . . . .	24
2.5.2.4	Water quality index . . . . .	26
2.5.2.5	Subsurface seawater intrusion . . . . .	27
2.6	Shift in the Shoreline of the Indus Delta and the Area Taken Away by the Sea . . .	28
2.6.1	Digital shoreline analysis system (DSAS). . . . .	29
2.6.2	Analysis of shoreline changes . . . . .	30
2.6.3	Manual quantification of change in shoreline . . . . .	30
2.6.4	Variation in tidal floodplain area and the area taken away by the sea . . . . .	31
2.6.5	Vulnerability of the Indus delta due to coastal flooding. . . . .	31
2.7	Impacts of Seawater Intrusion on Socio-economic Conditions of the People Living in the Delta . . . . .	32
2.7.1	The sample size and selection of respondents. . . . .	32
2.7.2	Data collection . . . . .	32
2.7.3	Measurement of poverty in the study area . . . . .	35
2.7.4	Limitations of the study . . . . .	35
3.	RESULTS AND DISCUSSION . . . . .	36
3.1	Spatial and Temporal Change in Vegetation of the Indus Delta . . . . .	36
3.1.1	Vegetation . . . . .	36
3.1.2	NDVI . . . . .	39
3.1.3	Mangroves . . . . .	40
3.2	Temporal Variation in Land Surface Temperature (LST) and its Effect on the Flora of the Delta . . . . .	44



3.2.1	Land surface temperature (LST) . . . . .	44
3.2.2	Climate change and Pakistan . . . . .	47
3.2.3	WorldClim data . . . . .	48
3.2.4	Comparison of rainfall and temperature between 1960 to 1990 and 1991-2017 .	49
3.2.5	River flow below Kotri barrage . . . . .	51
3.3	Spatial and Temporal Variation in Soil Salinity of the Delta. . . . .	52
3.3.1	Introduction . . . . .	52
3.3.2	Soil texture . . . . .	52
3.3.3	Soil density . . . . .	54
3.3.4	Electrical conductivity (EC) . . . . .	54
3.3.5	Soil pH . . . . .	56
3.3.6	Soil exchangeable sodium percentage (ESP) . . . . .	56
3.3.7	Percentage of soil samples with EC, pH, and ESP beyond the permissible limits .	57
3.3.8	Spatial distribution of soil salinity . . . . .	58
3.3.9	Temporal variation in soil salinity . . . . .	59
3.4	Spatial Variation in Surface & Groundwater Quality in the Delta . . . . .	61
3.4.1	Surface water . . . . .	61
3.4.1.1	Physicochemical analysis of surface water . . . . .	61
3.4.1.2	Correlation between the WQI and different water quality parameters . . . . .	65
3.4.1.3	Analysis of water quality regarding WQI and SPI. . . . .	66
3.4.2	Groundwater . . . . .	70
3.4.2.1	Statistical and spatial analysis of groundwater quality . . . . .	70
3.4.2.2	Water quality analysis based on water quality index (WQI) . . . . .	76
3.4.2.3	Subsurface seawater intrusion . . . . .	80
3.5	Shift in the Shoreline of the Indus Delta and the Area Taken Away by the Sea . . .	81
3.5.1	Shoreline position at different locations . . . . .	81
3.5.2	Shoreline change rates (1972-2017) . . . . .	82
3.5.3	Shoreline change rates during 1972-1990 and 1990-2017 periods . . . . .	87
3.5.4	Manual quantification of change in shoreline . . . . .	88
3.5.5	Variation in tidal floodplain area and the area taken away by the sea . . . . .	89

3.5.6	Temporal variation in the area underwater in tidal floodplains . . . . .	91
3.5.7	Vulnerability of the Indus delta due to coastal flooding. . . . .	92
3.6	Impacts of Seawater Intrusion on Socio-economic Conditions of the People Living in the Delta . . . . .	93
3.6.1	Socioeconomic characteristics of the respondents. . . . .	93
3.6.2.	Income, expenditure, and source of income. . . . .	94
3.6.3	Climate change Impacts . . . . .	96
3.6.4	Impact of seawater intrusion . . . . .	98
3.6.5	Magnitude of poverty in the delta . . . . .	102
3.7	Dissemination of Research Results . . . . .	104
3.8	Research Output. . . . .	104
4.	RECOMMENDATIONS . . . . .	105
	References . . . . .	108
	Appendix 1 Socio-Economic Survey Questionnaire (Indus delta) . . . . .	122
	Appendix-2 Newspaper Articles . . . . .	123
	Appendix 3 Seminar Advertisement . . . . .	124
	Appendix 4 Media Coverage . . . . .	125
	Appendix 5 Research Output . . . . .	127
	Appendix 5a Research Papers . . . . .	127
	Appendix 5b Thesis. . . . .	127
	Ph.D. . . . .	127
	M.E. . . . .	127
	Appendix 5c Conference/Seminar Presentations. . . . .	128



# LIST OF FIGURES

Fig. 1.1:	Location map of Indus Delta . . . . .	3
Fig. 1.2:	The decrease in the size of Indus delta (a) size of the delta in 1833 and (b) size of the delta today . . . . .	4
Fig. 2.1:	Maps of Sindh showing Pinyari river originating from river Indus during 1833 and 1883 AD . . . . .	9
Fig. 2.2:	Delineated Indus delta (based on a map of Sindh 1833 AD) . . . . .	9
Fig. 2.3:	Delineated Indus Delta compared to that given by Google Earth. Red line shows the boundaries of delta delineated for use in the present study while Greenline shows the delta given by Google Earth . . . . .	10
Fig. 2.4:	Snapshots taken during ground truthing data. . . . .	13
Fig. 2.5:	Flow chart of the supervised classification . . . . .	14
Fig. 2.6:	Tidal floodplain of the Indus Delta. . . . .	15
Fig. 2.7:	Spatial distribution of soil sampling locations in the delta. . . . .	18
Fig. 2.8:	Snapshots taken during soil sampling from Indus Delta. . . . .	19
Fig. 2.9:	GIS map of surface water sampling locations. . . . .	21
Fig. 2.10:	Snapshots taken during surface water sampling . . . . .	22
Fig. 2.11:	GIS map of groundwater sampling locations . . . . .	24
Fig. 2.12:	Snapshots taken during groundwater sampling . . . . .	25
Fig. 2.13:	Shoreline of delta divided into four zones. . . . .	28
Fig. 2.14:	Schematic diagram of the baseline and the transects for manual calculation of the net shoreline movement. . . . .	31
Fig. 2.15:	GIS map of groundwater sampling locations . . . . .	33
Fig. 2.16:	GIS map of socio-economic sampling survey locations . . . . .	34
Fig. 3.1:	Area under vegetation from 1990 to 2017 . . . . .	37
Fig. 3.2:	Vegetation masks for the last 28 years (1990-2017) . . . . .	38
Fig. 3.3:	Variation in NDVI for the last 28 years (1990-2017) . . . . .	39
Fig. 3.4:	Relationship between NDVI and the wheat crop yield . . . . .	40
Fig. 3.5:	Spatial and temporal variation in mangrove cover in tidal floodplains of Indus delta during the last 28 years (1990-2017). . . . .	41
Fig. 3.6:	Spatial variation in mangrove cover in the tidal floodplains of Indus delta during Feb. 2017 . . . . .	42
Fig. 3.7:	Percentage of tidal floodplains of the Indus delta under dense and sparse mangrove forests, water and barren floodplains (Feb. 2017). . . . .	43
Fig. 3.8:	Spatial and temporal variation in the Land Surface Temperature (LST). . . . .	45

Fig. 3.9:	Temporal change in the area having LST more than 30 °C	46
Fig. 3.10:	Relationship between NDVI and LST of Indus Delta	47
Fig. 3.11:	Spatial and temporal variation in mean monthly temperature of Indus delta (1960-1990)	48
Fig. 3.12:	Spatial and temporal variation in mean monthly temperature of Indus delta (1960-1990)	49
Fig. 3.13:	Comparison of the mean monthly temperature of Indus Delta between the periods 1960-1990 and 1991-2017.	50
Fig. 3.14:	Comparison of mean monthly rainfall of Indus Delta between the periods 1960-1990 and 1991-2017.	50
Fig. 3.15:	Temporal variation in Indus river flow below Kotri barrage	51
Fig. 3.16:	Zero flow days below Kotri barrage downstream	51
Fig. 3.17:	Spatial variation in soil texture of the top 0-20 cm layer in the Indus delta (top) and the percent of samples with different soil textures (bottom).	53
Fig. 3.18:	The spatial distribution of dry density at various soil depths.	54
Fig. 3.19:	Depth-wise variation in average EC of the soil profile. Error bars represent the 95% Confidence Interval in data.	55
Fig. 3.20:	Interpolated spatial distribution maps of EC at various soil depths in the Indus delta	55
Fig. 3.21:	Interpolated spatial distribution maps of pH at various soil depths in the Indus Delta	56
Fig. 3.22:	Interpolated spatial distribution maps of ESP at various soil depths in the Indus Delta	57
Fig. 3.23:	Percentage of samples with EC, pH, and ESP beyond the threshold values	58
Fig. 3.24:	Interpolated maps of spatial distribution of soil salinity by soil depth, 0-20, 20-40 and 40-60 cm	59
Fig. 3.25:	Temporal variation in soil salinity (a) 1972 (b) 2017	60
Fig. 3.26:	Spatial distribution of EC of surface water bodies	63
Fig. 3.27:	Percentage of samples beyond the permissible limit for various water quality parameters	65
Fig. 3.28:	Interpolated GIS map of the spatial distribution of turbidity	71
Fig. 3.29:	Interpolated map of the spatial distribution of water quality parameters.	73
Fig. 3.30:	Interpolated map of the spatial distribution of Ca	74
Fig. 3.31:	Interpolated map of the spatial distribution of Mg	75
Fig. 3.32:	Interpolated map of the spatial distribution of As	76



Fig. 3.33: Classification of groundwater of Indus delta based on WQI . . . . .	77
Fig. 3.34: Interpolated map of subsurface seawater intrusion in Indus delta . . . . .	80
Fig. 3.35: The position of the shorelines at different times, baseline, transects and the location of major creeks along the entire deltaic coastline . . . . .	82
Fig. 3.36: Shoreline change rate at different transects along coastline estimated by (a) EPR and (b) LRR . . . . .	83
Fig. 3.37: Shoreline change rate in different zones along the coastline . . . . .	84
Fig. 3.39: Net shoreline movement (NSM) at different zones along the Indus delta shoreline (1972-2017). . . . .	86
Fig. 3.40: Mean shoreline change rates and NSM at different zones along Indus delta shoreline for the periods 1972-1990 and 1990-2017 (a) Mean shoreline change rates and (b) NSM . . . . .	88
Fig. 3.41: NSM calculated manually at different zones along the Indus delta shoreline (1972 to 2017). . . . .	89
Fig. 3.42: Unclassified and classified satellite images of tidal floodplain area of Indus delta in 1972 and after 45 years in 2017. . . . .	90
Fig. 3.43: Shoreline positions of Indus delta in 1972 and 2017 and the area taken away by the sea . . . . .	91
Fig. 3.44: Temporal variation in area underwater in the tidal floodplain area . . . . .	91
Fig. 3.45: Risk prone areas of Indus delta due to coastal flooding . . . . .	92
Fig. 3.46: Age group distribution of the respondents of the survey. . . . .	94
Fig. 3.47: Main sources of income of the respondents of the Indus Delta . . . . .	95
Fig. 3.48: Monthly income of the respondents . . . . .	95
Fig. 3.49: Variations in climatic parameters of the Indus delta during the last 25 years from the respondents' perspective . . . . .	97
Fig. 3.50: Some of the common diseases prevailing in the Indus delta as reported by the people . . . . .	98
Fig. 3.51: Variations in the level of poverty in the Indus delta from the respondents' perspective . . . . .	103
Fig. 4.1: The layout of proposed coastal highway cum levee . . . . .	105

## LIST OF TABLES

Table 2.1: Area of the Indus Delta (based on literature) . . . . .	8
Table 2.2: Area of the active Indus Delta . . . . .	8
Table 2.3: Landsat satellite imagery (from 1990 to 2017) used for the vegetation analysis . .	12
Table 2.4: Landsat satellite imagery (from 1990 to 2017) used for the LST analysis . . . . .	17
Table 2.5: Summary of calculated weight, relative weight and WHO standards for selected physicochemical parameters . . . . .	26
Table 2.6: Indicators for estimation of subsurface seawater intrusion . . . . .	27
Table 2.7: Meta information of the satellite imagery used in quantifying shift in shoreline . . . . .	29
Table 2.8: DSAS transect description of the study area . . . . .	30
Table 3.1: Area of the delta under vegetation and corresponding percentage from 1990 to 2017 . . . . .	36
Table 3.2: Area under mangrove cover during the last 28 years (1990-2017) . . . . .	42
Table 3.3: Temporal variation in the area of delta under different temperature ranges . . . . .	46
Table 3.4: Area under each type of soil salinity (USDA, 1954) . . . . .	58
Table 3.5: Temporal variation in the area under water, vegetation and soil salinity in the Indus delta . . . . .	59
Table 3.6: Summary of statistical analysis of various physicochemical parameters of surface water bodies . . . . .	62
Table 3.7: Water Quality Index (WQI) for sampled surface water bodies of the Indus delta . .	67
Table 3.8: Data matrix for various physicochemical parameters of groundwater of Indus delta . . . . .	70
Table 3.9: Categories of water based on water quality index (WQI) . . . . .	76
Table 3.10: Classification of groundwater samples based on water quality index . . . . .	77
Fig. 3.38: Spatial variation in shoreline change rates (a) estimated through EPR at different transects along the shoreline and (b) spatial distribution of erosion and accretion along the entire shoreline of the delta . . . . .	85
Table 3.11: Summary of shoreline change rate based on NSM, EPR, and LRR for the period 1972-2017 . . . . .	86
Table 3.12 (a): Increase in tidal floodplain area in 45 years (1972-2017) . . . . .	90

Table 3.12 (b): Area of Indus delta degraded and taken away by the sea in 45 years . . . . .	90
(1972-2017) . . . . .	90
Table 3.13: Survey response regarding housing/accommodation. . . . .	94
Table 3.14: Sources of energy, roads, vehicle, agricultural lands, and livestock in the Indus delta. . . . .	96
Table 3.15: Relation between change in temperature and decrease in the fish catchment . . .	97
Table 3.16: Main issues faced by the people of the Indus delta due to seawater intrusion. . .	100
Table 3.17: Relation between seawater intrusion and vegetation . . . . .	100
Table 3.18: Relation between seawater intrusion and soil salinity. . . . .	101
Table 3.19: Relation between the seawater intrusion and the quality of the ground and surface water . . . . .	101
Table 3.20: Relation between seawater intrusion and the income of the respondents . . . . .	102
Table 3.21: Measurement of poverty headcount, poverty gap, and severity of poverty in the Indus delta community . . . . .	102
Table 3.22: Distribution of respondents based on their level of poverty . . . . .	103



# ACKNOWLEDGMENT

The U.S.-Pakistan Center for Advanced Studies in Water (USPCAS-W), Mehran University of Engineering & Technology, Jamshoro, Pakistan, is gratefully acknowledged for providing financial support for the project “**Climate Change: Assessing impact of seawater intrusion on Soil, Water and Environment in Indus Delta using GIS and Remote Sensing tools**” under the Applied Policy Research Grants. Support, encouragement, and inspiration of Dr. Kazi Suleman Memon, Manager Research, USPCAS-W, Mehran University of Engineering and Technology, Jamshoro during report write up and reviewing it is highly acknowledged. Moreover, United States Geological Survey (USGS), Japan Aerospace Exploration Agency (JAXA), National Aeronautics and Space Administration (NASA), Pakistan Meteorological Department (PMD), and Google Earth are also acknowledged for offering free of cost historic satellite imageries, Digital Elevation Model (DEM), historical meteorological data, and spatial data, respectively. Logistic support provided by Mr. Akhtar Samo (Wilderness Tourism Development Foundation) during ground truthing of creeks is also acknowledged.

Finally, technical assistance of Ghulam Shabir Solangi, Ph.D. Scholar; Munsif Langah, Research Assistant; Kashif Solangi and Ali Raza Siddiqui, M.E. students is highly appreciated and acknowledged.

# ACRONYMS AND SYMBOLS

AOI	Area of Interest
BCM	Billion Cubic Meters
BI	Brightness Index
CI	Confidence Interval
CRS	Crop Reporting Services
DEM	Digital Elevation Model
DN	Digital Numbers
DSAS	Digital Shoreline Analysis System
dS/m	Deci Siemens per Meter
EC	Electrical Conductivity
EPR	End Point Rate
ESP	Exchangeable Sodium Percentage
ETM	Enhanced Thematic Mapper
FGT	Foster Greer Thorbeck
GIS	Geographical Information System
GLOVIS	Global Visualization Viewer
GPS	Global Positioning System
ha	Hectare
IPCC	Intergovernmental Panel on Climate Change
IDW	Inverse Distance Weighted
KII	Key Informant Interview
LRR	Linear Regression Rate
LST	Land Surface Temperature

MAF	Million Acre Feet
mg	Milligrams
mg/L	Milligram/Liter
MSS	Multispectral Scanner System
NDSI	Normalized Difference Salinity Index
NDVI	Normalized Difference Vegetation Index
NSM	Net Shoreline Movement
NIR	Near Infrared
NTU	Nephelometric Turbidity Unit
OLI	Operational Land Imager
PMD	Pakistan Meteorological Department
ppm	Parts per Million
ppb	Parts per Billion
R <sup>2</sup>	Coefficient of Determination
SCE	Shoreline Change Envelope
SAR	Sodium Adsorption Ration
SD	Standard Deviation
SI	Salinity Index
SPI	Synthetic Pollution Index
TDS	Total Dissolved Solids
TH	Total Hardness
TM	Thematic Mapper
TOA	Top of Atmospheric
USGS	United States Geological Survey

WHO	World Health Organization
WQI	Water Quality Index
WRS	World Reference System
WWF	World Wide Forum for Nature
$A_L$	Band-specific additive rescaling factor
$\rho_\lambda$	Top of atmospheric (TOA) Planetary Reflectance, without Correction for the Solar Angle.
$M\rho$	Band-specific Multiplicative Rescaling Factor
$A\rho$	Band-specific Additive Rescaling Factor
$Q_{cal}$	Quantized and Calibrated Standard Product Pixel Values (DN)
$\rho_\lambda$	TOA Planetary Reflectance
$\theta_{SE}$	Local Sun Elevation Angle
$\theta_{SZ}$	Local Solar Zenith Angle
$L_\lambda$	Top of Atmosphere Spectral Radiance
$M_L$	Band-specific Multiplicative Rescaling Factor
$Q_{cal}$	Quantized and Calibrated Standard Product Pixel Values
$K_1$	Band-specific Thermal Conversion Constant
$K_2$	Band-specific Thermal Conversion Constant
$T$	At-satellite Brightness Temperature (K)

# EXECUTIVE SUMMARY

Indus Delta, a designated Ramsar wetland, is the 5<sup>th</sup> largest and most vulnerable delta of the world. It spreads from Sir Creek in the east to Phitti creek in the west with the apex at Banoo town of district Sujawal, Sindh, Pakistan. This fan-shaped delta supports the 7<sup>th</sup> largest mangrove system of the world in vast tidal mud floodplains. The shoreline of the delta is exposed to withstand the highest average wave energy compared to other major deltas in the world. Many factors such as: decrease in the river flows to the delta resulting in a reduction in sediment deposition, surface and subsurface seawater intrusion, land subsidence, sea level rise, climate change, and anthropogenic activities, have all contributed to the shrinkage and degradation of one of the largest ecosystems of the world. During the flourishing days of the delta, there were seventeen river mouths (creeks) which are now decreased to only two active creeks *viz.* Khobar and Khar. The active delta occupied an area of about 1.30 million hectares (Mha) in 1833, which has now shrunk to only 0.1 Mha (92% reduction in the area).

Most of the reports about the gravity of the problem are based on sampling surveys conducted from time to time without any scientific evidence and application of the latest scientific tools and techniques. Hence, there is significant variability in the data about land, water, vegetation, and socioeconomic conditions of the coastal communities affected by seawater intrusion. These reports are usually not considered worth by the policymakers for implementations. Hence, keeping in view above facts the present study was conducted to assess the impacts of seawater intrusion on freshwater, land, vegetation, environment and socio-economic conditions of the people using remote sensing and geospatial tools. The study aims to provide evidence to develop a strategic action plan for the mitigation and the adaptation measures for saving the biodiversity of the delta, mitigating the adverse impact on the environment and other socio-economic conditions of people under current and future climate change scenarios.

The first most difficult task was a delineation of the boundaries of the Indus delta as different researchers have delineated different boundaries and reported different areas of the delta. Based on the old maps of Talpur (1833) and British era (1893), the Indus delta was delineated taking Banoo town as an apex of the delta while Sir Creek on the East and Phitti Creek on the West as two bottom points of the delta. The active delta occupied an area of about 13067 sq. km (1.30 Mha) in 1833.

The vegetated area of the delta during February varied between 2568 km<sup>2</sup> (19.6% of the entire delta) in 2015 and 47000 km<sup>2</sup> (35.9% of the delta) in 2010. No specific trend in the temporal variation of vegetation was observed as it increased gradually from



1990 to 2010, but it significantly decreased later. The area covered with mangrove forests was 103413 ha or 16% of tidal floodplains during 1990 which slowly decreased to 63296 ha or 9.81% of tidal floodplains in 2005 which again increased to 81324 ha or 12.6% of tidal floodplains in 2017, might be due to the planting of mangroves by the forest department and NGOs. Nearly 60% of the tidal floodplain was barren in 2017 while 31.5% was under water. Dense mangrove forests covered only 36245 ha or 5.6%, while sparse forests are on about 45079 ha or 7% of the tidal floodplains. Thus, mangrove forests occupied only 12.6% of the total tidal floodplains or about 6.2% of the Indus delta.

On average, there was an increase of  $1.74^{\circ}\text{C}$  in Land Surface Temperature (LST) of the Indus delta in the last 28 years (1990-2017). There was a fair but negative statistical correlation between the normalized difference vegetation index (NDVI) and the LST of the delta with a coefficient of determination  $R^2 = 0.65$ . Mean monthly air temperature of the Indus delta from February to November for the period 1991-2016 was  $0.7$  to  $1.3^{\circ}\text{C}$  higher compared to the period 1960-1990. While the mean monthly temperature in December and January dropped by  $0.6$  to  $0.7^{\circ}\text{C}$  (3 to 4%) for the period 1991-2016 compared to the period 1961-1991. Thus, summers of the delta are getting warmer while the winters are turning colder. A significant decrease up to 23% in mean monthly rainfall was observed during the period 1991-2016 for June, July and August compared to the 1960-1990 period. While an increase in mean monthly rainfall up to 100% was observed in September and October during the later period compared to the 1960-1990 period. The analysis of river flow below Kotri barrage revealed that about 80% of Indus river flow to the delta is decreased from 1935 to 2017.

Indus delta is dominated with soils which have fine textural class. It reflects that loam (37.78%) and clay loam (22.22%) textural classes are dominant in the soils of the delta. The dry density of soil in 0-20 cm depth varied from 1.20 to  $1.40\text{ g/cm}^3$  with an average value of  $1.30\pm 0.05\text{ g/cm}^3$ . EC of 56 to 66% soil samples collected from 0 to 60 cm depth of the delta was beyond the permissible limits given by FAO. Similarly, the pH of 14 to 17% samples and ESP of 72 to 79% samples were beyond the permissible limits. Soil categorization by salinity showed that 46% of the soils were saline-sodic, 22% sodic, 16% saline, and 16% were normal soils. These data indicate that sodium is a dominant cation in most of the soils. Spatial distribution soil salinity maps showed the highest salinity levels in those samples which were taken from the coast of the Arabian sea, which might be due to seawater intrusion.

Water quality of the surface water bodies revealed that 66% of water samples had EC, 64% had TDS concentration, and 58% had chloride concentration beyond the permissible limits suggested by FAO. Overall, 78% of the natural surface water bodies

(lakes) had saline water, which is unfit for drinking. Hence, based on FAO water quality guidelines for irrigation purpose, the water bodies were unsuitable even for the irrigation. Analysis of the satellite imagery revealed that water bodies in the entire delta have doubled in the last 28 years from 1600 sq. km to 3000 sq. km.

The groundwater quality analysis indicated that 62% of water samples had a salty and bitter taste, while pH, odor, and color values in most of the groundwater samples were within the permissible limits. Furthermore, 34% of samples were turbid, while 89% had EC, 67% had calcium, and 56% had magnesium values beyond the permissible limits. It is also indicated that 94% of groundwater samples had chloride concentration higher than the safe limits. Analysis for arsenic demonstrated that only 23% of water samples had an arsenic concentration beyond the allowable limit described by WHO, with values as high as 1999 ppb. Groundwater contaminated with arsenic is found in areas adjacent to the river Indus. Even RO plants installed by the Government at Keti Bandar had an arsenic concentration above the WHO permissible limit of 10 ppb.

Based on high chloride concentration ( $>250$  mg/L), Simpson ratio ( $>2.8$ ), chloride and bicarbonate ratio ( $>0.6$ ) in groundwater, it is estimated that subsurface seawater intrusion had affected about 1.15 Mha (88.3% of the delta) while only 0.15 Mha (11.7%) is still unaffected.

The temporal variation in the shoreline of Indus delta was analyzed for statistical parameters End Point Rate (EPR), Net Shoreline Movement (NSM) and Linear Regression Rate (LRR) using DSAS software and compared with manual calculations. The study concluded that the left side of the river Indus was more vulnerable to coastal erosion compared to the right side of the river. It might be due to the low mangrove population, oil extraction, and flat land slope on the left side compared to the right side of the delta. The net inward shift in the shoreline was quantified as  $860\pm 92$  m using DSAS software and  $1295\pm 260$  m through manual calculations. Higher shoreline change rate ( $34.3\pm 3.5$  m/year) was observed for the period 1990-2017 compared to the period 1972-2017 ( $28.4\pm 3.9$  m/year).

This study shows that 42607 ha land of Indus delta is degraded due to surface seawater intrusion. Thus, there was a 7.1% increase in the tidal floodplains area of the delta in the last 45 years. Out of total degraded land of 42607 ha, 31656 ha land is now under the seawater while 10951 ha new land is converted into the tidal floodplain area. It was further investigated that tidal floodplain area on the left bank of the Indus is about 4208 km<sup>2</sup> or about two times larger than the right side (2220 km<sup>2</sup>). Permanent water in tidal flood plains has increased from 7.1% to 18.1% of the total tidal floodplain area. In case a tsunami wave of 5 m height or a cyclone capable of raising sea level up to 5 m hits the coastal belt of the Indus delta, 9376 km<sup>2</sup> (71% of the delta) will be flooded

which reflects high vulnerability of submergence of the delta and risk of life of coastal communities of the delta.

The socio-economic survey of the Indus delta revealed that 39.3% of people were engaged in agriculture, 16.6% in fishing, 15.0% in govt. /private jobs and 12.7% were daily wage labors. Income data showed that 16% of the population of the delta had a monthly income less than Rs. 10,000; 62% had income between Rs. 10,000 to Rs. 30,000, while only 3% had income more than Rs. 70,000. Majority of the people (76.5%) believe that the temperature in the last 25 years has increased, while 97.2% reported a decrease in rainfall, 92.5% reported an increase in wind blowing/velocity during the summer and 88.9% sensed an increase in humidity in the delta. One-fifth of the people suffered from gastro, diarrhea, and chest and stomach problems, about 14.8% were affected by skin diseases, 16.4% had hepatitis, 9.2% had cancer, and 8.4% had sugar, blood pressure, heart, and kidney problems. 88.4% population of the Indus delta was below the poverty line in which 31.4% were very poor, 27.8% were moderately poor and 29.2% were poor.

Based on the present study, it is recommended that:

- Expand the already constructed 38 km long coastal highways up to 200 km on the left bank of the Indus by putting a bridge over the river Indus at Sajan Wari/ Kharo Chhan. This will function as defense-line against the surface seawater intrusion impeding further swallowing of the delta by sea. It will also provide coastal communities with quick and easy access to the markets of Karachi and attract the tourists and flourish tourism in the delta. As a result, socio-economic conditions of poor communities of the delta will be improved.
- Ensure an escape of 5000 cusecs of water throughout the year below Kotri barrage to check seawater intrusion in order to accommodate the needs for fisheries, environmental sustainability, and to maintain the river channel as recommended by International Panel of Experts (IPOE) in 2004. Also, ensure release of the total volume of 25 MAF in a five-year period (an annual equivalent amount of 5 MAF) below Kotri barrage as flood flows (Kharif period).
- The environmental river flow is useful in controlling seawater intrusion only in the active delta. Therefore, enough water flow in the river Indus, as well as canals originating from Kotri barrage, should be ensured for minimizing surface and subsurface seawater intrusion in the entire delta. It will not only minimize surface and subsurface seawater intrusion but also provide drinking water to coastal communities, fulfill freshwater needs of flora and fauna and result in mitigating the adverse impacts on the ecosystem of the delta.

- From field surveys and through satellite images, it is observed that irrigation channels in the delta have a significant role in controlling seawater intrusion in areas far from the river Indus. For this purpose, if possible, relic river channels should be restored such as Ochito and Old Pinyari. These channels will carry extra flood water to the sea during peak flood to shun the flood pressure on the main river and thus minimize the possibility of the levee breach. Meanwhile, this will also supply fresh water to the coastal communities living far away from the main river course. These channels will carry silt-laden water during floods and discharge into the sea away from the main river estuary. It will be supportive in silt deposition in areas where river water and silt usually do not reach. Consequently, it will be supportive in revitalizing the delta.
- Plantation of mangroves on the tidal floodplains, especially on the left bank of river Indus should be initiated and encouraged on an emergency basis. For this, community-based natural resource management committees should be established. Thick mangrove forests provide defense-line against natural calamities, such as: extreme tides, cyclones, and tsunamis; trap river silt to support accretion process along the coast; provide a natural breeding ground for fish, shrimps and other marine life; and provide wood, fodder, and livelihood to the coastal communities.
- Biosaline agriculture should be encouraged, especially in tidal floodplains and over the vast barren salt-affected soils lying between tidal floodplains and the canal irrigated areas of the delta. Cultivation should be introduced and encouraged by the Government of Pal grass, *Quinoa*, *Salicornia*, *Sea Aster*, *Spartina alterniflora*, etc. Biosaline agriculture will, undoubtedly, be a source of food and fodder for the coastal communities and livestock. Also, it will have a positive impact on the coastal environment.
- Most of the natural lakes in the delta are saline, which should be revived by adding fresh water during the monsoon period. Freshwater lakes can play a vital role in providing drinking water to the communities and can work as groundwater recharge hotspots.
- Shrimp and crab farming in natural water bodies, lakes and ponds of the delta should be encouraged.
- The Government should ban on overgrazing or cutting of mangroves for wood and on the use of fine mesh nets for catching small size fish and shrimps.
- Tourism Industry should be encouraged, especially boat cruising in the mangrove laden creeks in the delta, to improve socioeconomic conditions of poor local communities.

# 1. INTRODUCTION

## 1.1 River Delta

A river delta is a flat, low-lying area shaped at the mouth of a river (Arnell and Browne, 2007) where the river terminates into the sea or estuary/creek. It evolves through a process of centuries due to a decrease in the river flow velocity, resulting in sediment deposition and the creation of different mouths (creeks) of a river. These are developed and shaped by interaction with fluvial and marine forces (Wright, 1978). River deltas play a vital role in human civilization, as they are major agricultural production and population hubs in the world. Therefore, they are also called the “gifts” of rivers to the sea (Wright, 1978). River deltas are vital landscapes at the land-water interface which support dense populations and diverse ecosystems while also providing excessively bulk food and energy resources (Tejedor *et al.*, 2017).

The term “delta” was first used around 2500 B.C. by the Greek historian Herodotus because of the similarity in shape between the triangular alluvial deposits in the mouth of the Nile river and the Greek letter delta (*D*) (Wright, 1978; Hudson, 2005). River deltas are vulnerable to the global climate change and human activities (Bianchi and Allison, 2009) because deltas drastically depend on the water and sediment discharge of river systems, sea-level variation, and physical-oceanographic regimes of the coastal seas (Wright and Nittrouer, 1995).

## 1.2 Indus Delta

Indus Delta, a designated Ramsar wetland, is the 5<sup>th</sup> largest delta of the world (IUCN, 2003; Sohl *et al.*, 2006; Khan and Akbar, 2012; Baig *et al.*, 2017); some place it at 6<sup>th</sup> position (Peracha *et al.*, 2015) while some rank it as 7<sup>th</sup> largest delta (Majeed *et al.*, 2008; Mimura, 2008; Renuad *et al.*, 2013). The delta spreads from Sir Creek in the east to Phitti creek in the west with the apex at Banoo town where once Pinyaree River originated from the Indus and discharged into the sea via Sir Creek as also reported by Haig (1894). Before the construction of different diversion hydraulic structures over river Indus, there were seventeen river mouths (creeks) in the Indus Delta (Meynell and Qureshi, 1993; WWF, 2007), which have now decreased to only two active creeks *viz.* Khobar and Khar. During 1833 A.D., the active delta occupied an area of about 13900 sq. km which has shrunk to only 1067 sq. km (about 92% reduction in the area). IUCN (2005) reported the area of the active delta as 1190 sq.km. This fan-shaped

delta supports 7<sup>th</sup> largest mangrove forest (Amanullah *et al.*, 2014; Sultana *et al.*, 2014; Baig *et al.*, 2017) system in the world in vast tidal mud floodplains. Some researchers place the mangrove forest system of Indus delta at 13<sup>th</sup> position in the world (Majeed *et al.*, 2010). However, Indus delta no doubt supports the largest mangrove forests in arid regions of the world (Hecht, 1999; Hamid *et al.*, 2000; Ismail *et al.* 2014)

The Indus Delta is reported as one of the world's most vulnerable large deltas (Spalding *et al.*, 2010). Due to decrease in the river flows to the delta and resulting reduction in sediment deposition, subsurface seawater intrusion, land subsidence, and sea level rise and low rainfall due to climate change and anthropogenic activities, one of the largest ecosystems of the world is shrinking and degrading (Majeed *et al.*, 2010; Rasul *et al.*, 2012). The average wind velocity in the Indus delta during the monsoon months varies between 12 and 35 km per hour (Majeed *et al.*, 2010). The shoreline is exposed to withstand the highest average wave energy compared to other major deltas in the world (Wells and Coleman, 1984; Mountjoy, 2004). At a depth of 10 meters from the Indus delta shoreline, waves having the power of about 950 joules/sec/unit crest width are generated (Mimura, 2008). The texture of most of the soils in the Indus delta is clay and clay loam (Majeed *et al.*, 2010). Indus Delta provides livelihood to nearly 0.9 million coastal populations (Wood *et al.*, 2013).

### 1.3 Location and Climate

The Indus Delta is situated approximately 30 km to the east of Karachi City and spreads at latitude 23°47'25.20" N - 24°57'30.90"N and longitude 67°11'9.76"E - 68°44'46.23"E (Fig. 1). The climate of the delta is arid having an average annual rainfall less than 200 mm (Giri *et al.*, 2015) and temperature ranges between 23.8 °C and 28.7 °C (IUCN, 2002; Majeed *et al.*, 2010). The Indus delta mangrove ecosystem is unique and the only arid mangrove system of Asia which is highly resistant to extreme temperatures, seawater salinity and low precipitation (DasGupta and Shaw, 2013). About 80% of the rain falls during the monsoon period (June-September). Tides are of the mixed semi-diurnal type with two high and two low tides a day. The tidal range is about 3.5 m along the shoreline of the Indus delta. The vegetation in the tidal floodplains of the delta is dominated by mangrove forests (Leichenko and Wescoat, 1993).

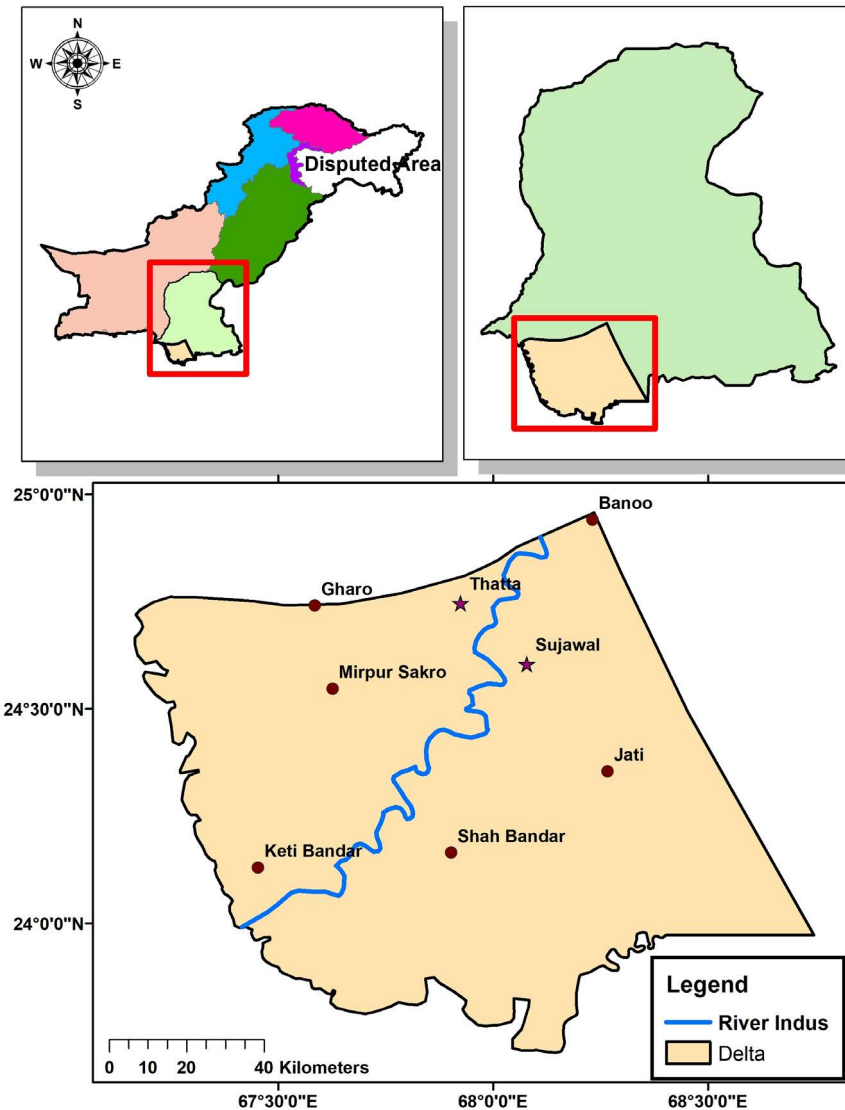


**Fig. 1.1: Location map of Indus Delta**

## 1.4 Issues of the Delta

### 1.4.1 Shrinking delta

It has been reported that river deltas of the world, including Indus delta, are shrinking due to morphological, hydrological, climatological, anthropogenic or geological factors (Oyedotun 2014; Addo, 2015). Indus delta, one of the largest eco systems of the world, is shrinking and degrading (Fig. 1.2) at an alarming rate due to anthropogenic and natural activities such as decrease in the river flows to the delta and the resulting reduction in sediment deposition, seawater intrusion, land subsidence, sea level rise and low rainfall due to climate change (Sidra *et al.*, 2010; Rasul *et al.*, 2012). Gupta (2008) reported that the life of Indus delta is dependent on the availability of freshwater and sediment. He suggested that the prosperity of delta requires a realistic assessment of the degradation of the delta and minimum volume of water and sediment needed

to prevent the disappearance of the delta. The total available freshwater flow in the Indus river system is about 180 billion cubic meters (BCM), while it deposits about 400 million tons of silt in the delta annually (Meynell and Qureshi, 1993; Nasir and Akbar, 2012). The 80% decrease in the freshwater flows in the river Indus below Kotri barrage (last barrage on the river Indus) and resulting 80% reduction in sediment load after the late 1950s is considered the main cause of the decrease in the size of the delta (Postel, 1999; Memon, 2005; Inam *et al.*, 2007; Kravtsova, 2009; Mahar and Zaigham, 2015). Some studies estimate a decrease in river flow to the delta even up to 90% (DasGupta and Shaw, 2013; Giosan *et al.*, 2006). Once all the creeks were live and received fresh river water, but now the active delta is reduced to only about 10% of its original size (ADB, 2005). Also, only Khobar and Khar creeks receive fresh water from the Indus and discharge into the sea (Inam *et al.*, 2007).

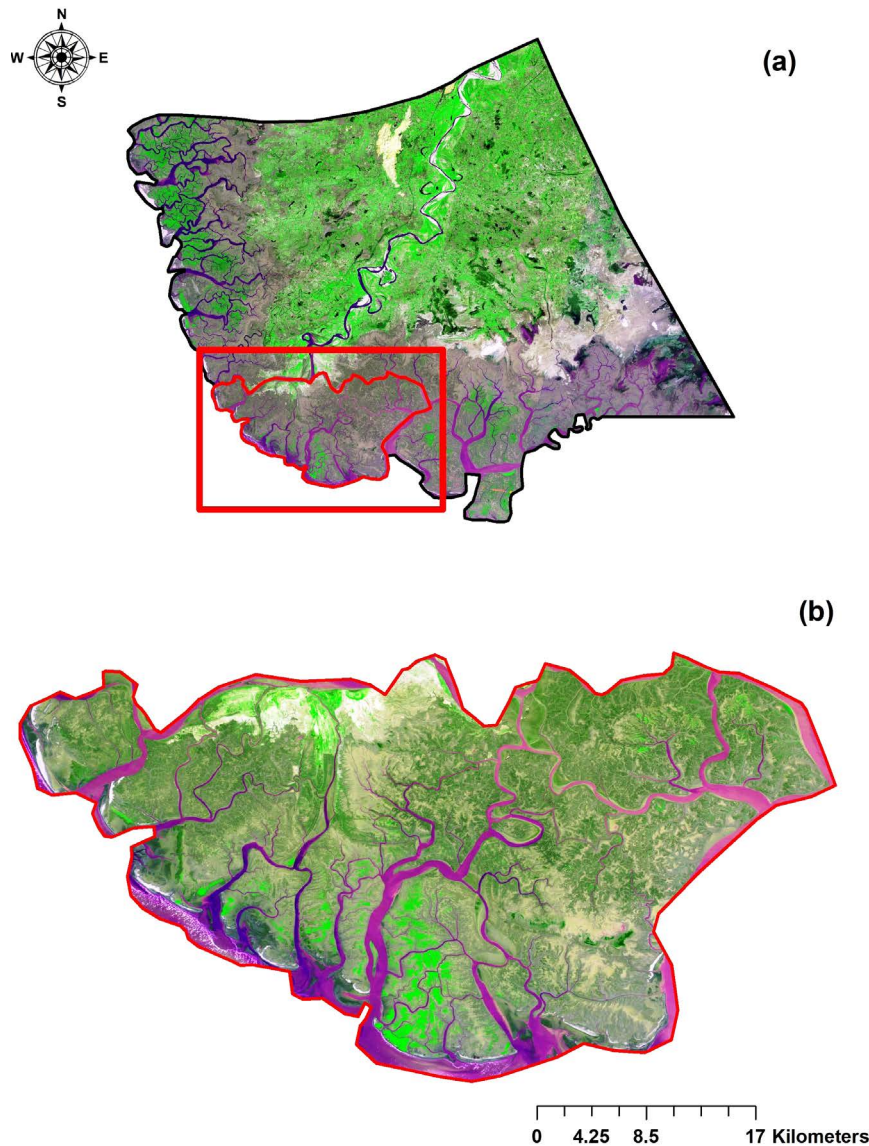


**Fig. 1.2: The decrease in the size of Indus delta (a) size of the delta in 1833 and (b) size of the delta today**



### 1.4.2 Seawater intrusion

Seawater intrusion is one of the main environmental issues in coastal areas, threatening coastal aquifers worldwide (Sherif *et al.*, 2012). It has been estimated that about 0.5 Mha of fertile agricultural land of the Indus delta (IRIN, 2001), or about 12% of the total cultivated land of the entire Sindh Province are degraded due to seawater intrusion (GOP, 2001). Different figures are reported about the total land submerged/taken away by the sea due to surface seawater intrusion. Chandio *et al.* (2011) reported that an area of about 80 acres of delta per day is being degraded due to seawater intrusion. DAWN (2008a) reported that the sea has occupied 1.3 million acres of delta and it continues to take away 80 acres per day. In another report, about 0.461 Mha of coastal land are reported as degraded due to seawater intrusion (DAWN, 2008b). Bokhari (2015) reported that about 0.486 Mha of the delta are degraded, which has caused migration of 0.25 million people. IUCN (2003) estimated about 1.2 Mha of land degraded due to seawater intrusion.

### 1.4.3 Degradation of water and vegetation

The Indus delta contains about 95% of the total mangrove forest of Pakistan, which provides shelter for migratory birds coming from Siberia (Giri *et al.*, 2015). About 97% of the total mangrove population belongs to *Avicennia marina* species (WWF, 2007). The mangrove ecosystem also provides habitat and breeding ground for the aquatic life and migratory birds; acts as a defense line against cyclones and Tsunamis; protects shorelines and seaports from erosion and siltation; provides fuel, fodder, and livelihood to the coastal communities. However, these mangrove forests are reported to be under threat due to a decline in fresh river water flow and seawater intrusion (Boon and Raven, 2012; Peracha *et al.*, 2017). They are decreasing at an alarming rate; the published literature shows a continuous decline from 380,000 ha in 1950 to 86,767 ha in 2005 (Ahmed and Shoukat, 2015). Khan (2015) and DAWN (2008b) reported that the mangrove forests until the 1980s were spread over about 260,000 ha of the Indus delta, which ranked them the largest arid zone mangrove forests in the world. However, they decreased to 160,000 ha or even less, in the 1990s. The latest studies report the figure as 80,000 ha. This has severely impacted fish, crab, prawn production as well as other aquatic life (DAWN, 2008b).

In coastal areas, groundwater salinization is associated with increased dissolved minerals and some other chemical constituents, such as chloride, magnesium, etc. (Dixon and Chiwell, 1992; Gimenez and Morell, 1997). Same is the case with coastal

areas of Sindh province of Pakistan; where groundwater contamination is increasing continuously, may be because of entry of saline water from the Arabian Sea into the aquifers as seawater contains salts and many trace metals (Patil *et al.*, 2012). Memon *et al.* (2011) reported that the groundwater of coastal areas of Sindh is not suitable for drinking purpose. Hence people usually use surface water to accomplish their domestic water demand.

#### **1.4.4 Climate change**

The topography of Indus delta is quite flat, which poses a higher risk of sea intrusion. It is reported that due to climate change, sea level has risen by 1.3 mm/year in the last 100 years (Stewart, 1989; Kusky, 2003) while it is 1.1 mm/year, based on the recorded data of the past 100 years at Karachi harbor (Quraishie, 1988). The flat topography of the delta makes coastal areas vulnerable to sinking. Rasul *et al.* (2012) predicted at least 5 °C rise in temperature over the Indus Delta by the end of the 21<sup>st</sup> century due to which domestic, animal and crop water requirements will rise 1.5 times over the present levels. They also projected that sea level rise will also increase and by the end of the 21<sup>st</sup> century, it will rise about 30 to 80 cm.

However, most of the reports about the gravity of the problem are based on sampling surveys conducted from time to time without any scientific evidence and application of the latest scientific tools and techniques. Hence, there is significant variability in the data about land, water, vegetation and socioeconomic conditions of the coastal communities affected by seawater intrusion. Without any scientific approach/evidence, these reports are usually not considered worth and hence do not get due considerations from the policymakers. Hence, keeping in view above facts the present study was conducted to assess the impacts of seawater intrusion on freshwater, land, vegetation, environment and socio-economic conditions of the people using remote sensing and geospatial tools. This study aims to provide definitive data to policy makers to help develop a strategic plan to mitigate the adverse impact of climate change on environment and to adopt measures for serving the biodiversity of the delta.

## 1.5 Objectives

The objectives of the present study were:

- I. To determine the spatial and temporal change in the vegetation of the Indus Delta
- II. To determine the spatial and temporal distribution of soil salinity in the delta
- III. To assess the spatial variation in surface and groundwater quality in the delta
- IV. To determine the temporal variation in Land Surface Temperature (LST) using Remote Sensing and determine its effect on the flora of the delta.
- V. To quantify the shift in the shoreline of the Indus delta and the area taken away by the sea
- VI. To assess the impacts of seawater intrusion on socio-economic conditions of the people living in the delta

## 2. MATERIALS AND METHODS

In this Chapter, materials and methodology used to accomplish the objectives of the present study are described in detail:

### 2.1 Delineation of Indus Delta

The first and most difficult task for carrying the present study was a delineation of the boundaries of Indus delta for collection of the required data. Different researchers/scholars have given different figures of the area of delta (Table 2.1 and 2.2) and delineated different boundaries of the delta and active delta (current live delta) in the literature.

**Table 2.1: Area of the Indus Delta (based on literature)**

S. No.	Area		Reference
	Sq. km	Hectares	
1	6,000	600,000	Meynell and Qureshi (1993); Khan and Akbar (2012); Giri <i>et al.</i> (2015); Memon (2005);
2	8,500	850,000	Ahmed and Shaukat (2015)
3	30,000	30,00,000	Leichenko <i>et al.</i> (1993); Renuad <i>et al.</i> (2013)
4	17,000	17,00,000	Syvitski <i>et al.</i> (2013)
5	16,000	16,00,000	Callaghan (2014)
6	41,440	41,44,000	Peracha <i>et al.</i> (2015)
5	5,000	500,000	Laghari <i>et al.</i> (2015)

**Table 2.2: Area of the active Indus Delta**

S. No.	Area		Reference
	Sq. km	Hectares	
1	260	2,600	Leichenko <i>et al.</i> (1993)
2	6,000	600,000	Peracha <i>et al.</i> (2015)

Thus, it was necessary to delineate the delta with some historical evidence. Old maps of Talpur (1833) and British era (1893) were used to delineate the delta (Fig. 2.1). During those days the Pinyari river/estuary originated from river Indus near Banoo town (District Sujawal) on the left bank of the river Indus and discharged into the Arabian sea through Sir Creek. Taking Banoo as an apex of the delta while Sir Creek on the east and Phitti Creek on the west as two bottom points of the delta, the Indus delta was delineated as shown in Fig. 2.2.

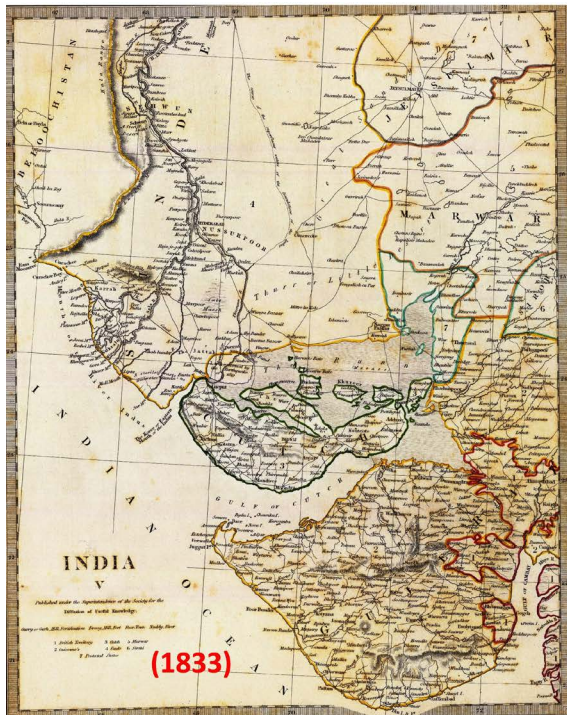


**Fig. 2.1: Maps of Sindh showing Pinyari river originating from river Indus during 1833 and 1883 AD**

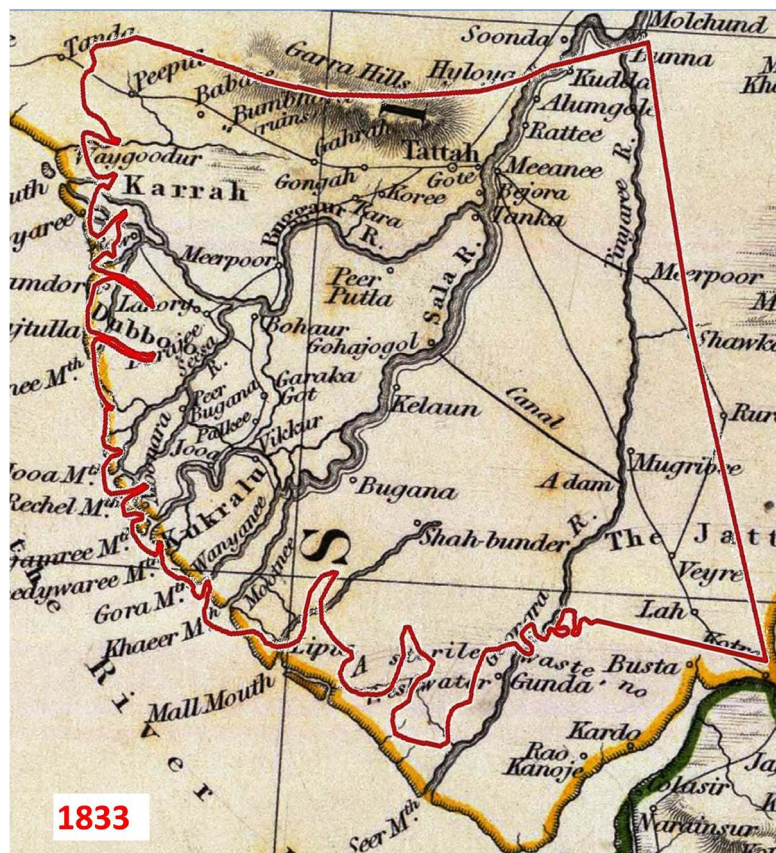


**Fig. 2.2: Delineated Indus delta (based on a map of Sindh 1833 AD)**

The delineated Indus delta for the present study has an area of 13067 sq.km (1.3 Mha). It covers almost the entire geographical boundaries of Sujawal and Thatta districts except for the mountainous area of the Thatta district. The apex of the delta is almost the same as delineated by Google Earth in the “Geographic Features” layer under “Borders and Labels” category (Fig. 2.3).

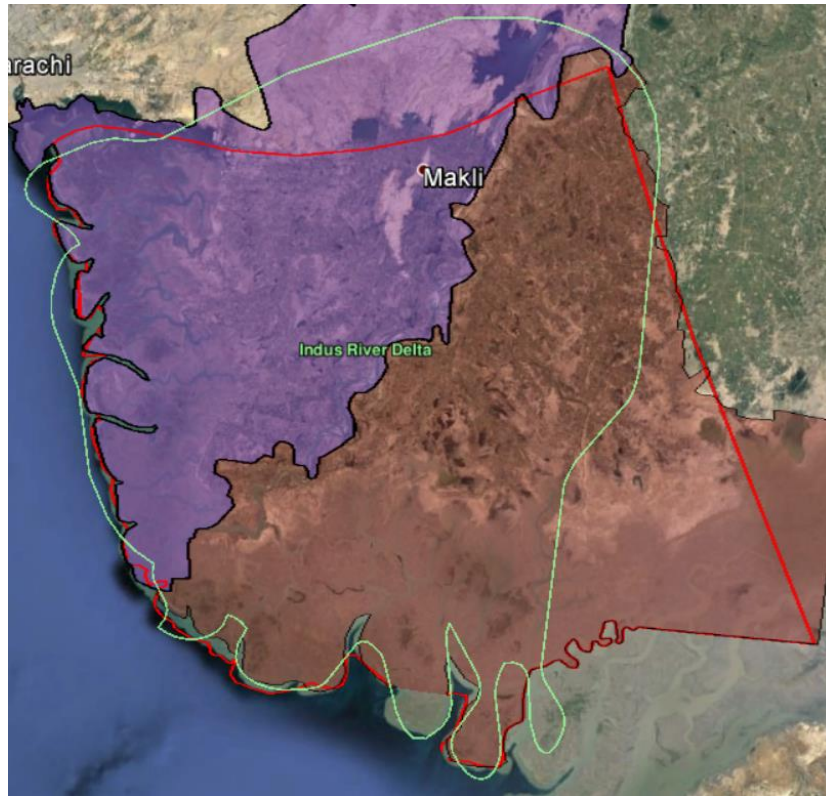


**Fig. 2.3: Delineated Indus Delta compared to that given by Google Earth. Red line shows the boundaries of delta delineated for use in the present study while Greenline shows the delta given by Google Earth**

## **2.2 Spatial and Temporal Change in Vegetation of the Indus Delta**

Vegetation is an indicator for assessing the environmental change and providing habitat to the wildlife. It is also a source of food, fuel, and shelter for humans. However, due to changing environmental conditions and anthropogenic activities, vegetation patterns are also affected in deltaic areas.

### **2.2.1 Satellite data**

To analyze the spatial and temporal variation in the vegetation of Indus delta, Landsat satellite data of last 27 years (from 1990 to 2017) were downloaded from the USGS Global Visualization Viewer (GloVis) and classified for quantification of vegetation. Google Earth temporal imagery and ground truthing data of 2016-17 were used for cross verification during image classification. The satellite imagery used for analysis

is summarized in Table 2.3. The area of interest (AOI), i.e. Indus delta in spreads in two tiles of the satellite image, hence the two satellite images having WRS (World Reference System) paths 151 and 152 and row 43 were mosaicked first and then the AOI was extracted from the entire scene using shapefile of the delta as a mask in “extract my mask” tool in spatial analyst toolbox of ArcGIS 10.3. The digital numbers (DN) of visible, near infrared and shortwave bands of the AOI were first converted to radiance and then to Top of Atmospheric Reflectance ( $\rho_{\lambda}$ ) following the methodology described by Chander *et al.* (2009) and Siyal *et al.* (2015) using equations 2.1 and 2.2. The atmospherically corrected images were used for the analysis.

$$\rho_{\lambda} = MpQcal + Ap \quad (2.1)$$

and

$$\rho_{\lambda} = \frac{\rho_{\lambda}'}{\cos(\theta_{SZ})} = \frac{\rho_{\lambda}'}{\sin(\theta_{SE})} \quad (2.2)$$

where:

$\rho_{\lambda}$  = Top of atmospheric (TOA) planetary reflectance, without correction for the solar angle.

$Mp$  = Band-specific multiplicative rescaling factor from the metadata

$Ap$  = Band-specific additive rescaling factor from the metadata

$Qcal$  = Quantized and calibrated standard product pixel values (DN)

$\rho_{\lambda}$  = TOA planetary reflectance

$\theta_{SE}$  = Local sun elevation angle. The scene center sun elevation angle in degrees is provided in the metadata (SUN ELEVATION).

$\theta_{SZ}$  = Local solar zenith angle;  $\theta_{SZ} = 90^{\circ} - \theta_{SE}$

**Table 2.3: Landsat satellite imagery (from 1990 to 2017) used for the vegetation analysis**

S. No	Year	Acquisition date	Path	Row	Day of year	d	$\theta_s$
1	1990	Feb. 10	151 <sup>a</sup>	43	41	0.98680	37.253531
2		Feb. 17	152 <sup>a</sup>		48	0.98814	38.963608
3	1995	Feb. 24	151 <sup>a</sup>	43	55	0.98959	39.025413
4		Feb. 15	152 <sup>a</sup>		46	0.98768	36.720616
5	2000	Feb. 14	151 <sup>b</sup>	43	45	0.98755	43.035698
6		Feb. 05	152 <sup>b</sup>		36	0.98596	40.742568
7	2005	Feb. 27	151 <sup>b</sup>	43	58	0.99036	46.663667
8		Feb. 18	152 <sup>b</sup>		49	0.98835	43.919991
9	2010	Feb. 09	151 <sup>b</sup>	43	40	0.98662	41.729947
10		Feb. 16	152 <sup>b</sup>		47	0.98794	43.632710
11	2015	Feb. 15	151 <sup>c</sup>	43	46	0.98774	44.574501
12		Feb. 06	152 <sup>c</sup>		37	0.98602	42.179202
13	2017	Feb. 20	151 <sup>c</sup>	43	51	0.98881	46.110403
14		Feb. 11	152 <sup>c</sup>		42	0.98698	43.506486

<sup>a</sup>Landsat 5; <sup>b</sup>Landsat 7; <sup>c</sup>Landsat 8

### 2.2.2 Ground truthing

Random georeferenced samples of vegetation were collected from the entire Indus delta during the year 2016-17. These georeferenced samples contained samples of vegetation, built-up areas, barren land, water, and mangroves. The ground truthing samples were collected from the entire project area using handheld Garmin GPS 62s (Fig. 2.4)





**Fig. 2.4: Snapshots taken during ground truthing data**

### 2.2.3 Image classification

Unsupervised and supervised classifications and vegetation index NDVI (Normalized Difference Vegetation Index) were used for identification of vegetated areas and preparation of vegetation masks; thus, quantification of temporal variation in the vegetation of Indus delta. For supervised classification, all the images of AOI were trained for vegetated and non-vegetated areas using Training Sample Manager in ArcGIS 10.3. Training samples were created by drawing polygons around locations already marked on the images using georeferenced field data and Google Earth imagery. All the samples of vegetation were merged into a single class. Then, the maximum likelihood algorithm was used to produce supervised classified vegetation masks of the delta. The whole process of supervised classification is summarized in the flowchart shown in Fig. 2.5.

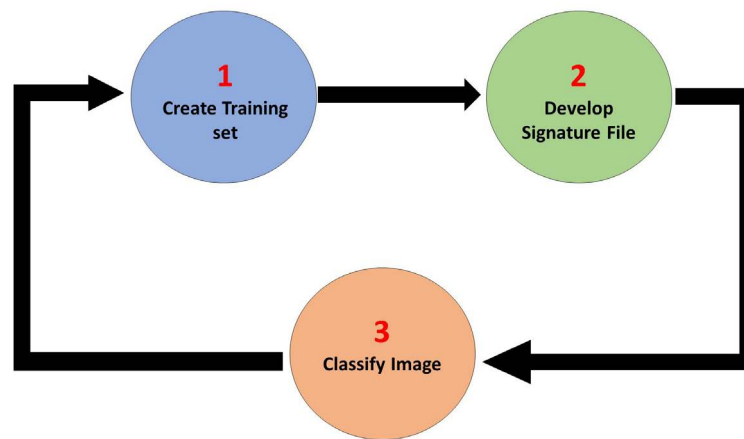


**Fig. 2.5: Flow chart of the supervised classification**

In unsupervised classification, the user identifies how many classes to generate and which bands to use. The software then clusters pixels into the set number of classes. The user then identifies the different classes and reclassifies them according to the specific requirement. In the present study, the raster satellite images were first classified into eight classes using unsupervised classification. Then these classes were reclassified into vegetated and non-vegetated classes by merging the similar classes.

### 2.2.4 NDVI

NDVI is determined from the visible and near-infrared light reflected by vegetation. Healthy green vegetation absorbs most of the visible sunlight which falls over it and reflects a large portion of the near-infrared light. Whereas, unhealthy or sparse vegetation reflects more visible light and less near-infrared light. NDVI was first presented by Kriegler *et al.* (1969), and it is calculated by subtracting the red band

from the near-infrared (NIR) band and dividing their difference by the sum of the two bands as given in equation 2.3.

$$NDVI = \frac{NIR-RED}{NIR+RED} \quad (2.3)$$

Calculations of NDVI for a given pixel always result in a number that ranges from minus one (-1) to plus one (+1); however, no green leaves give a value close to zero. Water has an NDVI value less than 0, bare soils between 0 and 0.1, and vegetation over 0.1. The increase in the positive NDVI value means greener the vegetation.

The area under vegetation was calculated for different years from the classified images (vegetation masks) to detect any temporal change in the vegetation. For this vegetation mask raster data of each reported year was first converted into vector data. Then using layer property “query builder,” the area of vegetation class for each year was calculated.

### 2.2.5 Temporal variation in mangroves

The tidal floodplain area, from the satellite images of the years 1990, 1995, 2000, 2005, 2010, 2015 and 2017 of Indus delta, was extracted as shown in Fig. 2.6. The extracted images of tidal floodplains were analyzed for mangroves population in the delta using supervised classification with maximum likelihood algorithm in ArcGIS 10.3. These images were categorized into three classes, viz. mangroves, barren tidal floodplain, and water.

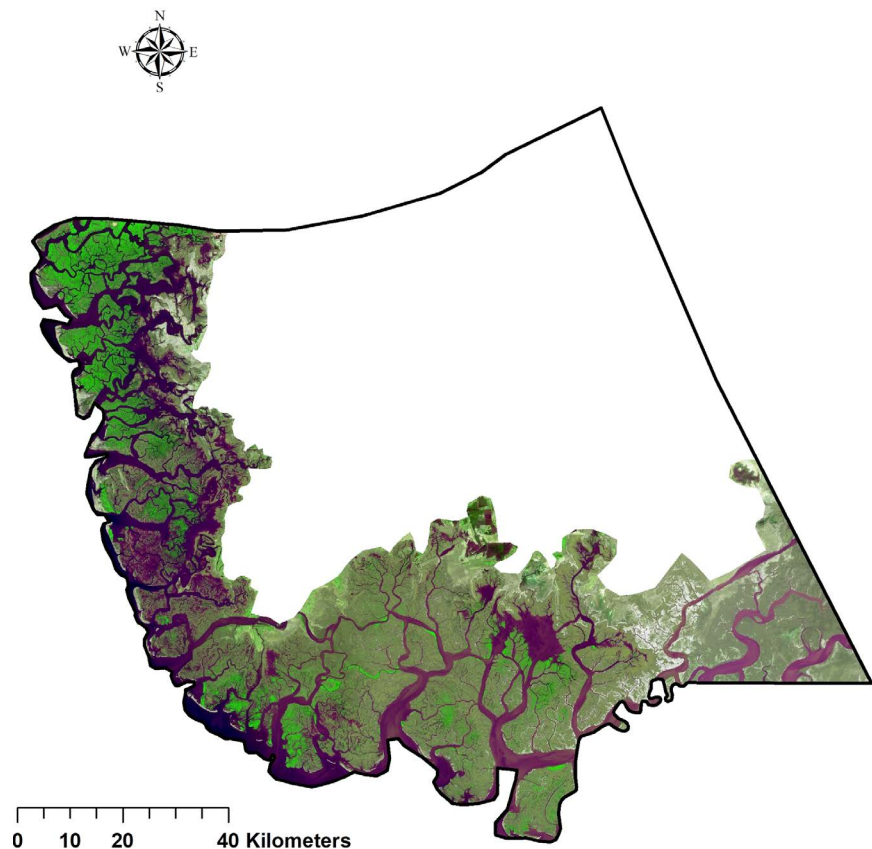


Fig. 2.6: Tidal floodplain of the Indus Delta

## 2.3 Temporal Variation in Land Surface Temperature (LST) and its Effect on the Flora of the Delta

### 2.3.1 Satellite data for land surface temperature

Landsat satellite data of the last 28 years (1990 to 2017) were used (Table 2.4) for quantification of temporal and spatial variation in land surface temperature (LST). The digital numbers (DN) of the thermal band (band 6 for Landsat 5 and 7 and band 10 for Landsat 8) of the AOI were first converted to Top of Atmospheric Spectral Radiance (TOA<sub>R</sub>) and then to land surface temperature using equations 2.4 and 2.5.

$$L_{\lambda} = M_L Q_{cal} + A_L \quad (2.4)$$

where:

$L_{\lambda}$  = Top of Atmosphere spectral radiance (TOA<sub>R</sub>) (Watts/(m<sup>2</sup> \* srad \* μm))

$M_L$  = Band-specific multiplicative rescaling factor obtained from the metadata file

$A_L$  = Band-specific additive rescaling factor obtained from the metadata file

$Q_{cal}$  = Quantized and calibrated standard product pixel values [Digital Numbers (DN)]

Then thermal band data were converted from TOA<sub>R</sub> to land surface temperature (LST) in centigrade using the thermal constants provided in the metadata file:

$$T = \frac{K_2}{\ln\left(\frac{K_1}{L_{\lambda}} + 1\right)} - 273 \quad (2.5)$$

Where

$T$  = At-satellite brightness temperature (K)

$L_{\lambda}$  = TOA spectral radiance (Watts/ (m<sup>2</sup> \* srad \* μm))

$K_1$  = Band-specific thermal conversion constant from the metadata

$K_2$  = Band-specific thermal conversion constant from the metadata

The satellite images used in the study along with values of band-specific multiplicative rescaling factor ( $M_L$ ), band-specific additive rescaling factor ( $A_L$ ), and thermal conversion constants ( $K_1$  and  $K_2$ ) are summarized in Table 2.4.

**Table 2.4: Landsat satellite imagery (from 1990 to 2017) used for the LST analysis**

Year	Acquisition date	Path	Row	Band number	$M_L$	$A_L$	$K_1$	$K_2$
1990	Feb. 10	151	43 <sup>a</sup>	B6	0.055375	1.18243	607.76	1260.56
	Feb. 17	152		B6	0.055375	1.18243	607.76	1260.56
1995	Feb. 24	151	43 <sup>a</sup>	B6	0.055375	1.18243	607.76	1260.56
	Feb. 15	152		B6	0.055375	1.18243	607.76	1260.56
2000	Feb. 14	151	43 <sup>b</sup>	B6	0.067	-0.06709	666.09	1282.71
	Feb. 05	152		B6	0.067	-0.06709	666.09	1282.71
2005	Feb. 27	151	43 <sup>b</sup>	B6	0.067	-0.06709	666.09	1282.71
	Feb. 18	152		B6	0.067	-0.06709	666.09	1282.71
2010	Feb. 09	151	43 <sup>b</sup>	B6	0.067	-0.06709	666.09	1282.71
	Feb. 16	152		B6	0.067	-0.06709	666.09	1282.71
2015	Feb. 15	151	43 <sup>c</sup>	B10	0.000334	0.10000	774.89	1321.08
	Feb. 06	152		B10	0.000334	0.10000	774.89	1321.08
2017	Feb. 20	151	43 <sup>c</sup>	B10	0.000334	0.10000	774.89	1321.08
	Feb. 11	152		B10	0.000334	0.10000	774.89	1321.08

<sup>a</sup> Landsat 5;    <sup>b</sup> Landsat 7;    <sup>c</sup> Landsat 8

### 2.3.2 Meteorological data

The meteorological data of two field stations, i.e., Thatta and Badin were acquired from the Pakistan Meteorological Department, Karachi. The monthly rainfall data from 1960 to 2016 for Badin station and from 2004 to 2016 for Thatta station were obtained as the later station started functioning in 2004. Also, the mean rainfall and temperature data from 1960 to 1990 of the study area were obtained from WorldClim (<http://worldclim.org/current>) by extracting the data of delta from the entire Global data given in raster tiff format with a spatial resolution of 1 km.

### 2.3.3 Flow below Kotri Barrage

The annual water flow (MAF) below Kotri barrage was acquired from the provincial irrigation department and was analyzed for determining the temporal variation in the flow and quantification of reduction in the river environmental flow.

## 2.4 Spatial and Temporal Variation in Soil Salinity of the Delta

### 2.4.1 Soil sampling

Georeferenced soil samples from 0-20, 20-40, and 40-60 cm soil depth were randomly collected from different locations of the study area (Fig. 2.7 and 2.8). Soil auger was used for collection of soil samples while the location of the sampling points was obtained using the handheld Garmin GPS. Total 375 soil samples from 125 different locations of the study area were collected and analyzed for various physicochemical parameters *viz.* texture, dry density, electrical conductivity (EC), hydrogen ion concentration (pH) and exchangeable sodium percentage (ESP).

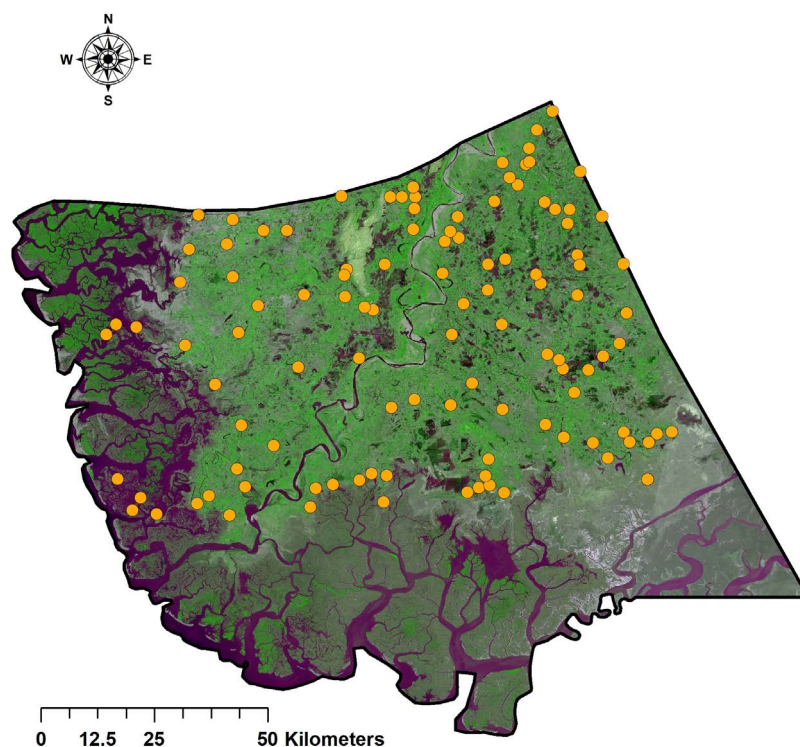


**Fig. 2.7: Spatial distribution of soil sampling locations in the delta**

### 2.4.2 Physicochemical analysis of soil samples

Soil particle size distribution of all samples was determined by Bouyoucos method using a hydrometer (Bouyoucos, 1936). Oven drying method was used for determination of the dry density of the soil samples. The electrical conductivity (EC) of the soil samples were determined at 25 °C using digital EC meter (Pessoa *et al.*, 2016). Sodium concentration was determined using flame photometer while the cations  $\text{Ca}^{+2}$  and  $\text{Mg}^{+2}$  were determined through titration method. The pH of soil saturation extracts was measured using pH meter. The results of these chemical analyses were used to calculate the sodium absorption ratio (SAR), and the exchangeable sodium percentage (ESP).



**Fig. 2.8: Snapshots taken during soil sampling from Indus Delta**

### 2.4.3 Mapping of soil salinity

Based on the analytical of data, thematic maps for various physicochemical parameters viz., electrical conductivity (EC), soil pH, exchangeable sodium percentage (ESP), texture, and dry density were prepared using ArcGIS 10.3 software. Spatial analysis 'Inverse Distance Weighted (IDW)' interpolation approach was used to develop the spatial distribution thematic maps. Based on physicochemical analysis of the soil samples, the delta was mapped with four soil salinity classes, i.e. normal (non-saline), saline, sodic or alkali and saline-sodic soils.

### 2.4.4 Salinity indices

The combination of GIS and Remote sensing are used to delineate salt-affected soils. Thus, mapping of salinity risk is nowadays carried out using different types of multispectral remote sensing data. Ghabour and Daels (1993) concluded that detection of soil degradation by conventional means of soil surveying requires a great deal of time, but remote sensing data and techniques offer the possibility for mapping and monitoring these processes more efficiently and economically. The most commonly used technique for a salinity index is the calculation of different indices and ratio images using infrared and visible spectral bands of satellite data. Following salinity indices were used to delineate the salt-affected areas of the delta.

- i. Normalized Difference Salinity Index =  $NDSI = \frac{red - nir}{red + nir}$  (Khan *et al.*, 2005)
- ii. Salinity Index =  $SI = \sqrt{blue \times red}$  (Khan *et al.*, 2001)
- iii. Brightness Index =  $BI = \sqrt{(red)^2 \times (nir)^2}$  (Khan *et al.*, 2005)



## 2.5 Spatial Variation in Surface and Groundwater Quality in the Delta

### 2.5.1 Surface water quality

#### 2.5.1.1 Water sample collection

The surface water samples were collected during July 2016 to May 2017 from 50 different surface water bodies *viz.* lakes, ponds, natural channels (except irrigation channels), and natural depressions located in the Indus delta (Fig. 2.9 and 2.10). Water samples were gathered in one-liter plastic bottles observing standard methods of water sampling. The samples were analyzed for different physicochemical parameters *viz.* turbidity, electrical conductivity, pH, total dissolved solids, calcium, magnesium, total hardness, chloride, alkalinity, and arsenic using standard methods and compared with water quality standards set by WHO and FAO for drinking and irrigation purposes, respectively

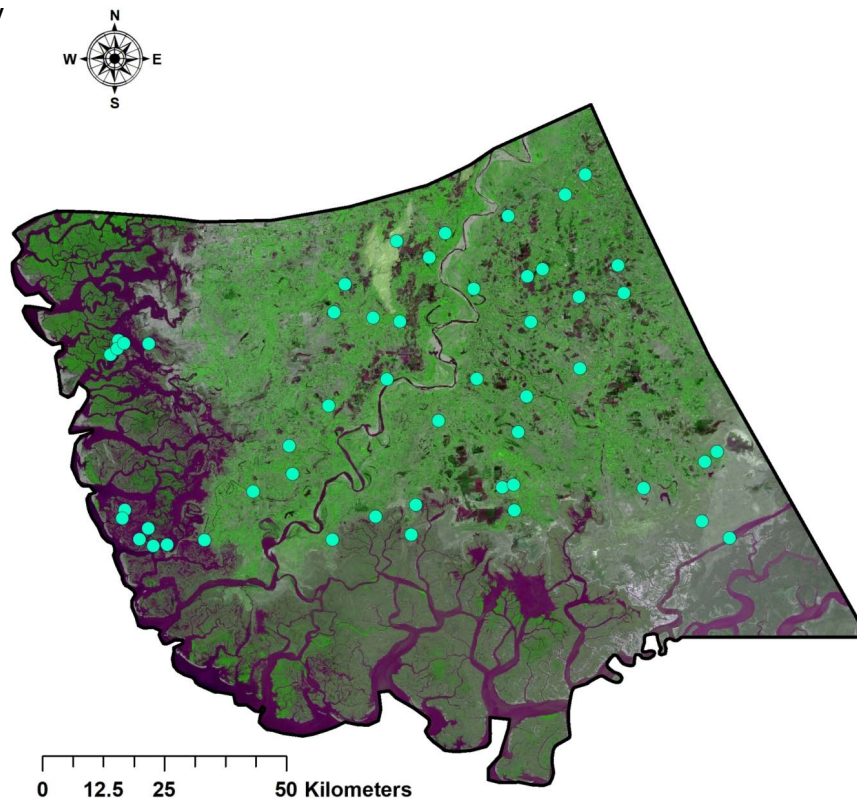


**Fig. 2.9: GIS map of surface water sampling locations**

Water quality parameters *viz.* turbidity, electrical conductivity, hydrogen ion concentration, and total dissolved solids were measured *in-situ* (Ketata-Rokbani *et al.*, 2011; Popovic *et al.*, 2016) using turbidity, EC, pH, and TDS meters, respectively, while calcium, magnesium, hardness, chloride, and water alkalinity were determined in the laboratory through standard methods (Shabbir and Ahmad, 2015), whereas arsenic

was determined using Merck arsenic kit. All the standard methods were followed from water sample collection, preservation, transportation and analysis of water samples in the laboratory.



**Fig. 2.10: Snapshots taken during surface water sampling**

### 2.5.1.2 Water quality indices

Water quality indices provide an overall picture of the suitability of water for various purposes (Tiwari and Mishra, 1985; Ma *et al.*, 2009). In the present study, the quality of surface water bodies of the Indus Delta was evaluated by using the Water Quality Index (WQI) and the Synthetic Pollution Index (SPI) by application of equations 2.6 and 2.7.

$$WQI = \frac{\sum_{i=1}^n W_i Q_i}{\sum_{i=1}^n W_i} \quad (2.6)$$

and

$$SPI = \sum_{i=1}^n \frac{C_i}{S_i} \times W_i \quad (2.7)$$

Where,  $W_i$  is the unit weightage of the  $i$ th parameter which was determined as a value inversely proportional to the standard value,  $Q_i$  is the sub-index of the  $i$ th parameter,  $S_i$  is the standard level for the  $i$ th parameter,  $n$  denotes the number of parameters and  $C_i$  is the observed concentration for each of the determined physicochemical water quality parameters.

## 2.5.2 Groundwater quality

### 2.5.2.1 Groundwater sampling

One hundred eighty groundwater samples were randomly collected from the hand pumps already installed in the Indus delta (Fig. 2.11 and 2.12). The samples were collected from those hand pumps which are widely used by the people for extracting water for their drinking and other domestic needs. Preference was given to those pumps which were installed at permanent public places, i.e., residential areas, schools, bus stops, restaurants, hospitals from where local population fetched water. The sampling locations were noted using a hand-held Garmin GPS (62s). During groundwater sampling, it was observed that the hand pumps were installed at shallow depths ranging between 5 to 15 m. The purging procedure based on the depth of hand pump was followed and after purging the bottles and their caps were thoroughly washed with the same groundwater. Then groundwater samples were collected in one-liter plastic bottles already washed and rinsed well with distilled water to remove any possible contamination. All the standard procedures were followed during the collection, handling, transportation and physicochemical analysis of the water samples.

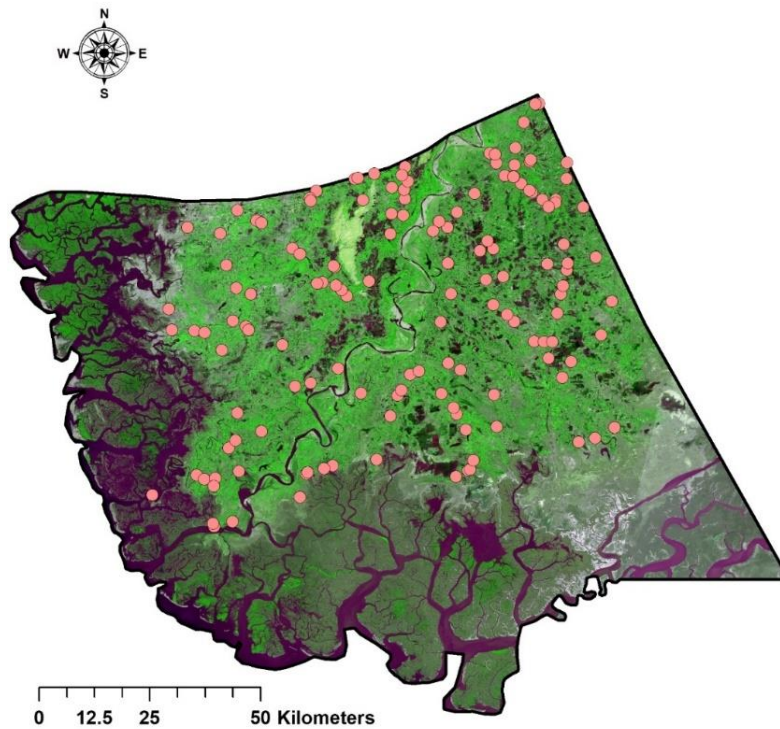


**Fig. 2.11: GIS map of groundwater sampling locations**

### **2.5.2.2 Physicochemical analysis**

The groundwater samples were assessed for various physicochemical parameters viz. turbidity, EC, TDS, pH, calcium (Ca), magnesium (Mg), chloride (Cl), total hardness (TH), and arsenic (As) in the laboratory. The turbidity, EC, TDS, and pH were determined by Turbidity meter (Lamotte Model – 2008, USA); EC meter (Hach Conductivity meter); TDS meter (Hach Model 44600, USA), and pH by Hanna Instrument (Model 8519 Italy), respectively. However, Ca, Mg, Cl, total hardness Cl and As were determined using 3500-Ca-D standard method (1992); 2340-C, Standard Method (1992); Titration (Silver Nitrate), Standard method (1992); EDTA titration, standard method (1992); and Merck Test Kit (0-0.5 mg/L), respectively. The drinking water quality standards suggested by WHO (2011) were used as benchmarks for various groundwater quality parameters.

### **2.5.2.3 Geospatial analysis and mapping**

The groundwater quality thematic maps for various physicochemical characteristics such as turbidity, EC, pH, TDS, Ca, Mg, Cl, and As were developed using a spatial interpolation “inverse distance weighted (IDW)” approach and then extracting the area of interest (AOI) using “extraction by mask” tool, by adding the shapefile of the study area. IDW is reported as an intuitive and efficient method (Balakrishnan *et al.*, 2011) to delineate the locational distribution of groundwater contamination.



**Fig. 2.12: Snapshots taken during groundwater sampling**

### 2.5.2.4 Water quality index

Three steps were followed while calculating the WQI. In the first step, the relative weight ( $W_i$ ) was calculated using equation (2.8)

$$W_i = \frac{w_i}{\sum_{i=1}^n w_i} \quad (2.8)$$

Where  $W_i$ ,  $w_i$ , and  $n$  were the relative weight, each parameter's weight, and the number of parameters, respectively.

In the second step, the water quality rating scale ( $Q_r$ ) for each of the selected parameters was calculated using equation (2.9).

$$Q_r = \frac{C_o}{C_p} \times 100 \quad (2.9)$$

Where  $C_o$  and  $C_p$  were the observed value of the physicochemical parameter in the analyzed water sample and the permissible limit for each of the selected parameters suggested by WHO for drinking purpose. Finally, in the third step, WQI was calculated using equation (2.10).

$$WQI = \sum W_i \times Q_i \quad (2.10)$$

The summary of calculated weight, relative weight and WHO standards for considered physicochemical parameters is given in Table 2.5.

**Table 2.5: Summary of calculated weight, relative weight and WHO standards for selected physicochemical parameters**

Parameter	WHO standards	Weight (wi)	Relative weight (Wi)
pH	8.5	3	0.14
TDS	1000 mg/L	3	0.14
Calcium	75 mg/L	2	0.10
Magnesium	50 mg/L	2	0.10
Total Hardness	500 mg/L	2	0.10
Chloride	250 mg/L	3	0.14
Turbidity	5 ppb	2	0.10
Arsenic	10 ppb	5	0.23
$\Sigma$		22	1.00

### 2.5.2.5 Subsurface seawater intrusion

The subsurface seawater intrusion was estimated considering the levels of indicators given below (Table 2.6) in the groundwater samples. The area affected due to subsurface seawater intrusion was estimated through interpolation of the ground water data.

**Table 2.6: Indicators for estimation of subsurface seawater intrusion**

S. No.	Description	Reference
1	The high levels of chlorides > 250 mg/L	Werner <i>et al.</i> (2013); Mtoni <i>et al.</i> (2013); Karanth (2014); El-Hoz <i>et al.</i> (2014); Supriyadi and Putro (2017).
2	The ionic ratio of Cl to (HCO <sub>3</sub> +CO <sub>3</sub> ) > 2.8	Ebrahimi <i>et al.</i> (2016)
3	Simpson's ratio > 2.8	Raghunath (1990); Jamshid and Mirbagheri (2011).
4	High correlations among chloride, magnesium, and sulfate, in association with EC in the Pearson correlation matrix	Sappa <i>et al.</i> (2015)
5	Chloride and bicarbonate ions ratio > 0.67	Bablani & Soomro, (2006).

## 2.6 Shift in the Shoreline of the Indus Delta and the Area Taken Away by the Sea

To enumerate the area-specific variation in the shoreline, the entire shoreline was divided into four zones namely Zone 1 (Sir-Wari) about 74 km, Zone 2 (Wari-Khoobar) about 62 km, Zone 3 (Khoobar-and Dabo) about 65 km and Zone 4 (Daboo-Phitti) about 75.6 km. Zones 1 and 2 lie on the Left Bank while Zones 3 and 4 are located on the Right Bank of the river Indus (Fig. 2.13).

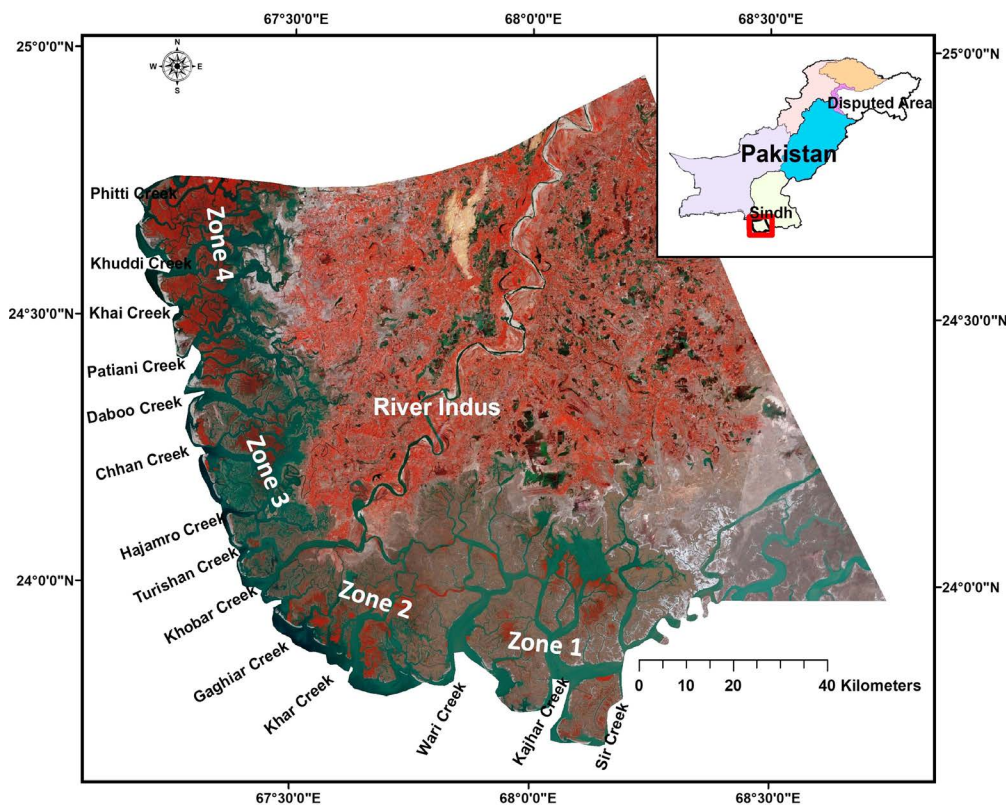


**Fig. 2.13: Shoreline of delta divided into four zones**

For the present study, the multitemporal Landsat MSS, TM, ETM+ and OLI imagery (Table 2.7), were acquired at Level-1T processing for the period 1972 to 2017 from USGS Global Visualization Viewer (GloVIS) website (<http://glovis.usgs.gov/>). Due to unavailability of systematic Landsat data before 1990, the selection of years for Landsat data is irregular.



**Table 2.7: Meta information of the satellite imagery used in quantifying shift in shoreline**

Satellite/Sensor	Acquisition date	Path/Row	Spatial resolution
Landsat 1/ MSS	Oct. 15, 1972	163/43	60
Landsat 3/ MSS	Jan. 18, 1979	163/43	60
Landsat 5/ TM	Nov. 8, 1987	152/43	30
Landsat 5/ TM	Feb. 17, 1990	152/43	30
Landsat 7/ ETM+	Feb. 05, 2000	152/43	30
Landsat 7/ ETM+	Feb. 16, 2010	152/43	30
Landsat 8/ OLI	Feb. 06, 2015	152/43	30
Landsat 8/ OLI	Feb. 11, 2017	152/43	30

Image acquired at the time of low tide is considered more suitable for shoreline mapping (Mujbar and Chandrasekar, 2014). Therefore, to compare the results on identical tidal condition, satellite images of only low tide periods were acquired. The spectral resolution of the image was improved for better visualization of coastal features using histogram equalization technique (Kaliraj *et al.*, 2014). The shorelines at Mean Low Water (MLW) of respective years were then carefully digitized in ArcGIS 10.3 and exported to vector (shape-file) format for further analysis.

### **2.6.1 Digital shoreline analysis system (DSAS)**

The Digital Shoreline Analysis System (DSAS) is a USGS (United States Geological Survey) freely available software extension which integrates with Environmental System Research Institute (ESRI) ArcGIS 10.3 to examine and quantify the past or present shoreline positions or geometry (Thieler *et al.*, 2009; Oyedotun, 2014). The DSAS calculates different statistical measures *viz.* Linear Regression Rate (LRR), Shoreline Change Envelope (SCE), Net Shoreline Movement (NSM), and End Point Rate (EPR). The statistical algorithm associated with this software quantifies the shoreline change rate at each transect from temporal geo-referenced shoreline vector data.

### 2.6.2 Analysis of shoreline changes

The inward movement of coastline with respect to a reference line (baseline) is called as landward shift (erosion) while outward movement of coastline with reference to the baseline is taken as seaward shift (accretion). The erosion is usually symbolized as negative (-) while accretion is denoted as positive (+). All the extracted shorelines from 1972 to 2017 were imported in ArcGIS 10.3 and buffer of 2 km was drawn around the shorelines after merging all the eight (1972, 1979, 1987, 1990, 2000, 2010, 2015, 2017) shorelines. The baseline was drawn at about 2 km distance landward, parallel to the shoreline orientation. Seaward transects, each of 3 km length, at an equal spacing of 200 m along the baseline were generated through DSAS software. Thus, the entire shoreline of the Indus delta was divided through 1373 transects placed perpendicular to the baseline at equal distance of 200 m (Table 2.8). Similarly, variations in shoreline for short periods, i.e., between 1972 to 1990 and 1990 to 2017 were also determined. The extracted shorelines were analyzed for statistical parameters End Point Rate (EPR), Net Shoreline Movement (NSM) and Linear Regression Rate (LRR) using DSAS.

**Table 2.8: DSAS transect description of the study area**

Parameters	Sir-Wari Creek (Zone 1)	Wari-Khobar Creek (Zone 2)	Khobar- Daboo Creek (Zone 3)	Daboo-Phitti Creek (Zone 4)
Number of Transects	367	312	325	369
Transect spacing (m)	200	200	200	200
Average baseline distance from shoreline (m)	2000	2000	2000	2000

### 2.6.3 Manual quantification of change in shoreline

A baseline of about 176 km, at about 3 km seawards from the shoreline was drawn along the delta (Fig. 2.14). Perpendicular transects were drawn towards the shoreline 1 km apart along the entire baseline. The baseline was smooth irrespective of the irregular length of the shorelines, while the length of transects varied depending on the distance between the baseline and the shorelines. The entire regular baseline

was 176 km; thus, there were 176 transects. At each transect, the linear distance, between the position of the shoreline in 1972 and 2017 was measured using the ruler tool in ArcGIS. The net movement of the shoreline at all transects was determined by taking an average of inward (compared to shoreline position in 1972) or outward shift of shoreline at all transects.

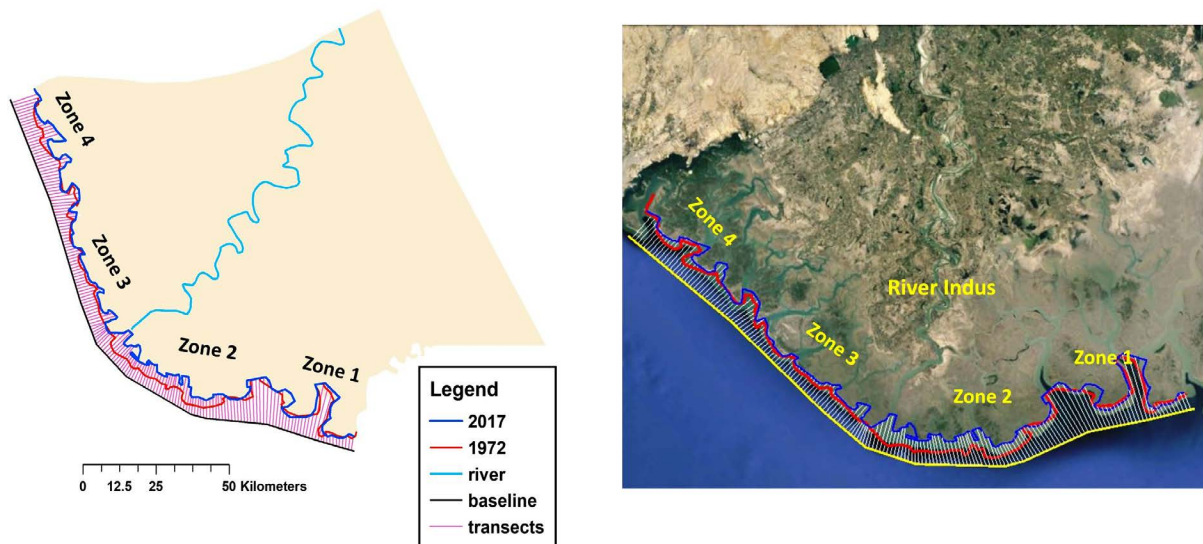


**Fig. 2.14: Schematic diagram of the baseline and the transects for manual calculation of the net shoreline movement.**

#### **2.6.4 Variation in tidal floodplain area and the area taken away by the sea**

Landsat imagery for the years 1972 and 2017 were used to extract the AOI, i.e. tidal floodplains after classifying the imagery for wetland area along the shoreline through supervised and unsupervised classification using ArcGIS 10.3. The surface seawater intrusion during the last 45 years (1972 to 2007) was quantified by comparing the change in shoreline and the landward increase in the tidal floodplain area.

#### **2.6.5 Vulnerability of the Indus delta due to coastal flooding**

SRTM 30m Digital Elevation Model (DEM) of the Indus delta was downloaded from the website <https://earthexplorer.usgs.gov/>. The entire Indus delta was covered through 4 tiles of the DEM which were mosaicked first and then the area of interest (AOI), i.e., Indus delta was extracted in ArcGIS 10.3 using the shapefile of the delta as a mask. The extracted DEM was categorized into sea flood risk map by classifying it into two classes based on the elevation of the area assuming a tsunami wave or a cyclone capable of raising sea level up to 5 m.

## 2.7 Impacts of Seawater Intrusion on Socio-economic Conditions of the People Living in the Delta

### 2.7.1 The sample size and selection of respondents

To assess the impacts of seawater intrusion on socio-economic conditions of the community living in the Indus Delta, a Key Informant Interview (KII) was carried out through a questionnaire. The appropriate sample size was determined using a formula developed by Cochran (1977):

$$n_0 = \frac{x^2 pq}{e^2} \quad (2.11)$$

Where,  $n_0$  = sample size,  $\chi^2$  = Abscissa of the normal curve that cuts off an area at the 95%,  $\chi = 1.96$ ,  $p$  = Estimated proportion of an attribute that is present in the population = 0.5,  $q = 1-p = 1-0.5 = 0.5$ , and  $e$  = desired level of precision equal to 0.05. Thus,

$$n_0 = \frac{(1.96)^2 \times 0.5 \times 0.5}{(0.05)^2} = 384$$

Using this formula, it was estimated that the sample size should not be less than 384, hence for the present study, 500 respondents of the study area were surveyed to conduct a valid and reliable study.

### 2.7.2 Data collection

Key Informant Interview (KII) survey was used to collect the primary data. All union councils (small administrative units) of the study area were sampled (Fig. 2.15). The participants/respondents of the survey were male and female, belonging to different age groups, communities and having different sources of income/occupations and different socio-economic levels/categories (Fig. 2.16). The survey was carried out from all the union councils so that it reflects the representation of all the people living in the delta.

Following parameters were considered in the Survey (KII Survey Questionnaire is given at Appendix-I)

- a. Current and previous occupation/current & previous source of income
- b. Socio-economic consideration change in farm income (past and present), living habits, any special diseases (not experienced before), etc.
- c. Any special/ adverse environmental conditions relative to past conditions
- d. Any perceived climatic change observed by the community

The information collected was analyzed to identify the impacts of seawater intrusion and whether those impacts are aggravating in time and space. The age group normally reflects the maturity level of the respondents; hence in the present study, no any respondent was under the age of 18 years.

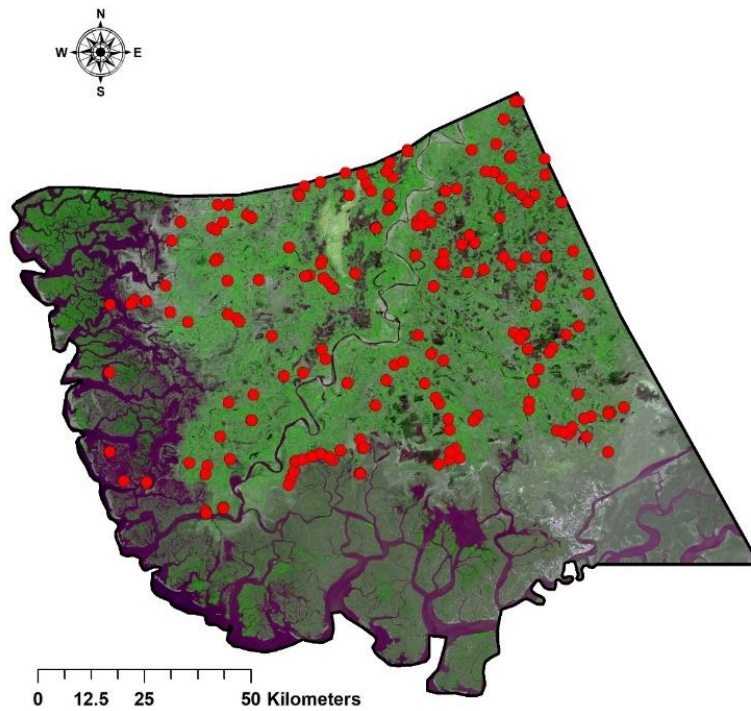


**Fig. 2.15: GIS map of groundwater sampling locations**



**Fig. 2.16: GIS map of socio-economic sampling survey locations**

### 2.7.3 Measurement of poverty in the study area

The Foster Greer Thorbecke techniques viz. headcount poverty index, the poverty gap, and the severity of the poverty index were used to determine the poverty measures in the study area. These techniques are mathematically expressed in equations 2.11, 2.12, 2.13 respectively.

$$P_{\infty} = \frac{1}{n} \sum_{i=1}^q \left( \frac{z - y_i}{z} \right)^0 \quad (2.12)$$

$$P_{\infty} = \frac{1}{n} \sum_{i=1}^q \left( \frac{z - y_i}{z} \right)^1 \quad (2.13)$$

$$P_{\infty} = \frac{1}{n} \sum_{i=1}^q \left( \frac{z - y_i}{z} \right)^2 \quad (2.14)$$

Where  $n$  is total sample size,  $q$  is the number of persons who are poor,  $z$  is the poverty line, and  $y_i$  is  $i$ th lowest income.

Headcount index measures the proportion of the population that is poor, but it does not indicate how poorer the poor are (Imran *et al.*, 2013). Whereas, the poverty-severity index averages the squares of the poverty gaps relative to the poverty line.

### 2.7.4 Limitations of the study

- i. Only those respondents were interviewed who were permanent residents of the Indus Delta and were above the age of 18 years
- ii. Respondents were asked for any significant change observed due to changes in climate over the last twenty years.
- iii. The data about income and expenditure was mainly collected from the memory of the respondents, as most of the uneducated respondents did not maintain the records of their income and expenditure.
- iv. Most of the respondents were reluctant to provide the required information such as income, expenditure, age, etc.
- v. Most of the female respondents of the study area were reluctant to agree for an interview.

### 3. RESULTS AND DISCUSSION

#### 3.1 Spatial and Temporal Change in Vegetation of the Indus Delta

##### 3.1.1 Vegetation

Table 3.1 shows the area under vegetation during February from 1990 to 2017, determined through supervised and unsupervised classifications along with the NDVI index. The vegetated area varied between 2568 km<sup>2</sup> (19.6% of the entire delta) during 2015 and 47000 km<sup>2</sup> (35.9% of the delta) in 2010. The variation in the calculated vegetated area due to the application of different techniques was from 51 to 154 km<sup>2</sup>.

**Table 3.1: Area of the delta under vegetation and corresponding percentage from 1990 to 2017**

Year	Unsupervised	Supervised	NDVI	Mean	% of delta	STD	SE	CI
	km <sup>2</sup>	km <sup>2</sup>	km <sup>2</sup>	km <sup>2</sup>		km <sup>2</sup>	km <sup>2</sup>	km <sup>2</sup>
Feb. 1990	3104	2850	3053	3002.3	22.98	134.37	77.58	152.047
Feb. 1995	2884	2941	3147	2990.7	22.89	138.36	79.88	156.561
Feb. 2000	4114	4056	4258	4142.7	31.70	104.01	60.05	117.692
Feb. 2005	4107	3986	4293	4128.7	31.60	154.64	89.28	174.991
Feb. 2010	4585	4717	4800	4700.7	35.97	108.43	62.60	122.694
Feb. 2015	2605	2510	2590	2568.3	19.66	51.07	29.49	57.792
Feb. 2017	2885	2648	2923	2818.7	21.57	149.02	86.04	168.627

STD = Standard Deviation SE = Standard error of mean CI = Confidence Interval @5%

No specific trend in temporal variation of vegetation was observed. It increased gradually from 1990 to 2010 but later it decreased significantly as shown in Fig. 3.1. It may be due to a decrease in the availability of irrigation water and the impact of



climate change (decrease in rainfall and increase in temperature).

The spatial and temporal variation in vegetation is portrayed in the form of vegetation masks (Fig. 3.2). No spatial variation in the vegetation was observed in all the years considered in the study. However, there was temporal variation in the vegetation. Vegetation masks for the years 2015 and 2017 show a decrease in the area of vegetation compared to other years. These maps show three distinct features of the delta, viz. mangroves (on south along seashore), irrigated vegetation in the mid and north of the delta and vast barren lands in between these two features.

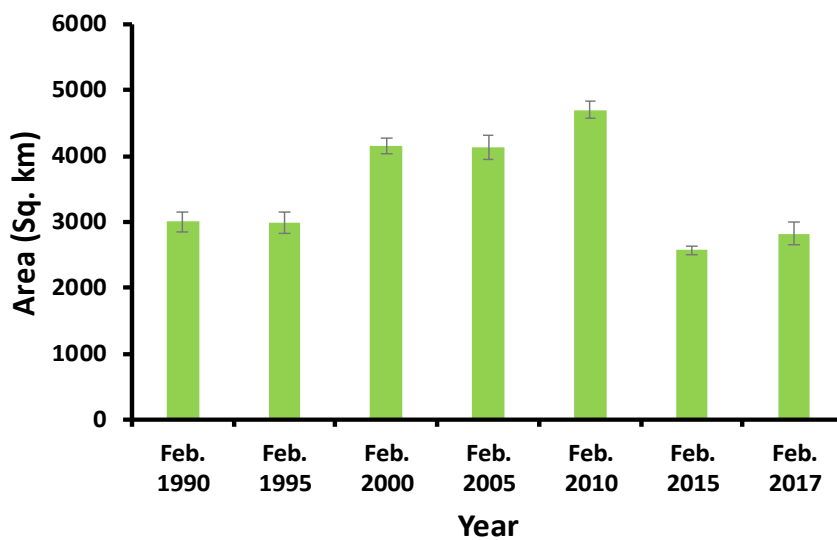


**Fig. 3.1: Area under vegetation from 1990 to 2017**

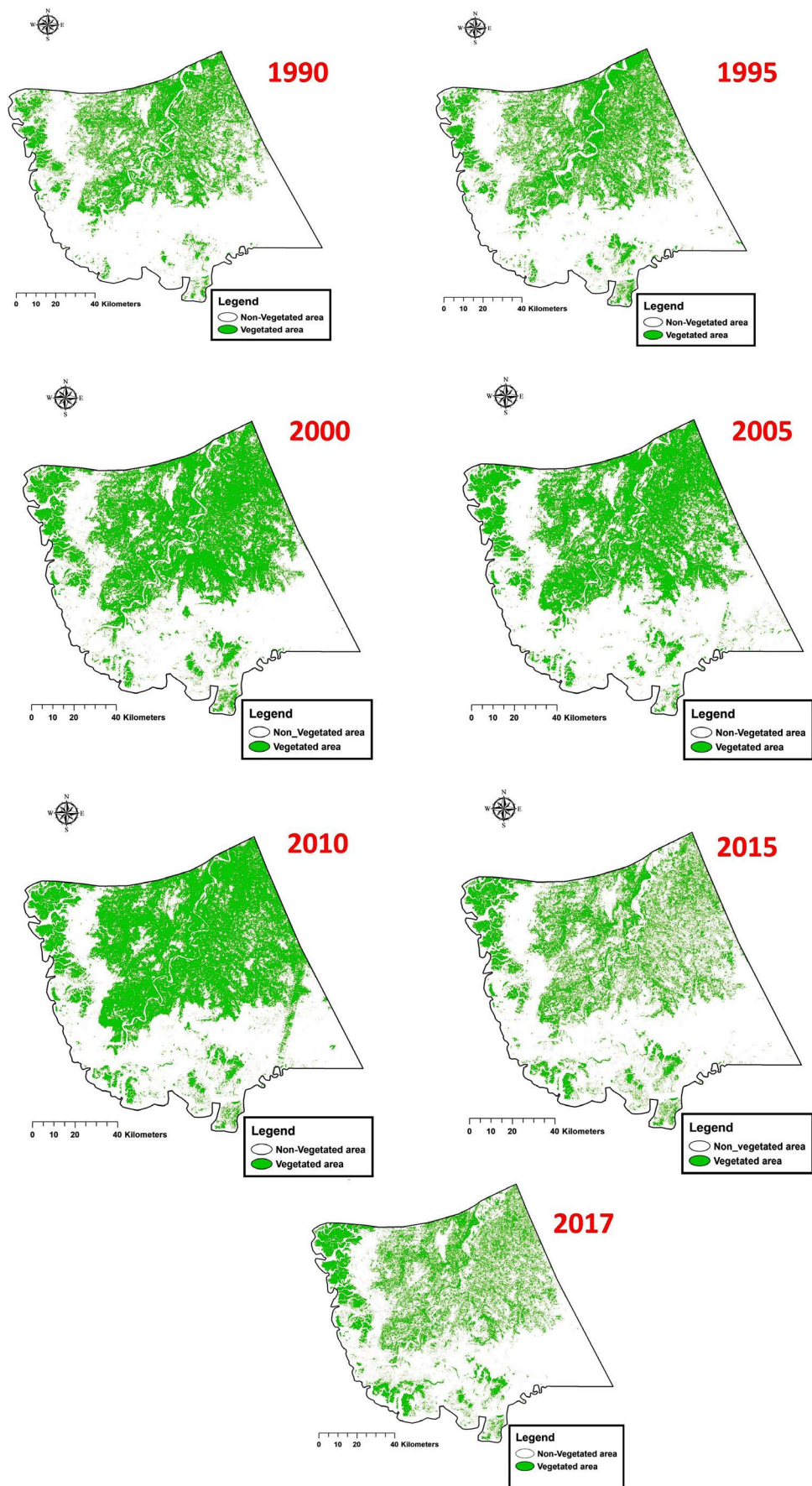


**Fig. 3.2: Vegetation masks for the last 28 years (1990-2017)**

### 3.1.2 NDVI

The temporal variation in the NDVI of the Indus delta from 1990 to 2017 is portrayed in Fig. 3.3. It shows that the highest NDVI of 0.725 was for the year 2005 followed by the year 2010 with NDVI of 0.712; while the lowest NDVI (-0.328) is for the year 2017. These NDVI values correspond with Fig. 3.1 which shows the temporal change in the area under vegetation of the delta. The green color in Fig. 3.3 depicts the positive values with lush green vegetation while brown color represents water and barren land with negative values of NDVI.

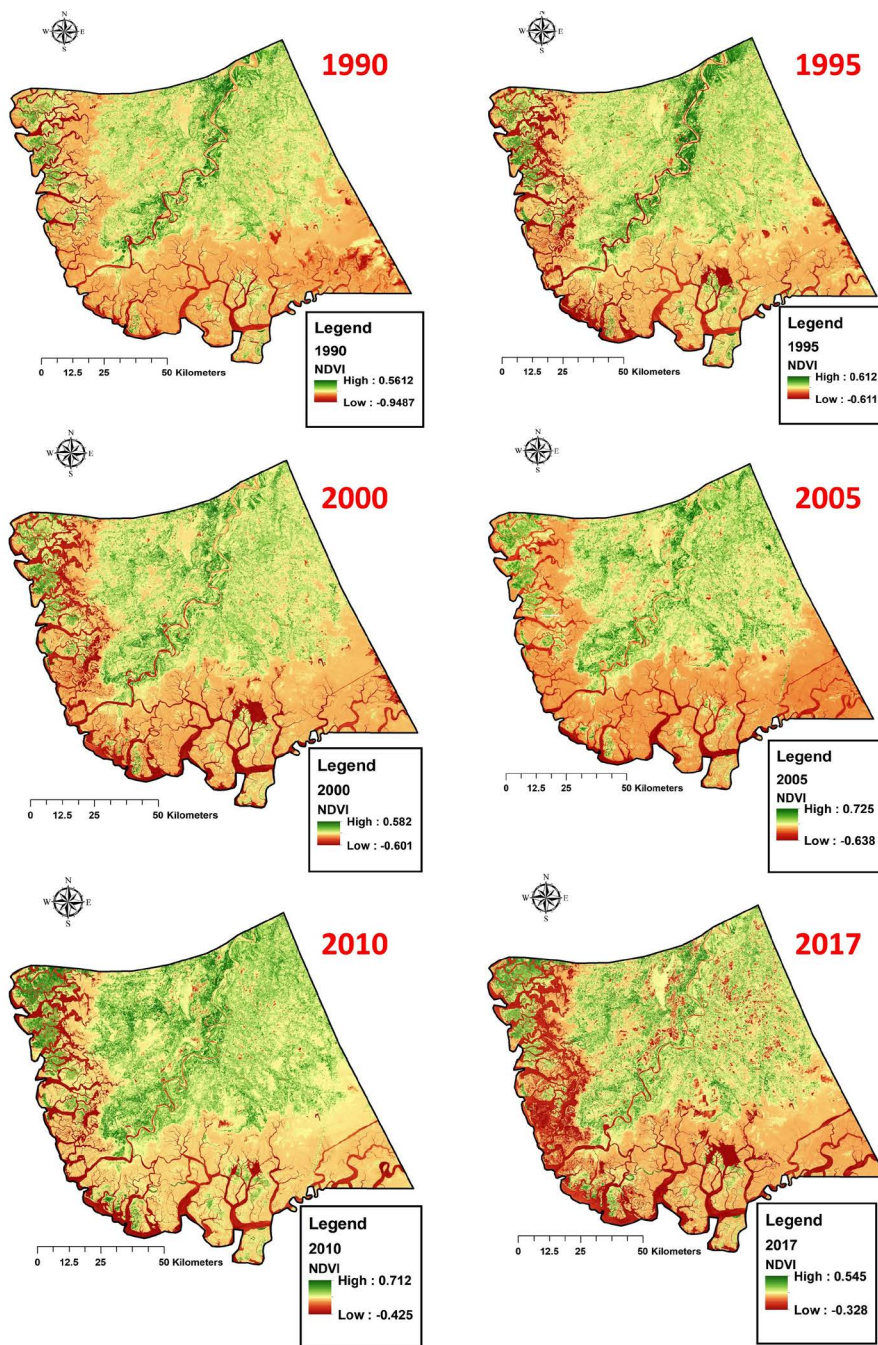


Fig. 3.3: Variation in NDVI for the last 28 years (1990-2017)

Based on the wheat crop yield data (obtained from Crop Reporting Services (CRS), Sindh) of the delta for different years, a statistical relationship between the yield and NDVI of the delta was developed as shown in Fig. 3.4 It shows a linear and positive relationship between the two variables, and it is described by the regression equation 3.1.

$$\text{Yield (wheat)} = 3.241x \text{ NDVI} - 0.3123 \quad (3.1)$$

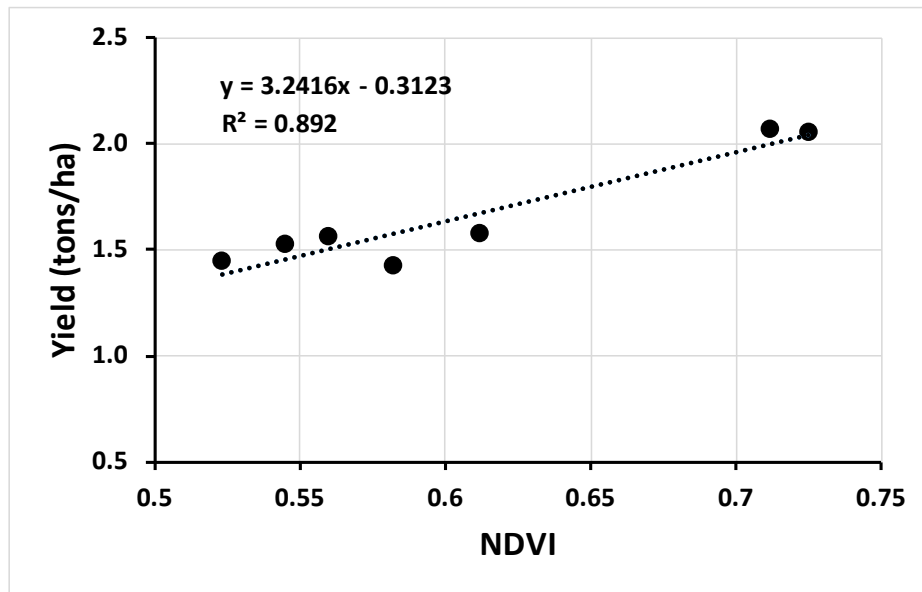
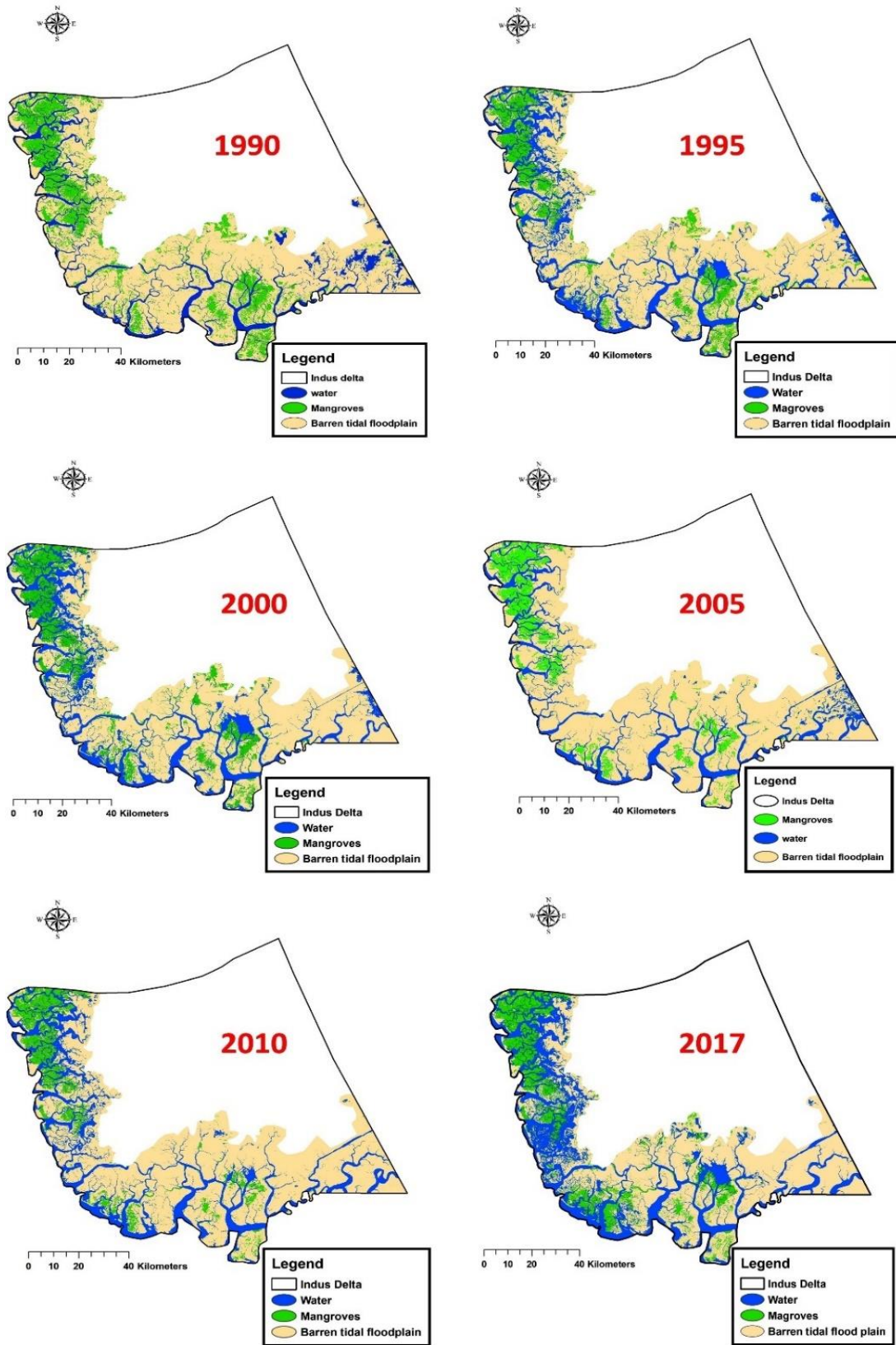


Fig. 3.4: Relationship between NDVI and the wheat crop yield

### 3.1.3 Mangroves

Fig. 3.5 shows the classified satellite images which portray temporal and spatial variation in mangrove cover in Indus delta from 1990 to 2017. These images depict that mangrove forests occupy more area of tidal floodplains on the right bank of the river Indus compared to the area under mangrove cover on the left bank of the Indus. The temporal change in area under mangrove cover during the last 28 years is quantified in Table 3.2. It shows that the area covered with mangrove forests was 103414 ha or 16% of tidal floodplains during 1990 which slowly decreased to 63296 ha or 9.81% of tidal floodplains in 2005 which again increased to 81324 ha or 12.6% of tidal floodplains in 2017. The increase in forest cover in 2017 might be due to massive mangrove plantation on vast tidal floodplains by NGOs, Forest Department, Government of Sindh and Civil Society in 2009 and 2013 (Rehman *et al.*, 2015; Daily Times, 2018).



**Fig. 3.5: Spatial and temporal variation in mangrove cover in tidal floodplains of Indus delta during the last 28 years (1990-2017)**

**Table 3.2: Area under mangrove cover during the last 28 years (1990-2017)**

Year	Area (ha)	Percentage of delta	Percentage of tidal floodplains
1990	103414	7.91	16.03
1995	82059	6.28	12.72
2000	80267	6.14	12.44
2005	63296	4.84	9.81
2010	65057	4.98	10.08
2017	81324	6.22	12.60

\*Delta area = 1306700 ha

The satellite image of 2017 was further classified into dense and sparse forests of mangroves, and the spatial variation in mangrove cover is shown in Fig. 3.6. It portrays that sparse mangrove forests are more on tidal floodplains located on left bank of the Indus while dense forests are mostly concentrated in the south-west of the delta on the right bank of the Indus.

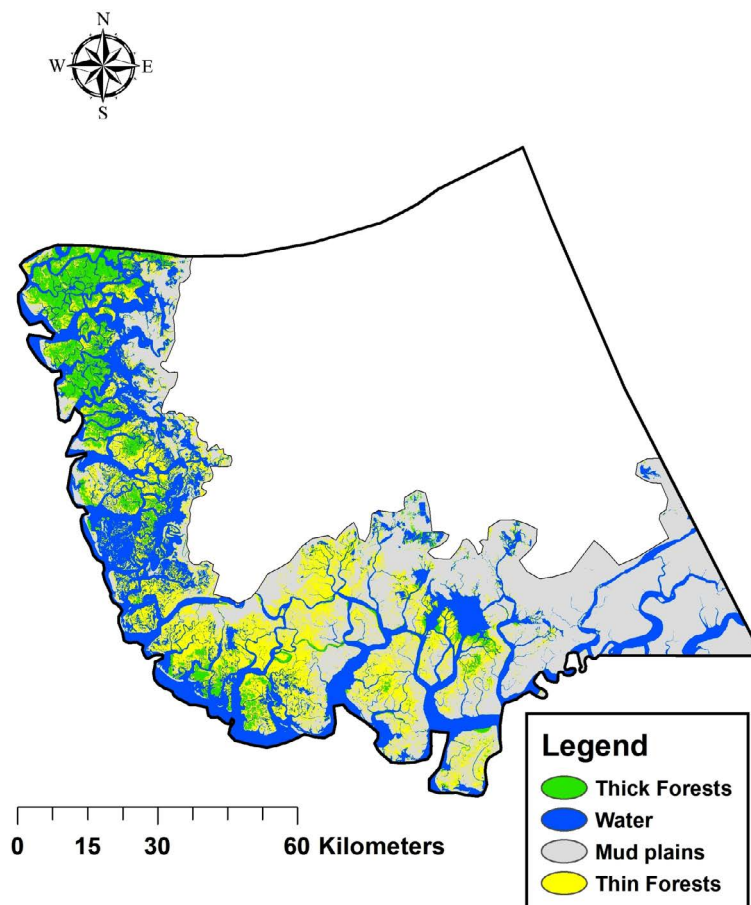


**Fig. 3.6: Spatial variation in mangrove cover in the tidal floodplains of Indus delta during Feb. 2017**

The percentage of the tidal floodplain area under dense and sparse mangrove forests, water, and barren floodplain during February 2017 is portrayed in the pie chart shown in Fig. 3.7. It depicts that nearly 60% of the tidal floodplain is barren while about 31.5% is under water. Dense mangrove forests cover only 36245 ha or 5.6% while sparse forests are on 45079 ha or 7.0% of the tidal floodplains. Thus, mangrove forests occupied only 12.6% of the total tidal floodplains or about 6.2% of the Indus delta.

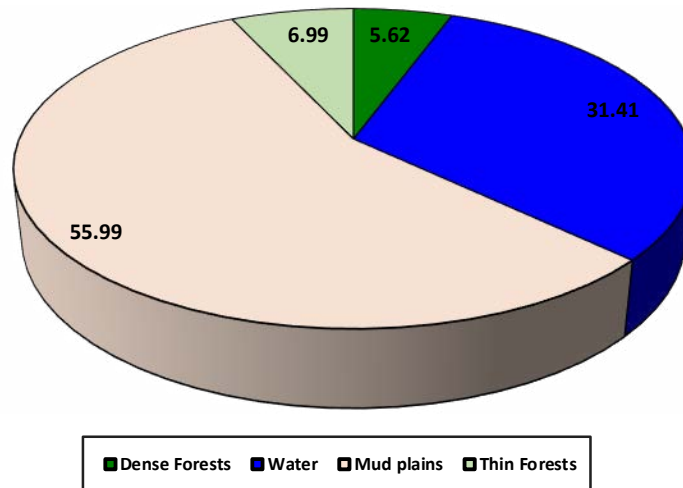


**Fig. 3.7: Percentage of tidal floodplains of the Indus delta under dense and sparse mangrove forests, water and barren floodplains (Feb. 2017)**

## 3.2 Temporal Variation in Land Surface Temperature (LST) and its Effect on the Flora of the Delta

### 3.2.1 Land surface temperature (LST)

The land surface temperature (LST) is an important factor controlling most physical, chemical and biological processes in the earth. Knowledge of the LST is necessary for many environmental studies and management activities of the earth surface resources. The LST results from energy exchange at the surface, and satellite-based monitoring can be regarded as an important prerequisite of regional or global observations of surface water, energy and radiation budgets. The LST is used as an indicator of climate change, hydrological cycle, evapotranspiration, urban climate, vegetation monitoring, environmental studies and others (Rehman *et al.*, 2015). In the present study, LST is measured from Landsat data, and it is linked with vegetation of the Indus delta.

The spatial and temporal variation in LST of the Indus delta during the month of February (1990-2017) is shown in Fig. 3.8 It shows that areas with water and vegetation have lower LST compared to towns and barren land. The temporal change in LST is more prominent in the south-east of delta (near Sir Creek) - may be because of change in hydrological features of the area due to the construction of Tidal Link Canal in the late 1990s. The area under temperature above 30 °C increased temporally from 511 ha in 1990 to 115304 ha in 2017 (Fig. 3.9) which confirms the temporal increase in LST in the delta as also reported by Rehman *et al.* (2015). Thus, the area of the delta having LST above 30 °C has increased more than 225 times in the last 27 years. Several factors may contribute to a temporal increase in LST, such as vegetation, surface water bodies, the increase in residential areas and overall global climate change.



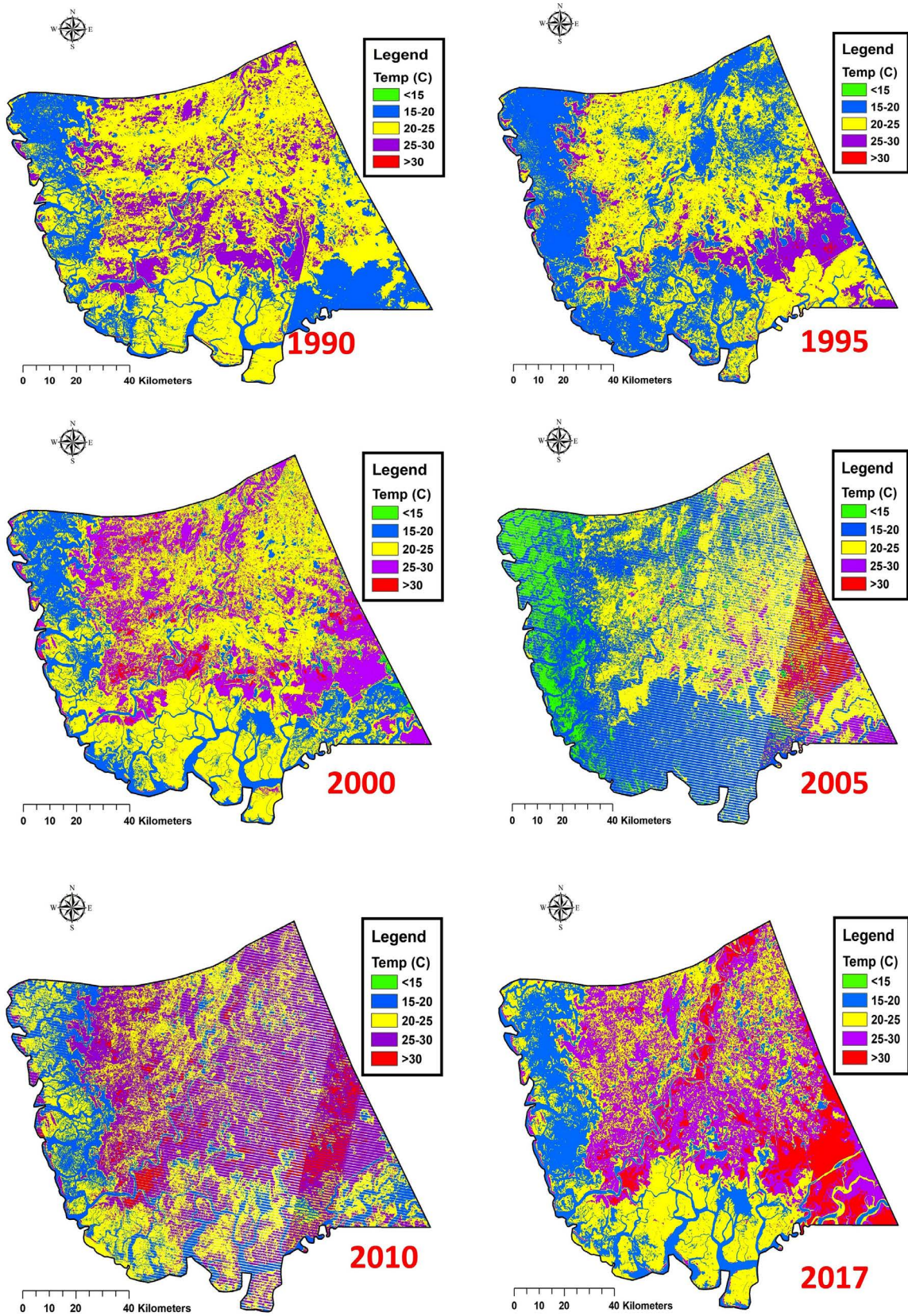


**Fig. 3.8: Spatial and temporal variation in the Land Surface Temperature (LST)**

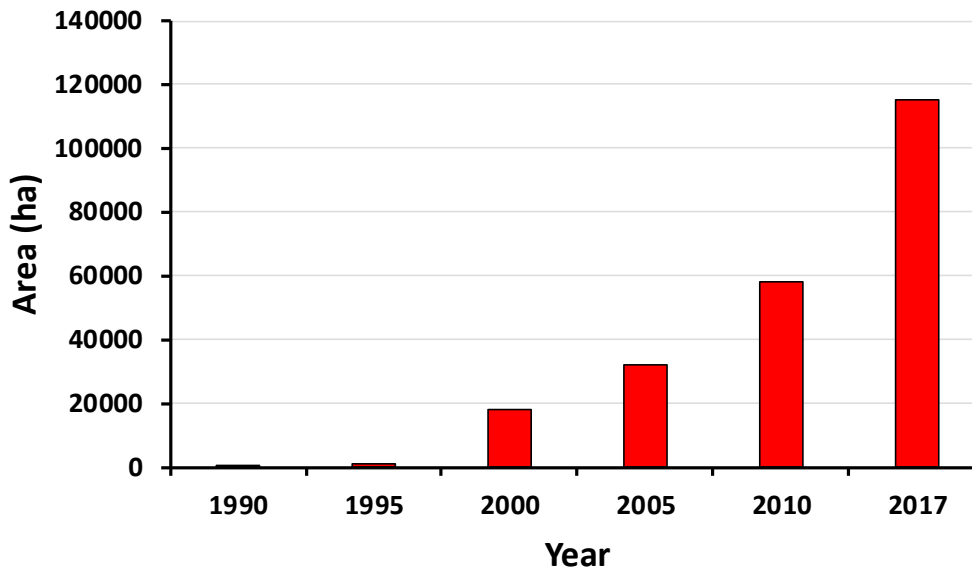


**Fig. 3.9: Temporal change in the area having LST more than 30 °C**

On average, there was an increase of 1.74 °C in LST of the Indus delta in the last 28 years (Table 3.3). It might be due to the current climate change scenario in Pakistan.

**Table 3.3: Temporal variation in the area of delta under different temperature ranges**

Temp (C)	1990		1995		2000		2005		2010		2017	
	Area (ha)	% of Delta	Area (ha)	% of Delta	Area (ha)	% of Delta	Area (ha)	% of Delta	Area (ha)	% of Delta	Area (ha)	% of Delta
<15	570	0.04	0	0.00	3228	0.25	123948	9.49	4	0.00	52	0.00
15-20	319627	24.46	523634	40.07	284694	21.79	601129	46.00	254956	19.51	272896	20.88
20-25	771611	59.05	631326	48.31	695205	53.20	455857	34.89	459033	35.13	525128	40.19
25-30	214390	16.41	150589	11.52	305309	23.36	85484	6.54	523691	40.08	393385	30.11
>30	511	0.04	1168	0.09	18281	1.40	31873	2.44	58343	4.46	115304	8.82
<b>Total</b>	<b>1306710</b>	<b>100.00</b>	<b>1306716.6</b>	<b>100.00</b>	<b>1306717</b>	<b>100.00</b>	<b>1298291</b>	<b>99.36</b>	<b>1296027</b>	<b>99.18</b>	<b>1306765</b>	<b>100.00</b>
Mean Temperature	22.10		21.08		22.70		20.04		23.99		23.84	

The impact of LST on the vegetation of the delta was evaluated by developing a relationship between LST and NDVI in Fig. 3.10. It shows that there was a fair but negative statistical correlation between NDVI and the LST with a coefficient determination ( $R^2$ ) = 0.65 and described by the equation 3.2. Thus, with an increase in LST of the delta, NDVI of the delta decreased as also reported by Yue *et al.* (2007); Huang and Ye (2015); Dong *et al.* (2018).

$$\text{LST (}^\circ\text{C)} = -19.034 \times \text{NDVI} + 34.14 \quad (3.2)$$

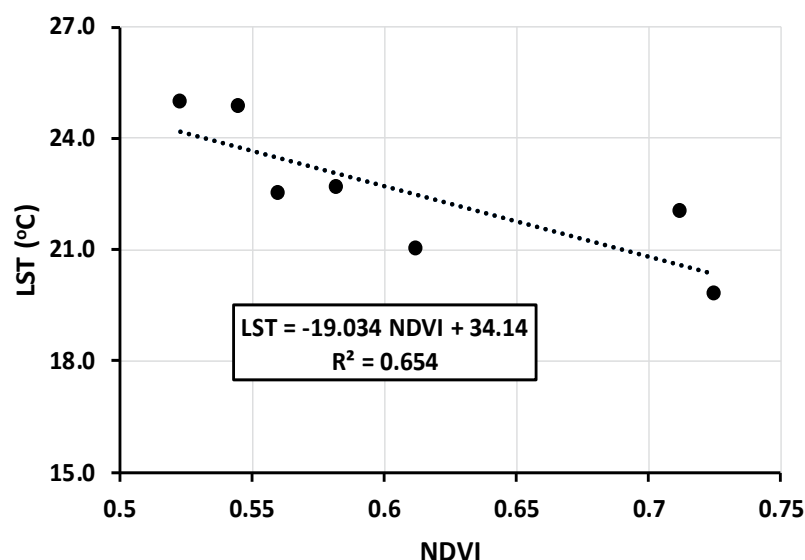


**Fig. 3.10: Relationship between NDVI and LST of Indus Delta**

### 3.2.2 Climate change and Pakistan

Climate change is an established fact affecting food, fresh water, agriculture, natural ecosystems, health, biodiversity and socioeconomic sectors around the globe (Rasul *et al.*, 2012). The increase in the global temperature was recorded as 0.76 °C during last century but in the first decade of 21<sup>st</sup> century 0.6 °C rise has been noticed (Van Vuuren *et al.*, 2008; Rasul *et al.*, 2012). Pakistan is vulnerable to climate change because of its location in a geographical region where the temperature increases are expected to be higher than the global average (Allison, 2009; Rasul *et al.*, 2012). Being in the arid and semi-arid region, it largely depends on the river irrigation system which is mainly fed by the Hindu Kush-Karakoram-Himalayan (HKH) glaciers which are reportedly melting rapidly due to global warming. Thus, the country will face risks of variability in monsoon rains, floods, and extended droughts.

Sindh, being the lowest riparian of Indus River System, is going to be affected more due to the impact of climate change. Decrease in water availability due to insufficient flow below Kotri barrage and the global rise in sea level will severely affect the Indus delta and its flora, fauna, environment and socio-economic conditions of the people living in Delta. Thus, quantifying the alteration in climatic factors such as temperature and rainfall in the Delta will be supportive in creating awareness about these impacts and resilience among the local communities will reduce the misery and getting people prepared for combating the calamity.

### 3.2.3 WorldClim data

The spatial and temporal variations in mean monthly temperatures of Indus delta from 1960 to 1990 are presented in Fig. 3.11. It shows that areas along the Arabian sea coast are 1 to 2 °C warmer than rest of the delta during winter while they are 1 to 3 °C colder during spring, summer, and autumn. It is because of the impact of closeness to the sea which remains warmer than land during the winter while it is colder compared to land during the rest of the months. The mean minimum temperature was 17.9 °C recorded in the month of January while the maximum mean temperature was 33.3 °C recorded in the month of June.

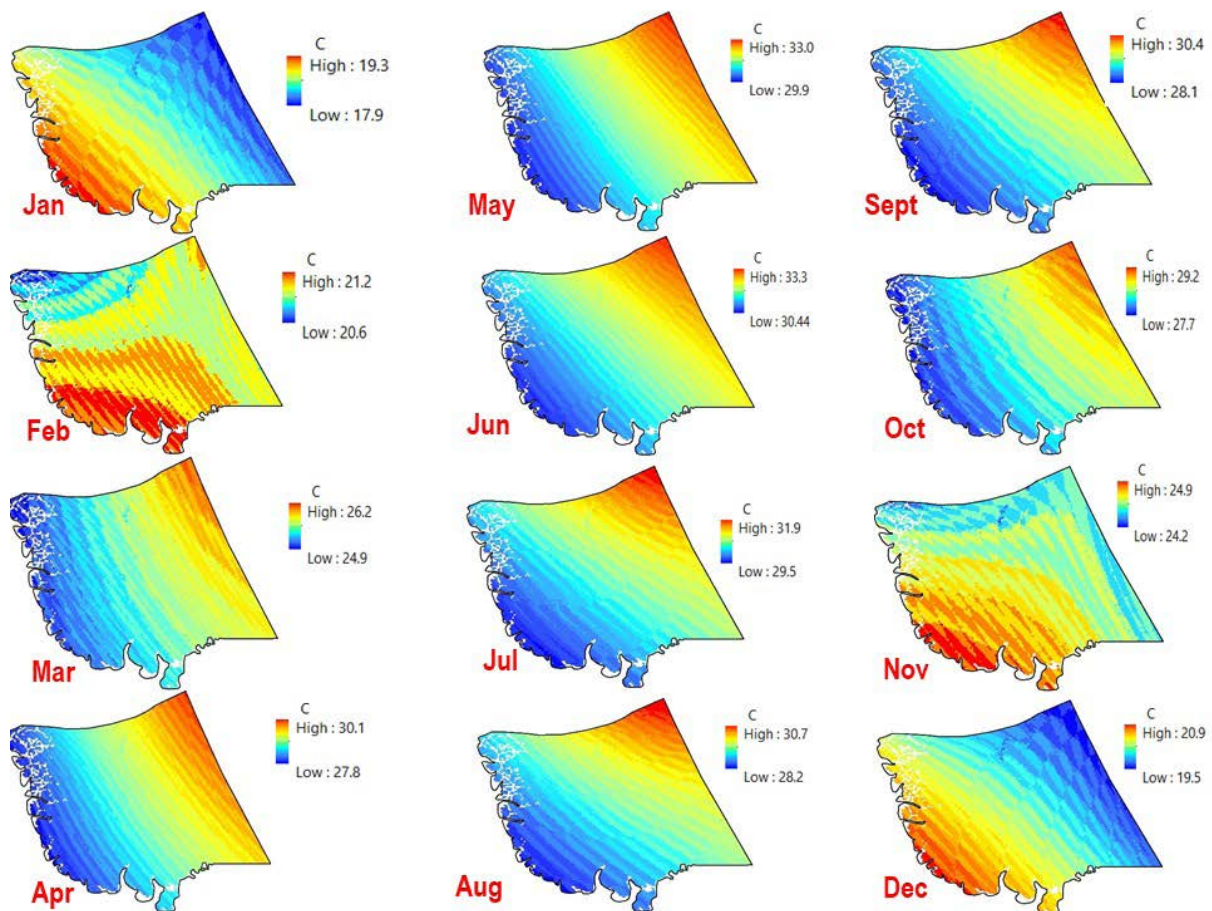


**Fig. 3.11: Spatial and temporal variation in mean monthly temperature of Indus delta (1960-1990)**

Fig. 3.12 shows spatial and temporal variation in mean monthly rainfall in Indus delta from 1960 to 1990. It depicts that the maximum rainfall in the delta occurred during July, August and September with mean maximum rainfall of 131 mm, 85 mm and 77 mm, respectively. While minimum mean rainfall of 0 to 7 mm was observed during November, December, January, February, March, April, May and October; rainfall was higher in the south-west during winter while it is higher in the south-east during monsoon.

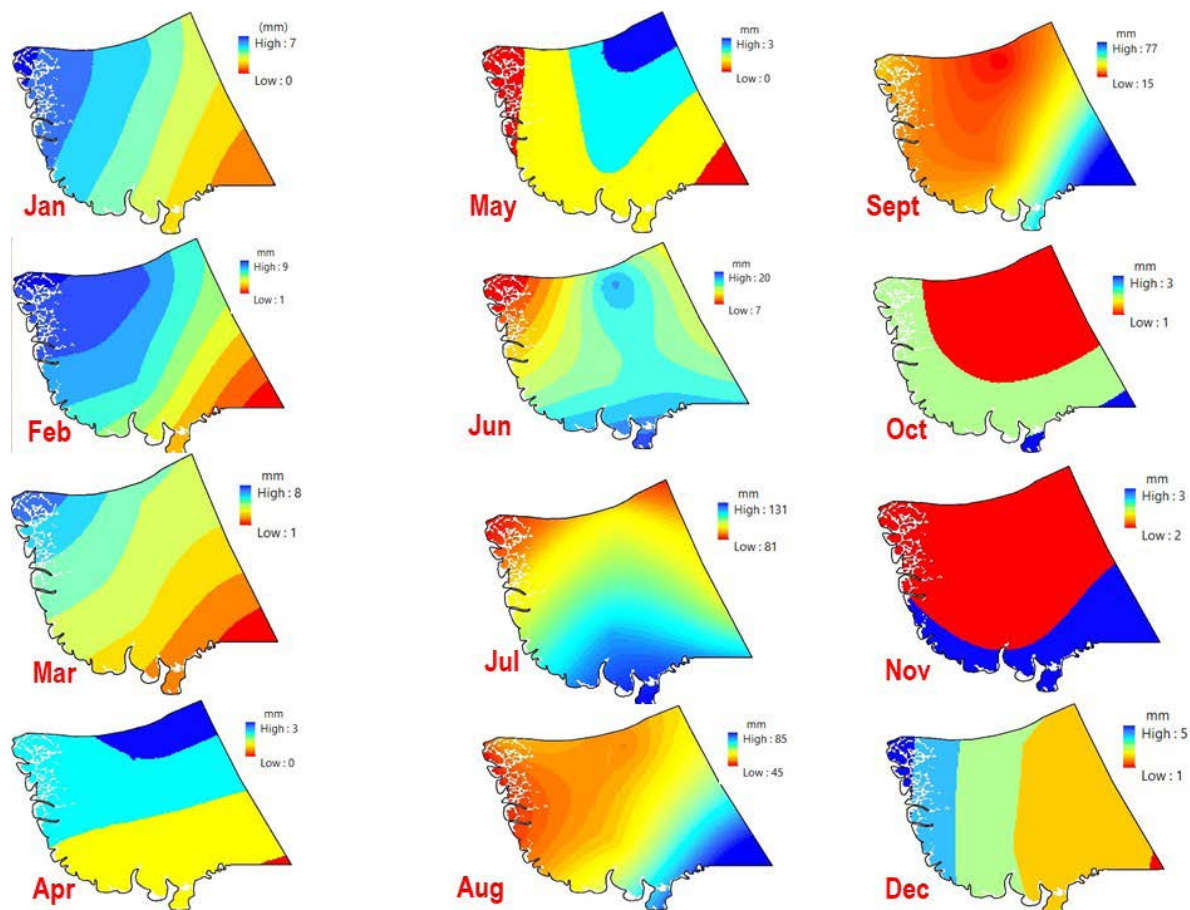


**Fig. 3.12: Spatial and temporal variation in mean monthly temperature of Indus delta (1960-1990)**

### 3.2.4 Comparison of rainfall and temperature between 1960 to 1990 and 1991-2017

Comparison of temperature variation between two periods 1960-1990 and 1991-2017 is shown in Fig. 3.13 It depicts that mean monthly temperature of Indus delta from February to November for the period 1991-2017 is 0.6 to 0.7 °C (3 to 4%) higher compared to period 1960-1990. While the mean monthly temperature in December and January has dropped by 0.6 to 0.7 °C (3 to 4%) for the period 1991-2016 compared to the period 1960-1990. Thus, summers of the delta are getting warmer while winters are turning colder. Chaudhry (2017) also reported an increase of about 0.5 °C in annual mean temperature in Pakistan. It might be due to the impact of global climate change which has more impact on Pakistan, especially on Sindh province.

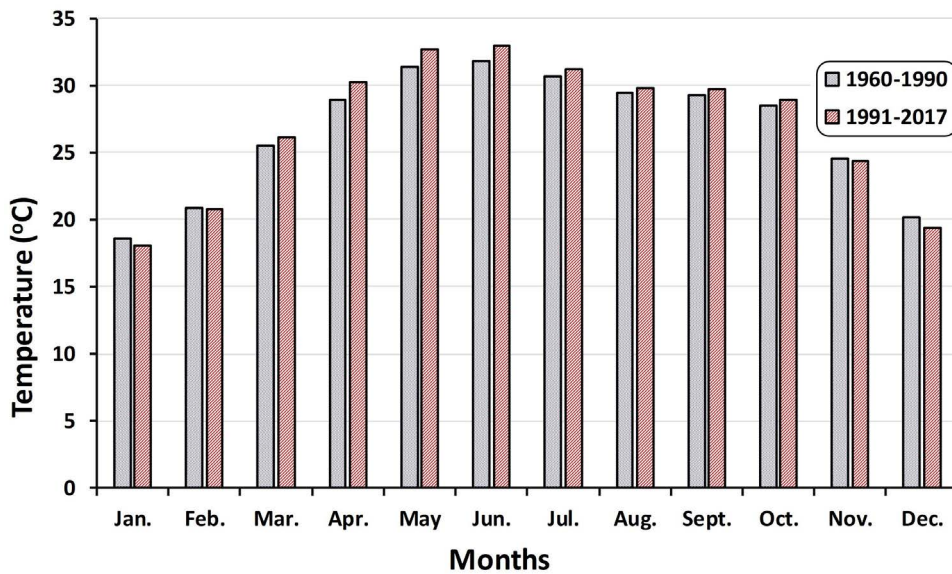


**Fig. 3.13: Comparison of the mean monthly temperature of Indus Delta between the periods 1960-1990 and 1991-2017**

Fig. 3.14 shows a comparison of mean monthly variation in rainfall between two periods 1960-1991 and 1991-2017. There is a vivid variation in the rainfall especially during monsoon months viz. from June to September. A significant decrease up to 23% in mean monthly rainfall was observed during the period 1991-2017 for June, July and August compared to the 1960-1990 period. While 100% increase in mean monthly rainfall was observed for September and October during the later period compared to 1960-1990 periods, Dyoulgerov *et al.* (2011) reported about 10-15% lower rainfall in the Indus Delta and projected that it would severely degrade the country's wetland and mangrove ecosystems.

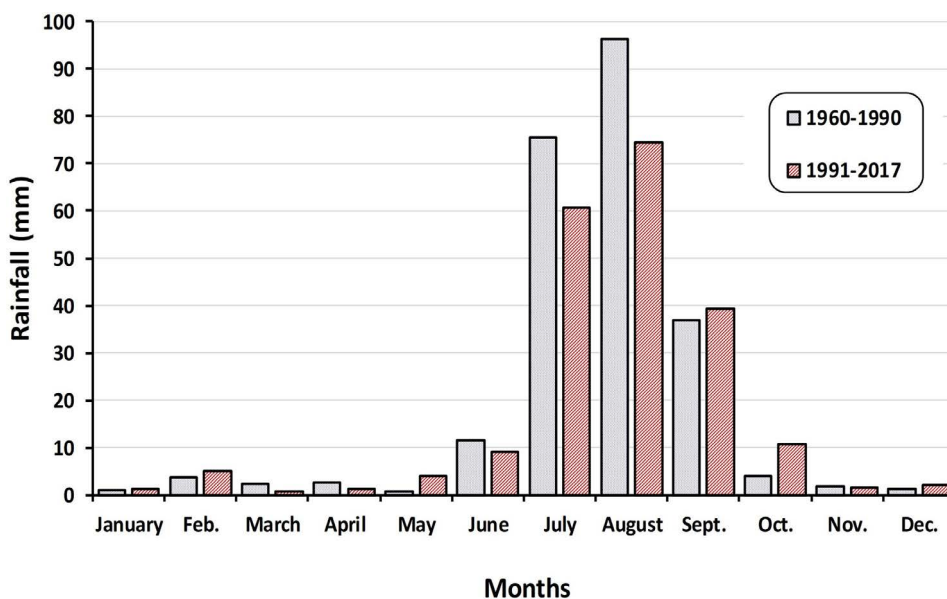


**Fig. 3.14: Comparison of mean monthly rainfall of Indus Delta between the periods 1960-1990 and 1991-2017**

### 3.2.5 River flow below Kotri barrage

The analysis of the data of annual flow below Kotri barrage in billion cubic meters (BCM) from 1937 to 2017 revealed that there was an overall decrease in flow to the extent of 80% especially after commissioning of Tarbela dam in 1976 (Fig. 3.15). As a result, there is about 90 to 400 million tons per year decline in incoming sediment to delta (Aziz and Khan, 2001; Amjad *et al.*, 2007). However, due to heavy rainfalls during the 1990's and availability of water, river flow below Kotri barrage increased. Overall there is a decreasing trend in flow below Kotri Barrage after the construction of the Tarbela dam.

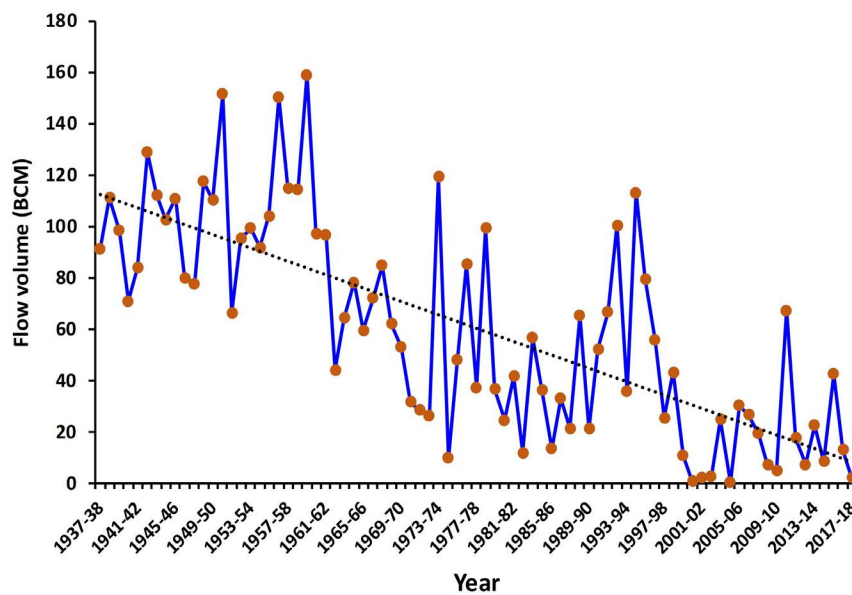


Fig. 3.15: Temporal variation in Indus river flow below Kotri barrage

The number of days with no flow below Kotri barrage has also drastically increased after 1970s and now mainly confined to monsoon period for about 60 to 80 days (Fig. 3.16).

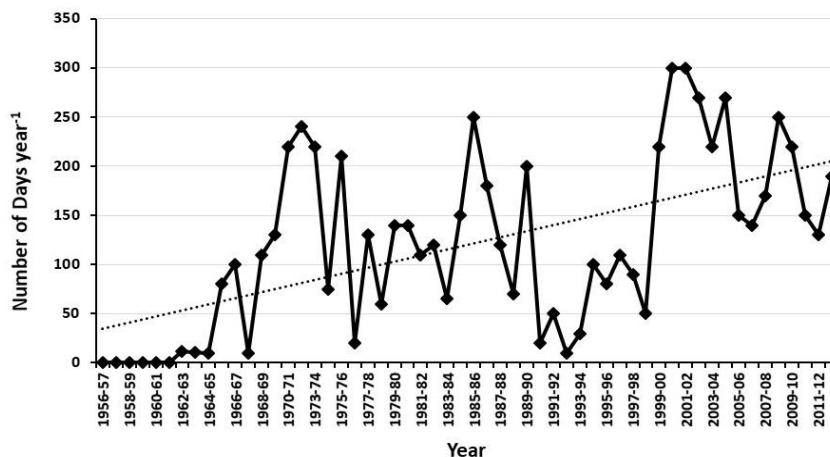


Fig. 3.16: Zero flow days below Kotri barrage downstream

## 3.3 Spatial and Temporal Variation in Soil Salinity of the Delta

### 3.3.1 Introduction

Soil salinization is the accumulation of soluble salts in the root zone resulting in the changing of normal soil into the salt-affected soil (Siyal *et al.*, 2002; Asfaw *et al.*, 2016). Soil salinity is a growing environmental hazard (Hillel, 2000) that impacts the growth of many crops. In arid and semi-arid regions of the world, soil salinization is the most common land degradation process (Asfaw *et al.*, 2016). Estimates reveal that about one-third of the irrigated land in the world is severely affected by soil salinity problem (Abbas and Khan, 2007). The soluble salts affect the physical, chemical, and biological properties of the soil.

In coastal areas, soil salinization is a common and serious problem affecting crop cultivation and ecology of the delta (Yu *et al.*, 2014). Indus Delta being near the Arabian sea is threatened with an increased level of seawater. Hence massive agricultural lands have either simply become part of the sea or changed into salt affected with salts visible on the surface of the agricultural lands and hence are not suitable for agricultural practices. Mapping of soil salinity using GIS and Remote sensing with different vegetation and salinity indices provide a simple and easy way of knowing how much damage has occurred due to soil salinity. The outcome of the present study will certainly provide a sound foundation for policymakers, analysts, and researchers to devise a strategic action plan for the mitigation of salinity hazard in the delta. An articulation of land reclamation measures will not only be constructive and favorable for the ecosystem but also will revamp the socio-economic conditions of the local communities.

### 3.3.2 Soil texture

Fig. 3.17 shows the spatial variation in soil texture of the top 0-20 cm layer in the Indus delta. It reflects that loam (37.78%) and clay loam (22.22%) are dominant textural classes in the topsoil layer of the Indus delta while 14.07% soil samples had clay, 8.89% had silty clay, 7.41% had silty clay loam, 5.93% had silty loam. While 2.22% had sandy clay loam and 10% soil samples had lighter texture. The lower soil layers (20-40 and 40-60 cm) had nearly similar soil texture distribution pattern. Thus, the delta is dominated with soils having fine textural class. It might be because of the location of the Indus delta at the tail end of the river Indus. The coarse-textured sediment is deposited in upper regions while the river brings sediment dominated



with fine particles at the tail end, i.e., Indus delta. In a report FFC (2005) revealed that particle size distribution of suspended sediment in river Indus below Kotri on average contains 5.0% sand, 49.6% clay and 45.4% silt; hence the alluvial soils of the delta are predominantly fine-textured soils.

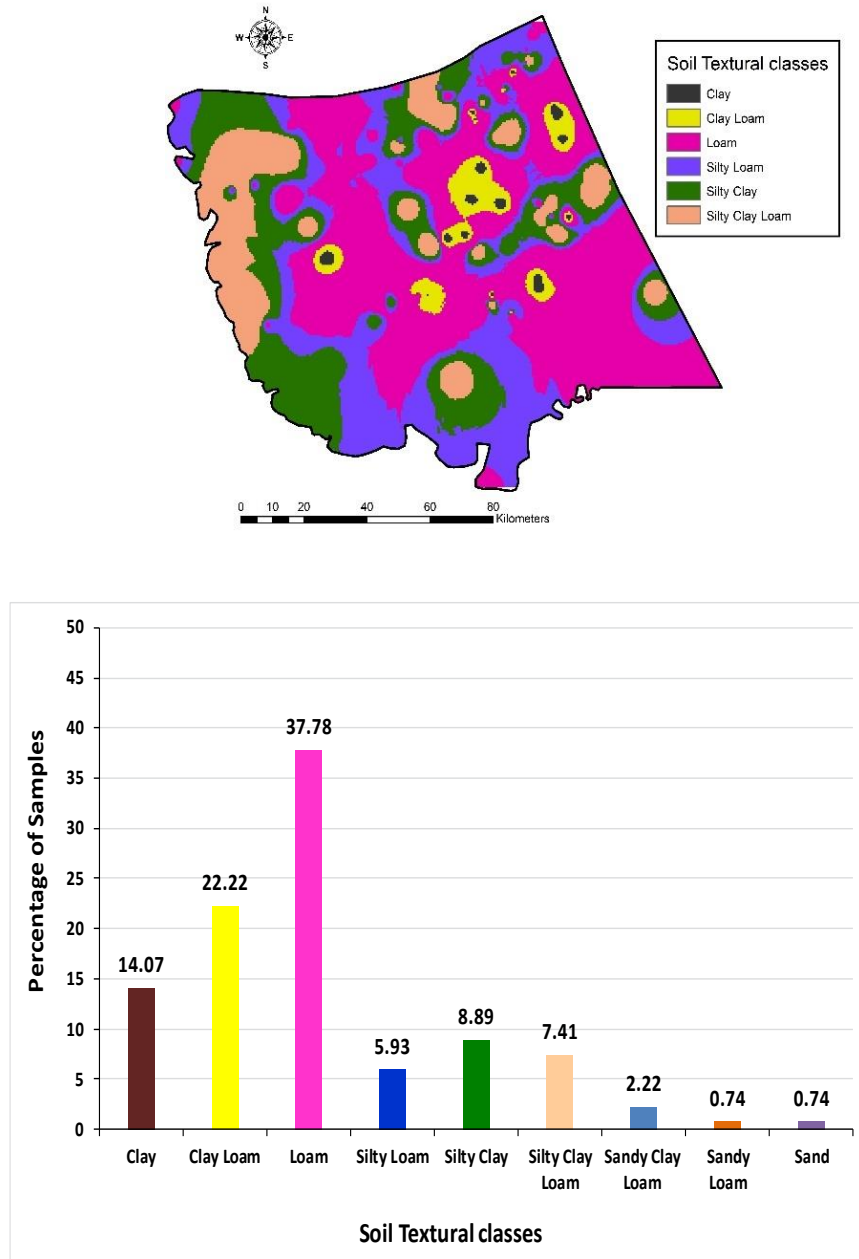


**Fig. 3.17: Spatial variation in soil texture of the top 0-20 cm layer in the Indus delta (top) and the percent of samples with different soil textures (bottom)**

### 3.3.3 Soil density

In the study area, the dry density of soil at 0-20 cm soil depth varied from 1.20 to 1.40 g/cm<sup>3</sup> with an average value of 1.30±0.05 g/cm<sup>3</sup>. At 20-40 cm, dry density varied from 1.19 to 1.44 g/cm<sup>3</sup> with an average value of 1.27±0.04 g/cm<sup>3</sup>, while the corresponding values at 40-60 cm varied from 1.17 to 1.40 g/cm<sup>3</sup> with an average value of 1.26±0.02 g/cm<sup>3</sup>. Spatial distribution of dry density at different soil depths is shown in Fig. 3.18.

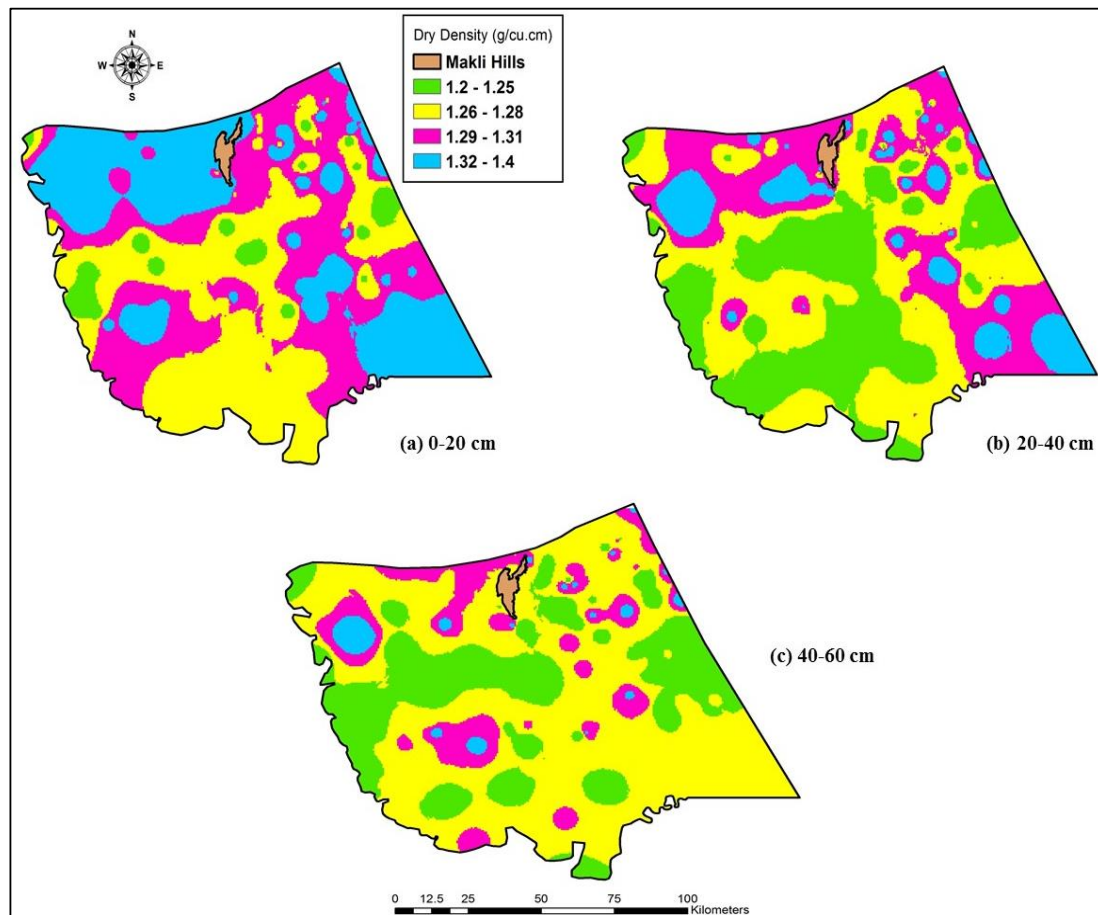


**Fig. 3.18: The spatial distribution of dry density at various soil depths**

### 3.3.4 Electrical conductivity (EC)

Electrical conductivity (EC) of soil saturation extract of soil samples taken from 0-20 cm soil depth varied between 0.45 to 55.2 dS/m with an average of 14.28±2.4 dS/m while at 20-40 cm soil depth it fluctuated between 0.56 to 48.8 dS/m with an average of 11.52±2.1 dS/m (Fig. 3.19). Similarly, EC of bottom soil layer (40-60 cm) varied between 0.7 to 36.3 dS/m with an average of 9.6±1.7 dS/m. Thus, there was decreasing EC of soil with increasing soil depth (0-60 cm). The higher values of EC in the topsoil are due to the migration of salts from lower soil layers with the capillary movement of water in the top layer where the water evaporates leaving salts on the surface.

In the upper soil layer, 66.4% of the soil samples had EC values greater than the safe limit of 4 dS/m, hence lying in the category of salt-affected soils. Whereas, about 56.8% of soil samples in the bottom layer had EC values beyond the permissible range of 4 dS/m. The spatial distribution of EC at various soil depths is shown in Fig. 3.20.

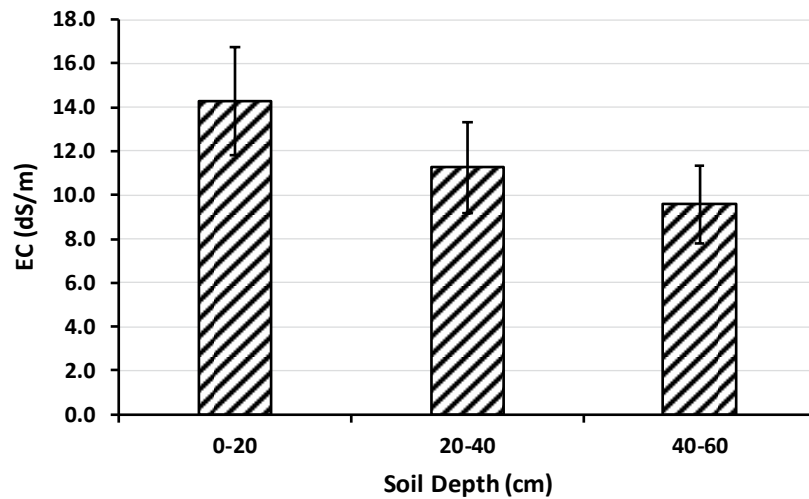


**Fig. 3.19: Depth-wise variation in average EC of the soil profile. Error bars represent the 95% Confidence Interval in data**

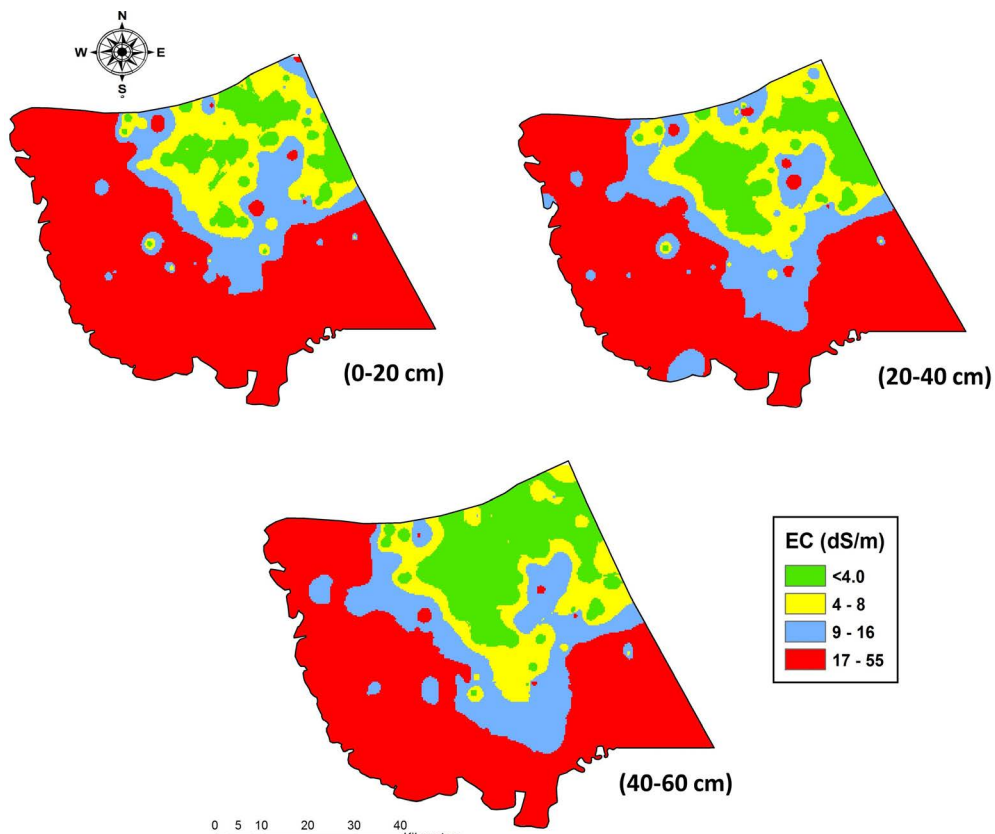


**Fig. 3.20: Interpolated spatial distribution maps of EC at various soil depths in the Indus delta**

### 3.3.5 Soil pH

The hydrogen ion concentration (pH) of saturation extract of soil samples taken from 0-20 cm soil depth fluctuated between 6.8 and 11.42 with an average value of 8.62. A general decline in average pH values was noticed at the said depths below 20 cm, the values being 7.99 and 8.01 at 20-40 cm and 40-60 cm, respectively. Generally, the soils having pH value greater than 8.5 are considered as sodic soils. The pH of soil samples collected along tidal floodplains had higher pH values (Fig. 3.21).

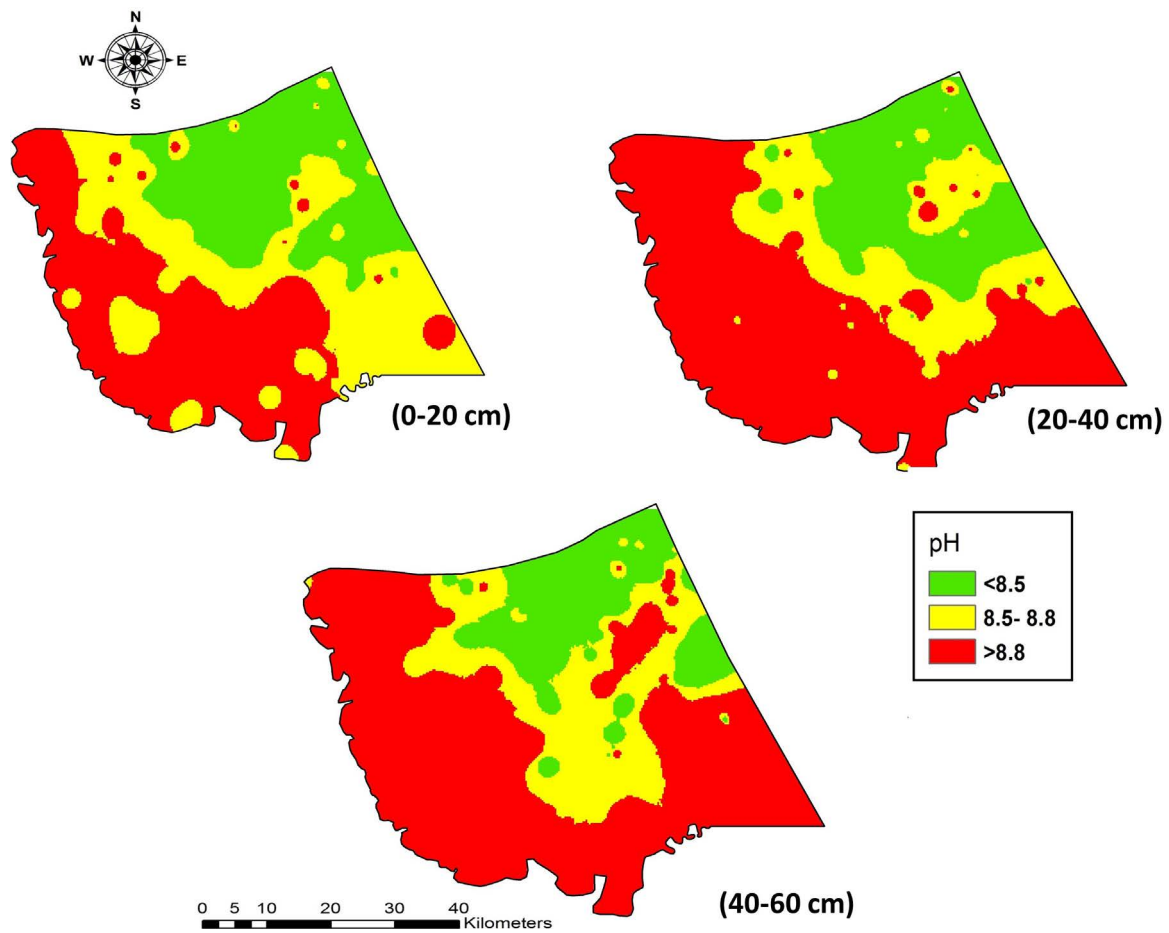


**Fig. 3.21: Interpolated spatial distribution maps of pH at various soil depths in the Indus Delta**

### 3.3.6 Soil exchangeable sodium percentage (ESP)

In the study area, exchangeable sodium percentage (ESP) in 0-20 cm soil depth ranged from 1.37 to 65 with an average of  $25.2 \pm 2.6$ . In 20-40 cm soil depth, the ESP values ranged from 5 to 65 with an average of  $26.6 \pm 2.4$ . However, about 50% samples had ESP values greater than the safe limit of 15. The exchangeable sodium percentage (ESP) values in 40-60 cm soil depth ranged from 3.6 to 65 with an average of  $27.1 \pm 2.5$ . About 40%

of the samples soil had ESP values greater than the threshold value of 15. Fig. 3.22 shows the spatial distribution of ESP for 0-20, 20-40, and 40-60 cm soil depths.

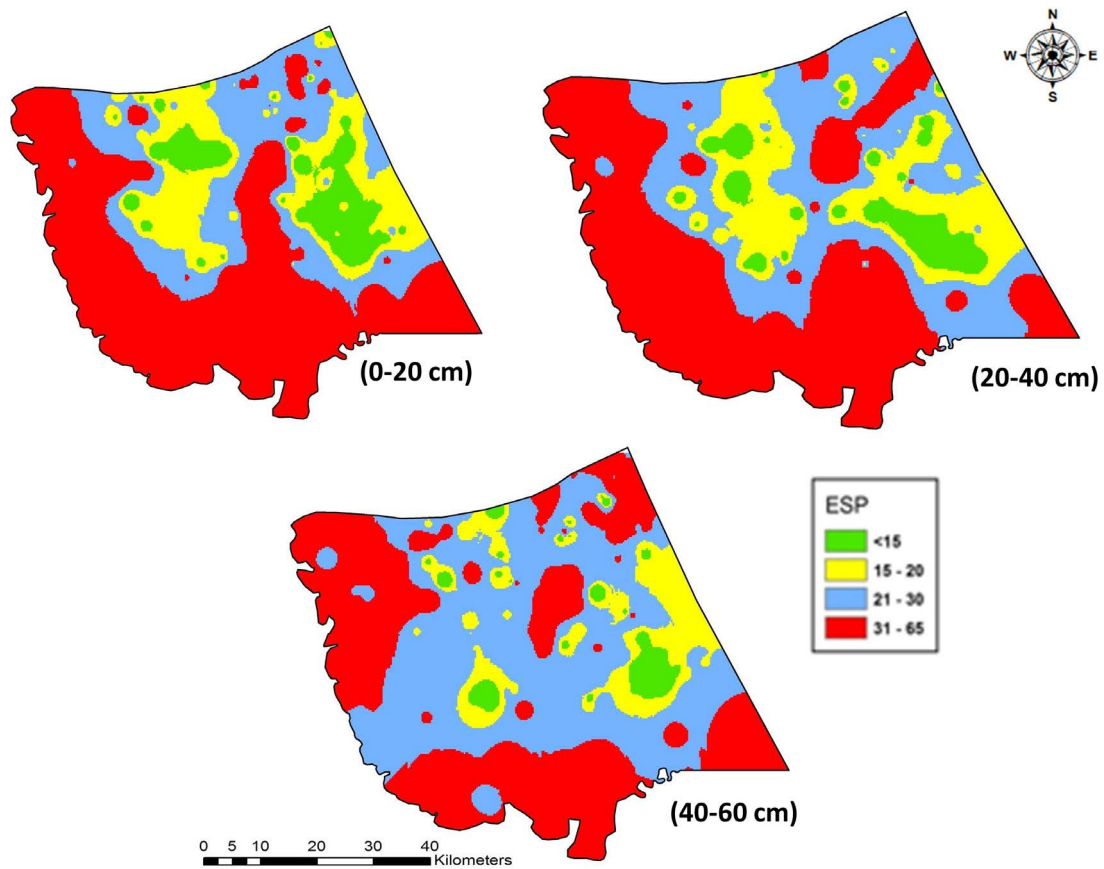


**Fig. 3.22: Interpolated spatial distribution maps of ESP at various soil depths in the Indus Delta**

### 3.3.7 Percentage of soil samples with EC, pH, and ESP beyond the permissible limits

The overall soil salinity presented in Fig. 3.23 shows that EC of 56 to 66% of soil samples collected from 0 to 60 cm depth was beyond the permissible limit of 4 dS/m given by FAO (1985). Similarly, pH of 14 to 17% and ESP of 72 to 79% of soil samples was beyond the permissible limit of 8.5 and 15, respectively. It depicts that sodium salts are dominant cations in these soils.

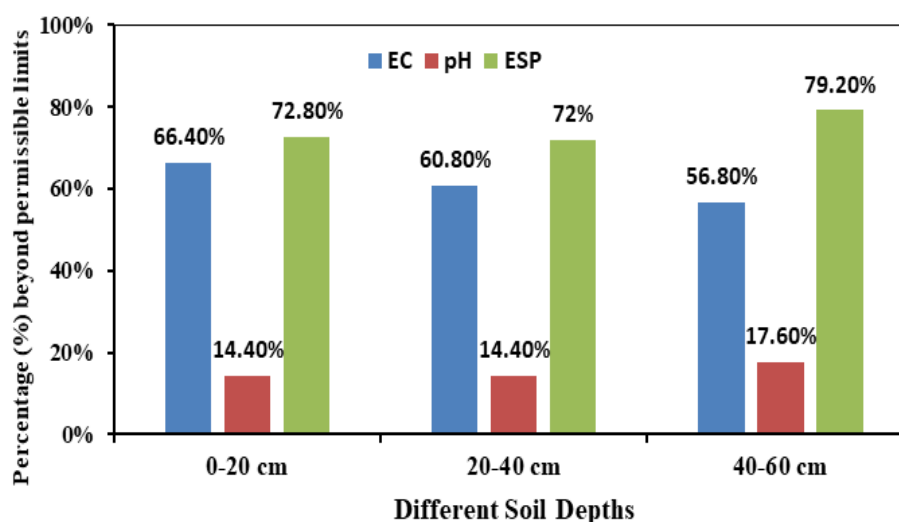


**Fig. 3.23: Percentage of samples with EC, pH, and ESP beyond the threshold values**

### 3.3.8 Spatial distribution of soil salinity

Based on ground truthing data, interpolated thematic maps for various soil salinity classes, i.e., normal, saline, sodic, and saline-sodic soils for all the three soil depths viz. 0-20 cm, 20-40 cm, and 40-60 cm were prepared (Fig. 3.24), and area under each soil class was calculated from the interpolated maps and presented in Table 3.4.

**Table 3.4: Area under each type of soil salinity (USDA, 1954)**

S. No.	Type of salt-affected soil	Area (km <sup>2</sup> ) by soil depth		
		0-20 cm	20-40 cm	40-60 cm
1	Normal	2025 (15.5%)	2836 (21.7%)	2855 (21.9%)
2	Saline	2144 (16.4%)	1590 (12.2%)	1872 (14.3%)
3	Sodic	2872 (22.0%)	2404 (18.4%)	2878 (22.1%)
4	Saline-sodic	601 (46.1%)	6225 (47.7%)	5452 (41.8%)

These data revealed that the salinity in the topsoil was higher than that in subsoil indicating that the salt in the subsoil moved up and accumulated in topsoil. Overall 46% soils were saline-sodic, 22% sodic, 16.4% saline and 15.5% were normal soils. Thus, soils of the delta were dominated with sodium salts. The interpolated spatial distribution soil salinity maps showed that there is strongest level of salinity in those samples which were taken from the coast of the Arabian sea which might be due to seawater intrusion (Fourati *et al.*, 2015).

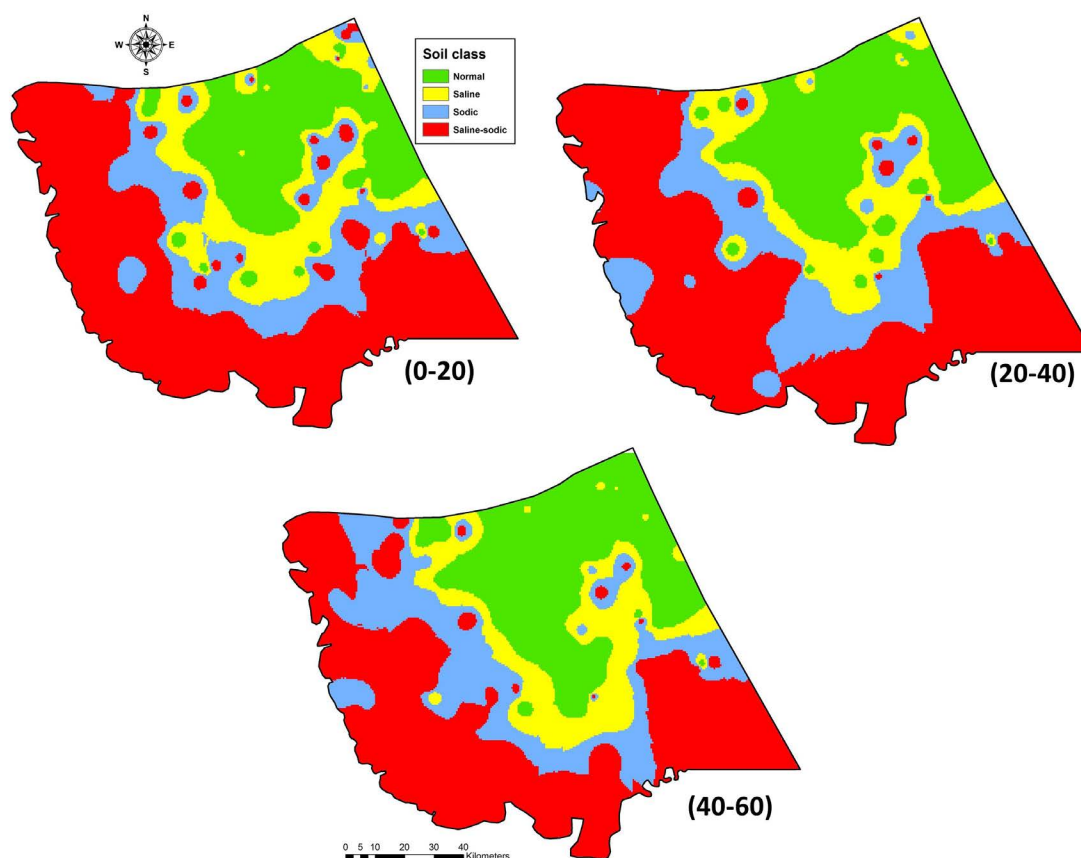


**Fig. 3.24: Interpolated maps of spatial distribution of soil salinity by soil depth, 0-20, 20-40 and 40-60 cm**

### 3.3.9 Temporal variation in soil salinity

The temporal variation in soil salinity of Indus delta in (Fig. 3.25) shows that vast area of the delta is under the grip of soil salinity especially those which are along the coastline of the delta. The area under water has increased significantly from 9% to 24% of the delta especially in the tidal floodplains during the last 45 years (1972 to 2017). Vegetation decreased from 36% to 22% while soil salinity increased from 33 to 43% of the delta. The variations in soil salinity are quantified in Table 3.5.

**Table 3.5: Temporal variation in the area under water, vegetation and soil salinity in the Indus delta**

Year	Water		Vegetation		Salt-affected		Others	
	ha	%	ha	%	ha	%	ha	%
1972	122450	9.37	467990	35.81	435600	33.34	280663	21.48
2017	318665	24.39	293115	22.43	571349	43.72	123467	9.45

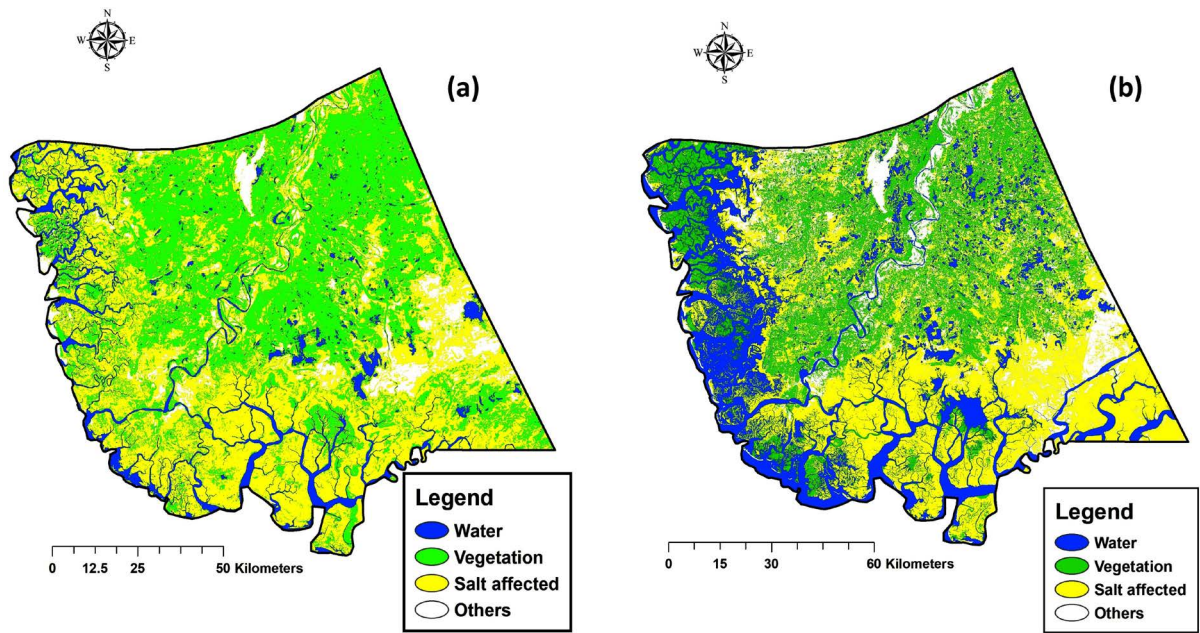


**Fig. 3.25: Temporal variation in soil salinity (a) 1972 (b) 2017**



## 3.4 Spatial Variation in Surface & Groundwater Quality in the Delta

### 3.4.1 Surface water

Freshwater is a vital resource for the existence of life and a healthy ecosystem on the planet of earth. Rivers, lakes, glaciers, and aquifers are the primary sources of fresh water. It is reported that in the Indus River delta, the groundwater is not suitable for drinking purpose (Memon *et al.*, 2011; Husain *et al.*, 2012). Hence people living in the delta usually depend on surface water to meet their domestic water demand. Natural wetlands, lakes, ponds, irrigation canals, and natural depressions are the primary sources of fresh surface water in the Indus delta. However, these freshwater resources are exposed to a variety of pollutants originating from the point and nonpoint sources such as domestic and industrial sewage and agricultural and industrial wastes which are difficult to control, evaluate, and monitor (Ahuja, 2003). The water quality of any specific area either surface or sub-surface is ascertained by the chemical, physical and biological parameters of water (Ewaid and Abed, 2017). The concentration of such parameters beyond permissible limits is hazardous for human health as well as for agricultural production. Hence, the present study was conducted to evaluate the water quality status of surface water bodies in the Indus Delta

#### 3.4.1.1 Physicochemical analysis of surface water

The summary of the physicochemical analysis of surface water bodies of the Indus Delta is presented in Table 3.6.

The turbidity of surface water fluctuated from 1.15 to 129 NTU with a mean value of  $15 \pm 6.4$  NTU. The highest turbidity of 129 NTU was observed in the surface water drain located in the union council (small administrative unit) of Kar Malik, District Sujawal. The higher levels of turbidity in water are accompanied by disease-causing bacteria (Patil *et al.*, 2012). Thirty eight percent samples had turbidity values within a safe limit and 62% samples had turbidity values higher than the safe limit of 5 NTU described by WHO for drinking purpose.

**Table 3.6: Summary of statistical analysis of various physicochemical parameters of surface water bodies**

Parameter	Unit	Min.	Max.	Mean	Standard deviation (SD)	Confidence interval (CI)
Turbidity	NTU	1.15	129	15	23.4	6.41
Electrical conductivity	dS/m	0.6	60	15	15.07	4.14
pH	---	7.62	8.64	8.0	0.28	0.08
Total dissolved Solids	mg/L	378	38272	9590	9657	2650
Calcium	mg/L	24	100	45	27.94	7.67
Magnesium	mg/L	55	305	76	79.73	21.88
Total hardness	mg/L	68	1354	368	361.91	99.33
Chloride	mg/L	440	17406	2197	3300.1	905.72
Arsenic	ppb	0	25	3.83	6.84	1.88

Electrical conductivity (EC) is the main parameter (Sivakumar *et al.*, 2011) which provides a primary indication for suitability of water for drinking and agriculture purposes (Patil *et al.*, 2012). The EC values of the samples fluctuated from 0.6 to 60 dS/m with an average value of  $15 \pm 4.14$  dS/m. The highest conductivity of 60 dS/m was observed in the surface water drain located in the southeast part of the delta. The study revealed that only one surface water lake located in the union council of Ladyoon had EC value within safe drinking water quality standards, while rest of the 49 surface water bodies had EC values beyond the drinking water quality standards (Fig 3.26). The highest EC values were observed in those water bodies which are near the Arabian sea. It might be due to the high evaporation rate, low rainfall, and intrusion of saline water from the Arabian sea into the delta. The EC is also an important indicator for assessing the suitability of water for irrigation purpose as the concentration of total salts is also estimated from EC of water (Ajayi *et al.*, 1990). According to the FAO (1985), the water having EC of less than 0.8 dS/m is considered suitable for irrigation purpose while water having EC greater than 3.0 dS/m affect the water uptake capability of most of the plants and thus decreases crop yield. From this perspective, 66% of the sampled surface water bodies had EC values higher than 3 dS/m and water could be considered unfit even for the irrigation purpose.

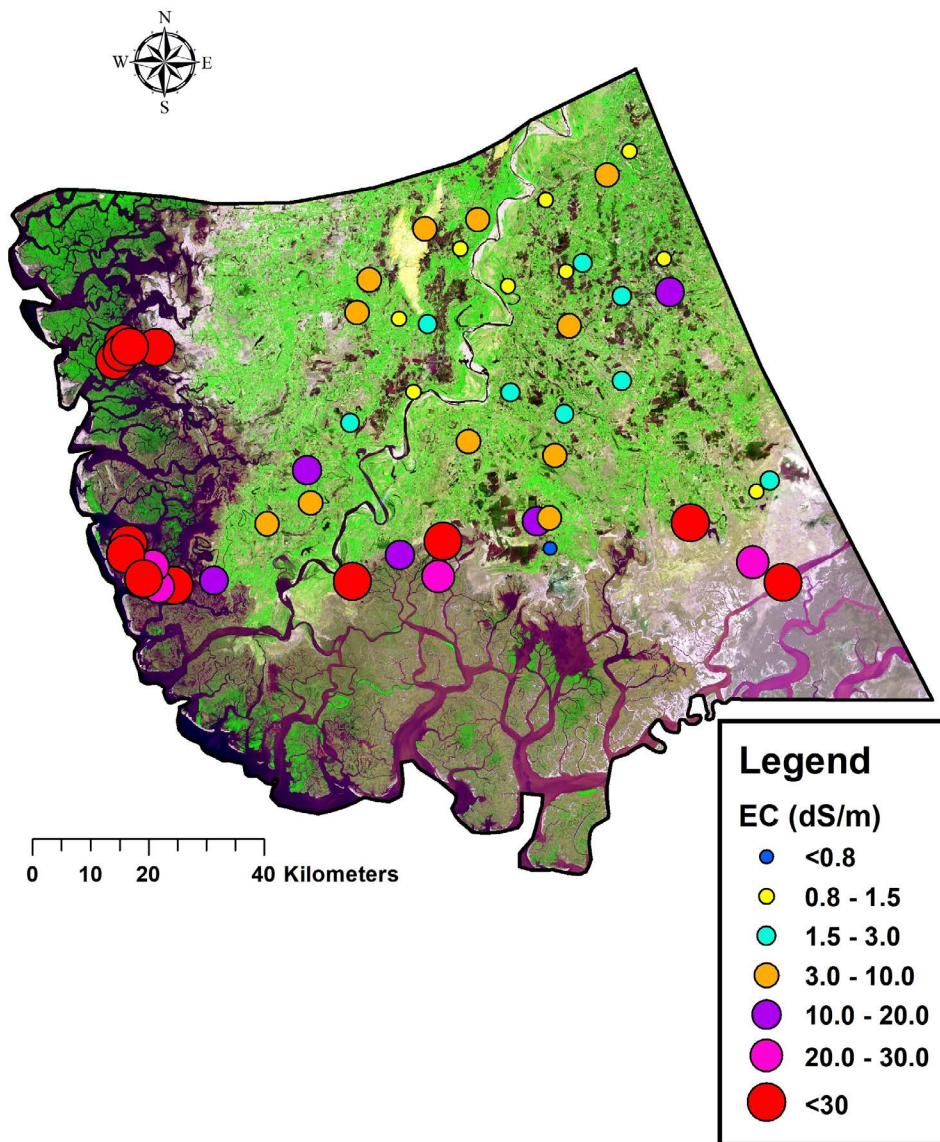


**Fig. 3.26: Spatial distribution of EC of surface water bodies**

The pH is a scale normally used to evaluate the acidity or alkalinity of water. Most of the aquatic creatures tolerate a restricted range of pH i.e., 6-8 (Ewaid, 2016). The surface water of the study area was normal to slightly alkaline in nature with pH values between 7.62 to 8.64 with a mean value of  $8.0 \pm 0.08$ . For regular irrigation, the pH values should be between 6.5 and 8.5, while pH values higher than 8.5 increases the soil sodicity hazards (Danko, 1997).

The concentration of total dissolved solids (TDS) in the sampled water bodies ranged between 378 and 38272 mg/L with a mean value of  $9590 \pm 2650$  mg/L. The lowest value of TDS was observed in a natural lake located in the union council of Ladyoon, whereas, the highest concentration was observed in the union council of Kar Malik, District Sujawal. Only a single surface water body (natural lake) had a TDS

concentration less than 500 mg/L, while rest of the surface water bodies had a higher concentration of dissolved solids. The water with TDS concentration more than 500 mg/L becomes unsuitable for drinking purpose (Smitha and Shivashankar, 2013) with an unpleasant taste and it may cause gastrointestinal irritation in the human body. As indicated by FAO (1985) the water having total dissolved solids (TDS) under 450 mg/L is considered as good, and that with more than 2000 mg/L is considered as unsatisfactory for irrigation purpose also (Adamu, 2013). Hence, under this criterion, the water of 64% of the sampled surface water bodies of the study area had TDS concentration higher than 2000 mg/L, hence not suitable even for irrigation purpose.

The chloride concentration was higher than the safe limit of 250 mg/L described by WHO for drinking water in most of the sampled water bodies of the study area. Its concentration fluctuated from 440 to 17406 mg/L with an average value of  $2197 \pm 905.7$  mg/L. The highest chloride concentration was detected in the natural lake located in the union council of Gaarho, district Thatta. The high concentration of chloride in most of the surface water bodies of the study area can be considered as an indication of entry of highly saline water into the water bodies (Supriyadi *et al.*, 2017). It increases the corrosive nature of water adversely affects human health and causes eye and nose irritation, and stomach problems (Patil *et al.*, 2012).

The irrigation water having chloride concentration between 70-350 mg/L causes no problems to plants, and severe problems are likely to occur if it contains chloride concentration greater than 350 mg/L. Based on this criterion, most of the surface water bodies had higher chloride concentration and could not be used for agriculture purpose.

The calcium concentration in the surface water bodies varied from 24 to 100 mg/L with an average value of  $45 \pm 7.67$  mg/L. According to WHO (2011) standards, the maximum allowable limit of calcium for drinking purpose is 75 mg/L. The magnesium concentration ranged from 55 to 305 mg/L with an average value of  $76 \pm 21.88$  mg/L, whereas, its allowable limit for drinking water is 50 mg/L. Severe problems are likely to occur if calcium and magnesium concentrations in water used for irrigation purpose are greater than 200 mg/L and 60 mg/L, respectively. Overall, 51% of the sampled surface water bodies of the study area had calcium and magnesium content beyond the safe limit, hence could be categorized as unsuitable for drinking and irrigation purpose.

The analysis of the water samples revealed that 36% had total hardness values greater than 300 mg/L and fell in the categories of hard to very hard water. The total hardness expressed as calcium carbonate ( $\text{CaCO}_3$ ) ranged up to 1354 mg/L with an average value of  $368 \pm 99.33$  mg/L, whereas, the maximum threshold limit for total hardness in drinking water is 500 mg/L (WHO, 2011). The presence of a higher concentration of hardness in water causes poor lathering with soap and deteriorates the quality of clothes (Patil *et al.*, 2012).

The arsenic concentrations in ten out of the fifty (20%) sampled water bodies located in the union councils of Mureed Khoso, Darro, Khan, Tar Khawaja, Kinjhar, Darya Khan Soho, Bijoro, Jar, Karampur, and Uddasi were above the safe limit for drinking purpose (WHO, 2011) and ranged from 10 to 25 ppb (Fig 3.27). This shows an alarming situation for the local communities who use such toxic water for their domestic and agricultural use. Arsenic contaminated water adversely affects human health, causes heart, liver, ocular and neuropathies diseases (Das *et al.*, 2012).

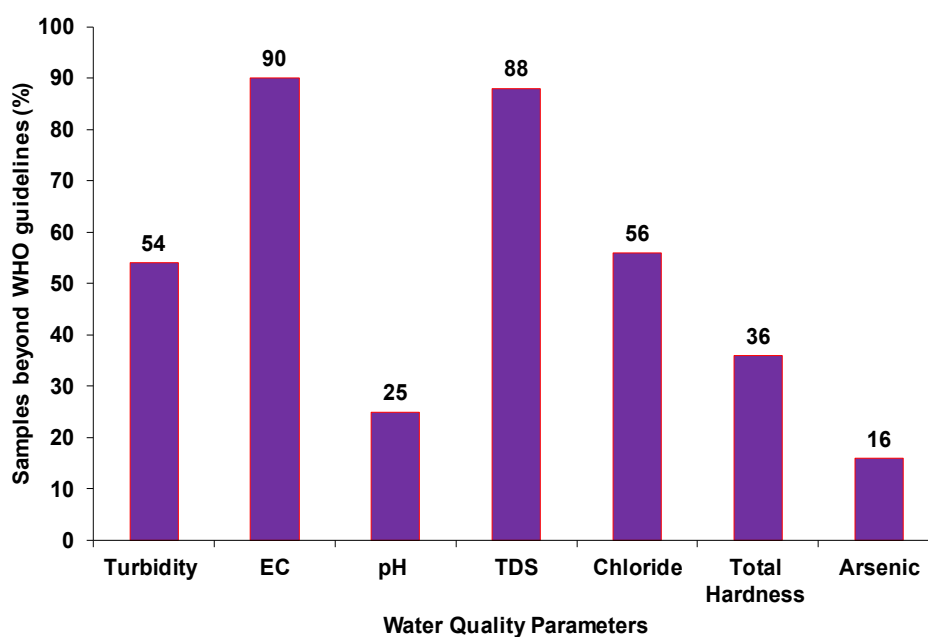


**Fig. 3.27: Percentage of samples beyond the permissible limit for various water quality parameters**

### 3.4.1.2 Correlation between the WQI and different water quality parameters

The correlation between the computed values of WQI and different water quality parameters (Alobaidy *et al.*, 2010) was established. Strong relationships were noted between WQI and electrical conductivity (EC), and total dissolved solids (TDS) with a coefficient of determination  $R^2 = 0.98$ , and  $0.99$ , respectively. Whereas, there was a

weak correlation between WQI and turbidity, pH, chloride, arsenic, and total hardness with a coefficient of determination of  $R^2 = 0.014, 0.019, 0.10, 0.11,$  and  $0.003,$  respectively. Thus, it is evident that EC and TDS were the major components affecting the calculated estimates of the WQI for surface water bodies of the Indus delta. The correlation between computed numerical indices (WQI and SPI) was also developed and found a significant trend between these numerical indices with a coefficient of determination  $R^2 = 0.75$  and described by regression Equation 3.3.

$$\text{SPI} = 1.0623 * \text{WQI} - 0.0136 \quad (3.3)$$

#### ***3.4.1.3 Analysis of water quality regarding WQI and SPI***

WQI based results (Table 3.7) show that only nine (18%) surface water bodies are classified as very poor with WQI levels between 76 to 100 (Ewaid and Abed, 2017) while rest of the forty-one (82%) surface water bodies lie in the category of unfit for drinking purpose with WQI value exceeding 100.

However, the results based on the SPI (Table 3.7) indicate that ten (20%) of the tested surface water bodies are classified as severally polluted with SPI estimates between 1.0 to 3.0, only one (2%) as moderately polluted and rest of the thirty-nine (78%) lie in the category of unfit for drinking purpose with an SPI value exceeding 3.0.

**Table 3.7: Water Quality Index (WQI) for sampled surface water bodies of the Indus delta**

Sample No.	Coordinates		Source	WQI Value	Classification	SPI Value	Classification
	Longitude	Latitude					
1	67.90276	24.1625	Sea creek	2750	Unfit for drinking	255.25	Unfit for drinking
2	67.95309	24.37344	Natural wetland	98.3	Very poor water	2.87	Severally polluted
3	68.02376	24.45111	Natural lake	453.2	Unfit for drinking	306.5	Unfit for drinking
4	68.09355	24.2074	Natural lake	84.0	Very poor water	2.91	Severally polluted
5	68.07106	24.25031	Chach lake	1764.5	Unfit for drinking	0.42	Unfit for drinking
6	68.18729	24.79169	Wetland	811.6	Unfit for drinking	104.4	Unfit for drinking
7	68.22477	24.82922	Thari lake	97.0	Very poor water	2.60	Severally polluted
8	67.45255	24.14417	Kori Creek	3936.6	Unfit for drinking	611.7	Unfit for drinking
9	67.52082	24.15231	Drainage canal	1565.3	Unfit for drinking	15.27	Unfit for drinking
10	67.61072	24.24239	Ochito canal	99.3	Very poor water	2.40	Severally polluted
11	67.75085	24.40145	Natural lake	294.4	Unfit for drinking	611.4	Unfit for drinking
12	67.85824	24.45016	Natural lake	88.0	Very poor water	2.94	Severally polluted
13	67.88196	24.55717	Natural lake	312.2	Unfit for drinking	13.25	Unfit for drinking
14	68.46769	24.3158	Natural lake	281.7	Unfit for drinking	103.8	Unfit for drinking
15	68.4453	24.29778	Natural lake	99.12	Very poor water	2.85	Severally polluted

16	68.491383	24.156311	Drainage Canal	4349.4	Unfit for drinking	126.2	Unfit for drinking
17	68.43974	24.18784	Natural lake	2466.7	Unfit for drinking	114.6	Unfit for drinking
18	68.21419	24.46997	Natural lake	308.3	Unfit for drinking	291.2	Unfit for drinking
19	68.12379	24.55609	Natural lake	974.6	Unfit for drinking	297.3	Unfit for drinking
20	68.29596	24.60979	Natural lake	1278	Unfit for drinking	815.7	Unfit for drinking
21	68.09246	24.25523	Natural lake	1021.3	Unfit for drinking	162.9	Unfit for drinking
22	68.11646	24.41800	Natural lake	215.0	Unfit for drinking	254.5	Unfit for drinking
23	67.83723	24.1958	Sea Creek	1472.0	Unfit for drinking	509.3	Unfit for drinking
24	67.75732	24.15304	Sea Creek	4719.0	Unfit for drinking	132.4	Unfit for drinking
25	67.91129	24.21738	Jani Shah Sea Creek	3876.0	Unfit for drinking	213.8	Unfit for drinking
26	67.41837	24.51607	Patiani Sea creek	3854.2	Unfit for drinking	295.3	Unfit for drinking
27	67.36214	24.52225	Patiani sub-creek	3401.3	Unfit for drinking	366.6	Unfit for drinking
28	67.3475	24.4959	Patiani sub-creek	3492.2	Unfit for drinking	417.5	Unfit for drinking
29	67.35999	24.50703	Patiani sub-creek	3260.0	Unfit for drinking	464.6	Unfit for drinking
30	67.37256	24.51642	Patiani sub-creek	3370.4	Unfit for drinking	529.5	Unfit for drinking
31	68.08241	24.75265	Natural lake	185.4	Unfit for drinking	254.7	Unfit for drinking
32	68.28537	24.66112	Natural lake	89.2	Very poor water	0.99	Moderately polluted
33	68.21278	24.60309	Natural lake	351.1	Unfit for drinking	2.85	Severally polluted



34	67.83234	24.56437	Natural lake	150.3	Unfit for drinking	712.8	Unfit for drinking
35	67.76093	24.57385	Natural lake	707.3	Unfit for drinking	2.93	Severally polluted
36	67.78073	24.62568	Natural lake	298.5	Unfit for drinking	117.3	Unfit for drinking
37	67.42661	24.14198	Sea creek	3144.6	Unfit for drinking	427.6	Unfit for drinking
38	67.41728	24.1741	Sea Creek	3220.1	Unfit for drinking	519.3	Unfit for drinking
39	67.37425	24.20829	Sea creek	3242.2	Unfit for drinking	641.5	Unfit for drinking
40	67.36965	24.1928	Sea Creek	3263.3	Unfit for drinking	824.5	Unfit for drinking
41	67.40112	24.15451	Sea Creek	3253.1	Unfit for drinking	977.5	Unfit for drinking
42	68.14568	24.65398	Natural lake	317.3	Unfit for drinking	916	Unfit for drinking
43	68.11794	24.64049	Natural lake	95.5	Very poor water	2.98	Severally polluted
44	68.01884	24.61757	Natural lake	88.7	Very poor water	2.76	Severally polluted
45	67.96613	24.72054	River lake	806.5	Unfit for drinking	570.1	Unfit for drinking
46	68.10094	24.3526	Natural lake	431.3	Unfit for drinking	162.9	Unfit for drinking
47	67.67789	24.3267	Natural lake	1260.4	Unfit for drinking	91.7	Unfit for drinking
48	67.87566	24.70585	Kalan Kot natural lake	783.4	Unfit for drinking	152.7	Unfit for drinking
49	67.93612	24.67523	Aaghmino Kori lake	153.3	Unfit for drinking	224.0	Unfit for drinking
50	68.33233	24.24889	Surface drain	6685.3	Unfit for drinking	230.5	Unfit for drinking

### 3.4.2 Groundwater

Groundwater is an essential natural resource which is widely utilized for domestic, industrial, agricultural, and recreational purposes (El-Hoz *et al.*, 2014). It is reported that about 33% of the total world population utilizes groundwater for drinking purpose (Nickson *et al.*, 2005). The water quality is a vital concern before its utilization for different purposes, such as domestic, agriculture, industrial (Sargaonkar and Deshpande, 2003).

Coastal aquifers are particularly more vulnerable due to the entry of highly saline seawater into the aquifers. In these areas, groundwater salinization is associated with increased dissolved minerals and some other chemical constituents, such as chloride, magnesium, etc. (Gimenez and Morell, 1997). Same is the case with coastal areas of Sindh province of Pakistan; where groundwater contamination is increasing continuously, may be because of entry of saline water from the Arabian Sea into the aquifers (Patil *et al.*, 2012). The present study was thus conducted to evaluate the quality of groundwater and develop a spatial distribution database for the different physicochemical parameters using GIS interpolation inverse distance weighted (IDW) and water quality index (WQI) approaches.

#### 3.4.2.1 Statistical and spatial analysis of groundwater quality

The analytical data matrix for the physicochemical parameters of the groundwater of the Indus delta is given in Table 3.8.

**Table 3.8: Data matrix for various physicochemical parameters of groundwater of Indus delta**

Parameter	Unit	Min.	Max.	Mean	Standard deviation (SD)	Confidence interval (CI)
Turbidity	NTU	4.4	99.2	6.9	10.92	1.70
Electrical Conductivity	dS/m	0.48	26.10	1.57	2.18	0.34
pH	---	6.5	8.9	7.8	0.42	0.06
Total Dissolved Solids	mg/L	304	16704	1222.2	1393.27	217.25
Calcium	mg/L	14.4	391.2	128.3	65.16	10.16
Magnesium	mg/L	2.2	486	112.8	98.76	15.4
Total Hardness	mg/L	35.8	660.4	240	130.16	20.30
Chloride	mg/L	117.7	6274.7	1381.4	995.05	155.16
Arsenic	ppb	0	200	13.43	30.48	4.75

The groundwater quality analysis indicated that 62% of water samples had salty and bitter taste, while odor and color values in most of the groundwater samples were within the permissible limits.

Turbidity is first to be noticed and is a useful parameter which mimics the quality of water. The presence of suspended particles in water makes the water cloudy and opaque, increases the concentration of distressing metals and other dangerous minerals and pesticides, thus adversely impacts the human health (Patil *et al.*, 2012). The turbidity values fluctuated between 4.4 to 99.2 NTU with a mean value of  $6.9 \pm 1.7$  NTU. The highest turbidity was observed in the groundwater of union council Jar, district Sujawal which might be due to the defective or poor-quality strainer filter material used in the hand pump. While lowest turbidity was found in the groundwater of union council Mirpur Bathoro, district Sujawal. The turbidity of most of the groundwater was within the limit of 10 NTU. Fig 3.28 portrays the spatial distribution of turbidity in the groundwater of the Indus delta.

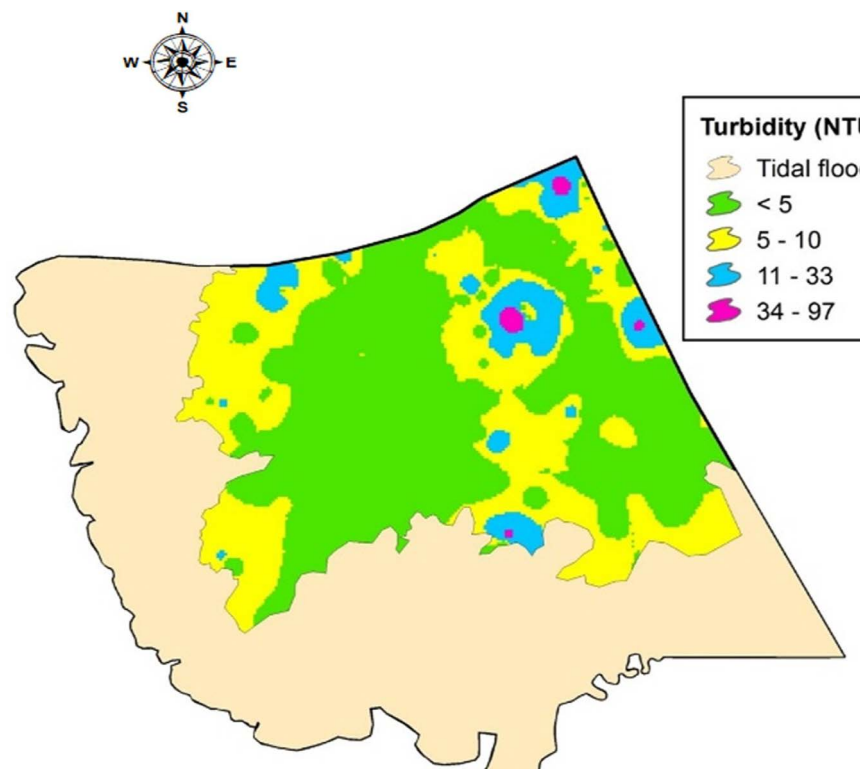


**Fig. 3.28: Interpolated GIS map of the spatial distribution of turbidity**

The electrical conductivity (EC) is also the primary parameter used to describe the presence of the salts in the groundwater. The availability of different dissolved minerals increases the conductivity values in the groundwater (Shabbir and Ahmed, 2015). The EC of the samples fluctuated between 0.48 to 26.10 dS/m with a mean value of  $1.57 \pm 0.34$  dS/m, though the acceptable range of EC for drinking water is 0.7 dS/m.

The highest electrical conductivity of 26.10 dS/m was observed in the groundwater of union council Ketī Bandar which is close to the Arabian Sea, while, the lowest EC of 0.48 dS/m was observed in the groundwater of union council Thatta, may be due to the proximity of river Indus. The interpolation of groundwater quality with respect to electrical conductivity demonstrated the higher concentration of dissolved minerals in groundwater in most areas of the delta (Fig. 3.29a).

In natural waters, the concentration of TDS is generally less than 500 mg/L. However, the water with TDS more than 500 mg/L is usually considered as unsatisfactory for drinking purpose, increases hardness and corrosive nature of water (Davis *et al.*, 2003). The overall suitability of water is usually based on the concentration of total dissolved solids present in water (Balakrishnan *et al.*, 2011). In the present study, the TDS concentration ranged from 304 to 16704 mg/L with a mean value of  $1222 \pm 217$  mg/L. The highest TDS of 16704 mg/L was observed in the groundwater of union council Ketī Bandar, district Thatta, while the lowest TDS value was observed in the groundwater of union council Thatta which is clearly shown in the spatial distribution map. The Fig. 3.29b depicts that major part of the study area has TDS values beyond the cutoff level of 500 mg/L, categorizing the groundwater unacceptable for drinking purposes. pH is also an essential parameter used to evaluate the quality of groundwater though it has no direct human health impact (Shabbir and Ahmed, 2015). The maximum allowable limit of pH as indicated by WHO (2011) for drinking water is 8.5, while required ideal pH is frequently varied between 6.5 to 8.5. The study demonstrated that groundwater samples had pH within range while few samples had slightly alkaline pH ranging up to 8.9 with a mean of  $7.8 \pm 0.42$ . Fig. 3.29c shows the spatial distribution of pH in the groundwater of the study area.

The chloride concentration in the study area varied between 117.7 and 6274.7 mg/L with an average of  $1381.4 \pm 155$  mg/L. In about 94% of the groundwater samples, the chloride concentration exceeded the permissible limit of 250 mg/L. The presence of chloride concentration in drinking water beyond the permissible limits has an adverse impact on human health, causes nose/eye irritation, stomach distress and expands destructive nature of water (Patil *et al.*, 2012). Fig. 3.29d shows the spatial distribution of chlorides in the groundwater of the study area. The presence of larger amounts of chloride in most of the groundwater samples are considered as an indication of the intrusion of saline water (Supriyadi *et al.*, 2017) in the groundwater of the study area.

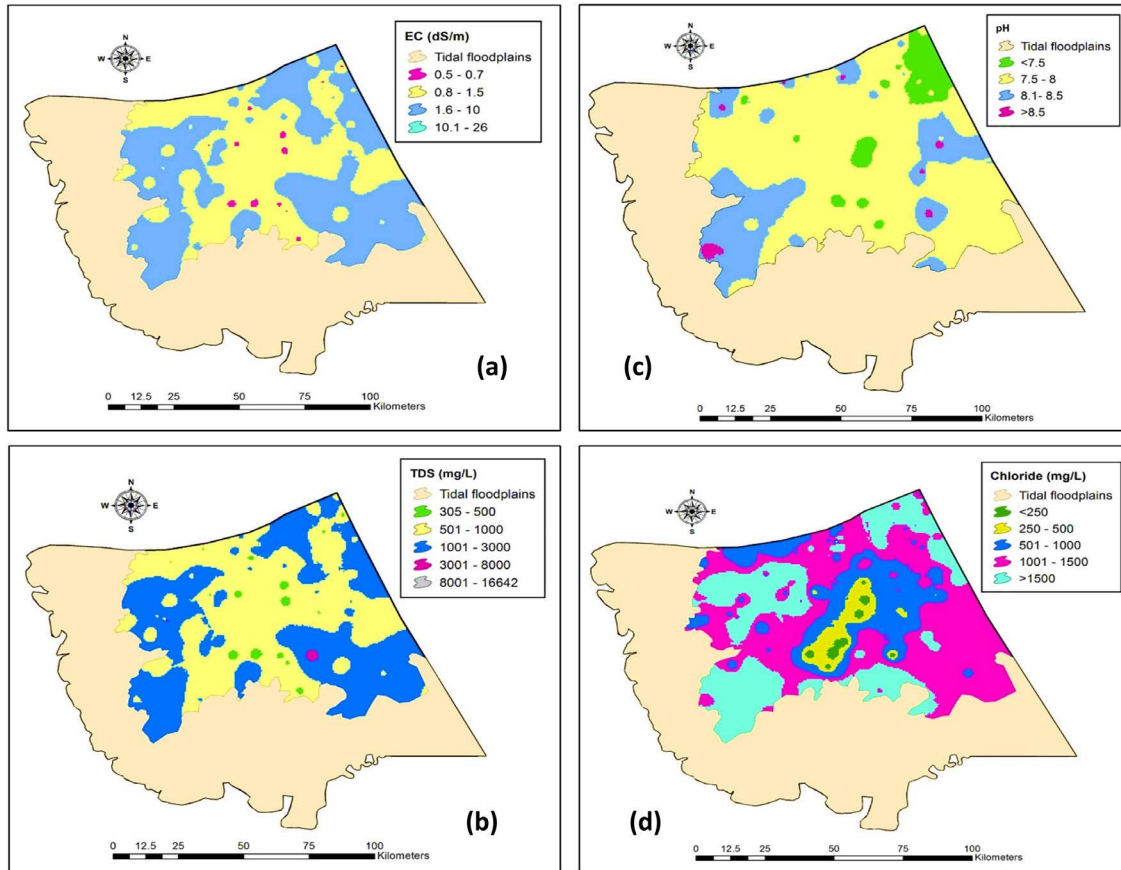


**Fig. 3.29: Interpolated map of the spatial distribution of water quality parameters**

The calcium concentration in the groundwater samples of the study area ranged between 14.4 to 391.2 mg/L with a mean value of  $128.3 \pm 10$  mg/L while, as per WHO (2011) the maximum permissible level of Ca in drinking water is 75 mg/L. About 33% of groundwater samples were within range, while the rest of the samples had Ca concentration beyond the permissible limit. The highest value of Ca in the groundwater was observed in the union council of Dhabeji, district Thatta, while lowest in the union council of Chuhar Jamali, district Sujawal. The spatial distribution of calcium concentration within the study area is shown in Fig. 3.30.

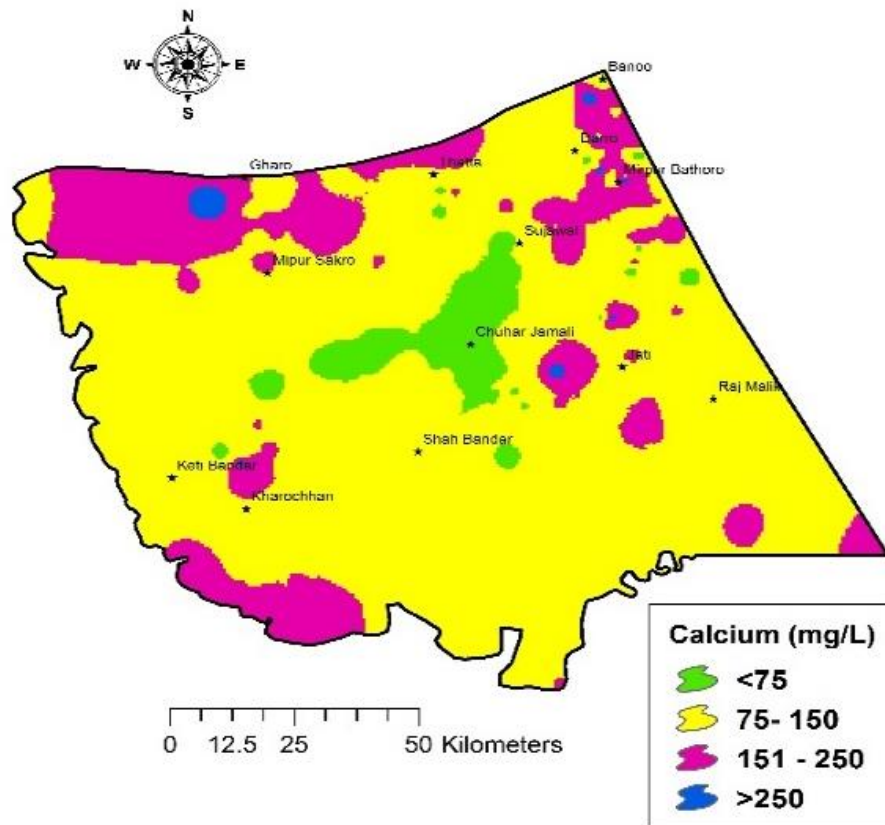


**Fig. 3.30: Interpolated map of the spatial distribution of Ca**

The magnesium concentration in the groundwater samples ranged between 2.2 and 486 mg/L with a mean value of  $112.8 \pm 15$  mg/L. The increased level of calcium and magnesium makes the water hard (Al-Ahmadi and El-Fiky, 2009). Overall, 43.7% of the groundwater samples had magnesium concentrations within the permissible limit of 50 mg/L, and the rest of the 56.3% had magnesium concentration beyond the permissible limit Fig. 3.31. The highest concentration of magnesium was observed in the groundwater of union council Jati, while lowest in the union council of Ali Bahar, district Sujawal.

The permissible limit of arsenic concentration in water for drinking purpose is 5-10 ppb (WHO, 2011). Almost one-fourth (23.4%) of groundwater samples of the study area were contaminated with arsenic concentration up to 200 ppb which was detected in the groundwater of union council Goongani, district Sujawal. The arsenic concentration differed significantly from area to area, but it is a serious threat to those people who

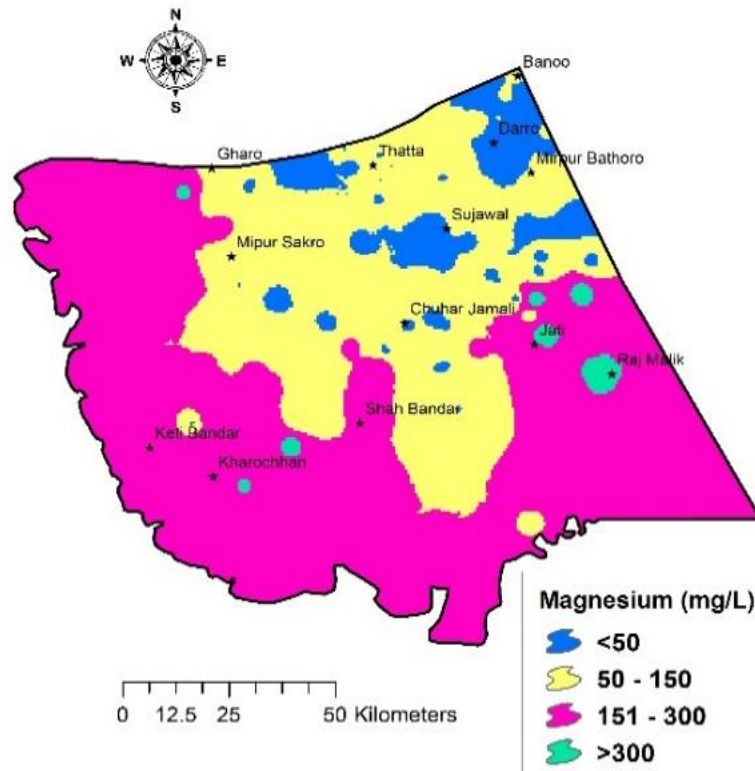


**Fig. 3.31: Interpolated map of the spatial distribution of Mg**

use that contaminated water. The presence of arsenic concentration beyond the cutoff level in water causes liver problems, cancer, cardiovascular, ocular, and neuropathy diseases (Das *et al.*, 2012). One of the conceivable sources of the presence of arsenic in the groundwater of the delta might be the geological formation of subsoil strata which contains enough arsenic compounds. The spatial distribution of arsenic (Fig. 3.32) shows that in some of the union councils (small administrative unit), the arsenic concentration was beyond the WHO standards set for safe drinking water.

The spatial distribution interpolated maps of various physicochemical parameters indicated that a very small portion of the study area has potable groundwater. In most of the area, the values of water quality parameters exceeded the respective maximum permissible limit suggested by WHO (2011). Hence, it required proper water treatment before use for drinking purpose. The quality of groundwater was mostly fresh in those areas where the pumps were installed near to irrigation water channels.

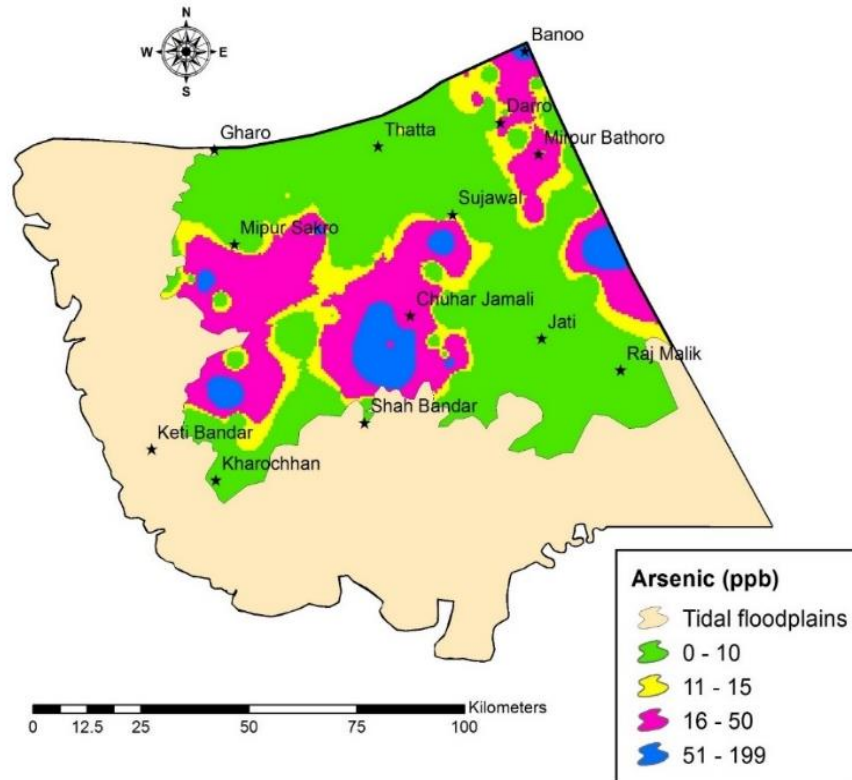


**Fig. 3.32: Interpolated map of the spatial distribution of As**

### 3.4.2.2 Water quality analysis based on water quality index (WQI)

Based on the computation of water quality index (WQI) values, the water is usually classified into five categories (Sahu and Sikdar, 2008) as given in Table 3.9.

**Table 3.9: Categories of water based on water quality index (WQI)**

WQI Range	Class of water	Category
<50	Excellent	1
50-100	Good	2
100-200	Poor	3
200-300	Very poor	4
>300	Unfit for drinking	5

Water Quality Index (WQI) calculations for the groundwater samples of the study area clearly show that most of the groundwater samples were classified as poor to very poor (Fig. 3.33). Only four out of 180 groundwater samples had WQI range below 50 while rest of the samples had WQI value beyond 50. Thus, groundwater needs proper treatment before use for the domestic purpose.



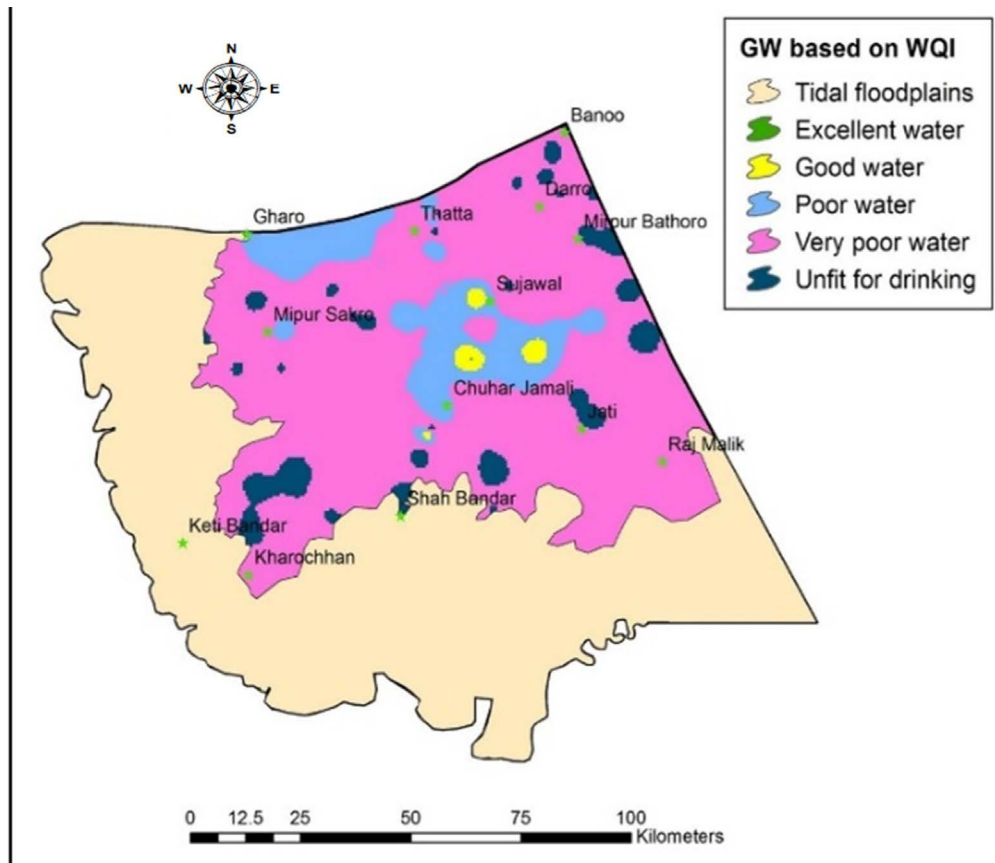


**Fig. 3.33: Classification of groundwater of Indus delta based on WQI**

For the present study, the classification of groundwater based on WQI is described in Table 3.10.

**Table 3.10: Classification of groundwater samples based on water quality index**

Sample No.	WQI	Classification	Sample No.	WQI	Classification	Sample No.	WQI	Classification
1	347.7	Unfit for drinking	61	299.7	Very poor	121	275.4	Very poor
2	49.2	Excellent	62	337.8	Unfit for drinking	122	184.5	Poor
3	496.4	Unfit for drinking	63	518.3	Unfit for drinking	123	192.6	Poor
4	178.7	Poor	64	268.5	Very poor	124	439.7	Unfit for drinking
5	93.5	Good	65	255.6	Very poor	125	397.4	Unfit for drinking

6	144.7	Poor	66	154.2	Poor	126	336.4	Unfit for drinking
7	49.1	Excellent	67	167.8	Poor	127	171.6	Poor
8	249.4	Very poor	68	298.5	Very poor	128	466.2	Unfit for drinking
9	47.0	Excellent	69	149.3	Poor	129	124.0	Good
10	665.1	Unfit for drinking	70	587.7	Unfit for drinking	130	269.2	Very poor
11	255.0	Very poor	71	232.0	Very poor	131	600.3	Unfit for drinking
12	274.6	Very poor	72	350.7	Unfit for drinking	132	259.4	Very poor
13	276.8	Very poor	73	394.2	Unfit for drinking	133	97.2	Good
14	445.6	Unfit for drinking	74	347.0	Unfit for drinking	134	176.1	Poor
15	381.2	Unfit for drinking	75	278.0	Very poor	135	100.1	Good
16	168.7	Poor	76	239.5	Very poor	136	96.4	Good
17	287.4	Very poor	77	351.0	Unfit for drinking	137	99.1	Good
18	435.8	Unfit for drinking	78	288.1	Very poor	138	98.3	Good
19	173.9	Poor	79	236.4	Very poor	139	154.1	Poor
20	462.7	Unfit for drinking	80	263.6	Very poor	140	132.0	Poor
21	372.4	Unfit for drinking	81	185.2	Poor	141	167.2	Poor
22	175.6	Poor	82	175.4	Poor	142	957.0	Unfit for drinking
23	228.5	Very poor	83	125.2	Poor	143	157.3	Poor
24	152.2	Poor	84	119.1	Poor	144	142.2	Poor
25	237.2	Very poor	85	118.1	Poor	145	416.4	Unfit for drinking
26	499.4	Unfit for drinking	86	263.3	Very poor	146	104.2	Poor
27	274.3	Very poor	87	238.3	Very poor	147	534.0	Unfit for drinking
28	128.2	Poor	88	119.3	Poor	148	99.2	Good

29	542.4	Unfit for drinking	89	118.0	Poor	149	394.1	Unfit for drinking
30	1122.2	Unfit for drinking	90	188.7	Poor	150	116.3	Good
31	282.8	Very poor	91	455.4	Unfit for drinking	151	256.1	Very poor
32	235.7	Very poor	92	451.6	Unfit for drinking	152	510.3	Unfit for drinking
33	336.8	Unfit for drinking	93	323.0	Unfit for drinking	153	135.3	Poor
34	127.1	Poor	94	394.2	Unfit for drinking	154	153.0	Poor
35	82.0	Good	95	347.0	Unfit for drinking	155	220.1	Very poor
36	47.6	Excellent	96	291.0	Very poor	156	215.4	Very Poor
37	168.8	Poor	97	267.5	Very poor	157	183.2	Poor
38	223.3	Very poor	98	350.7	Unfit for drinking	158	326.3	Unfit for drinking
39	248.9	Very poor	99	287.1	Very poor	159	411.3	Unfit for drinking
40	368.6	Unfit for drinking	100	236.3	Very poor	160	168.4	Poor
41	165.6	Poor	101	263.6	Very poor	161	189.1	Poor
42	174.1	Poor	102	185.2	Poor	162	209.3	Very poor
43	244.8	Very poor	103	185.3	Poor	163	147.3	Poor
44	265.2	Very poor	104	185.2	Poor	164	215.2	Poor
45	238.5	Very poor	105	149.1	Poor	165	99.2	Good
46	239.3	Very poor	106	198.0	Poor	166	773.3	Unfit for drinking
47	226.6	Very poor	107	263.3	Very poor	167	204.0	Poor
48	267.8	Very poor	108	238.1	Very poor	168	151.4	Poor
49	358.2	Unfit for drinking	109	119.3	Poor	169	347.8	Unfit for drinking
50	267.9	Very poor	110	108.0	Poor	170	298.3	Very poor
51	181.8	Poor	111	200.2	Poor	171	162.6	Poor
52	534.2	Unfit for drinking	112	455.4	Unfit for drinking	172	110.6	Good
53	167.5	Poor	113	451.5	Unfit for drinking	173	266.5	Very poor

54	244.1	Very poor	114	192.8	Very poor	174	538.5	Unfit for drinking
55	118.5	Poor	115	773.3	Unfit for drinking	175	246.4	Very poor
56	157.3	Poor	116	199.2	Poor	176	151.0	Poor
57	306.3	Very poor	117	184.3	Poor	177	793.4	Unfit for drinking
58	130.0	Poor	118	254.0	Very poor	178	170.2	Poor
59	600.4	Unfit for drinking	119	155.0	Poor	179	61.4	Good
60	142.5	Poor	120	152.5	Poor	180	348.5	Unfit for drinking

### 3.4.2.3 Subsurface seawater intrusion

The area of Indus delta affected by seawater intrusion illustrated in the interpolated map (Fig. 3.34). shows that seawater has intruded in vast areas of the delta such that its presence was observed in the wells near to Thatta and Sujawal towns. Based on high chlorides concentration ( $>250$  mg/L), Simpson ratio ( $>2.8$ ), chloride and bicarbonate ratio ( $>0.6$ ) in groundwater, the seawater intrusion interpolation map depicted that about 11540 sq. km (1.15 Mha) of land or 88.3% of the delta are affected by the seawater intrusion while 1527 sq. km (0.15 Mha) or 11.7% of the delta is unaffected due to the intrusion of seawater.

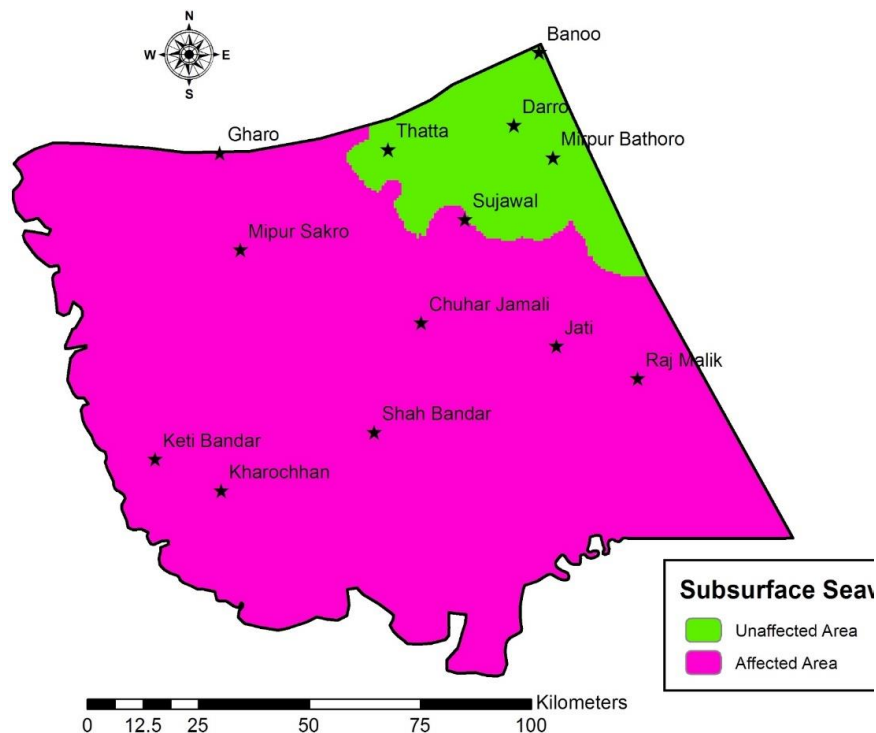


Fig. 3.34: Interpolated map of subsurface seawater intrusion in Indus delta

### **3.5 Shift in the Shoreline of the Indus Delta and the Area Taken Away by the Sea**

So far, very few studies have documented the degradation of the coastal areas of the Indus delta without any quantifiable data. Thus, the present study aims to quantify the coastal erosion and accretion and variation in the shoreline along the Indus delta under long-term scenario by analyzing the multi-temporal Landsat satellite images using Digital Shoreline Analysis System (DSAS) integrated with ArcGIS 10.3. The present quantitative study will be beneficial for coastal managers and decision makers for frequent analysis and spotlighting the geomorphologically vulnerable hotspots along the delta.

#### **3.5.1 Shoreline position at different locations**

(Fig. 3.35) illustrates the position of the shoreline at different times, and baseline, transects and location of major creeks along the entire Indus deltaic coastline. It depicts that 679 transects are on the left side while 694 transects are on the right side concerning the flow direction of the river Indus.

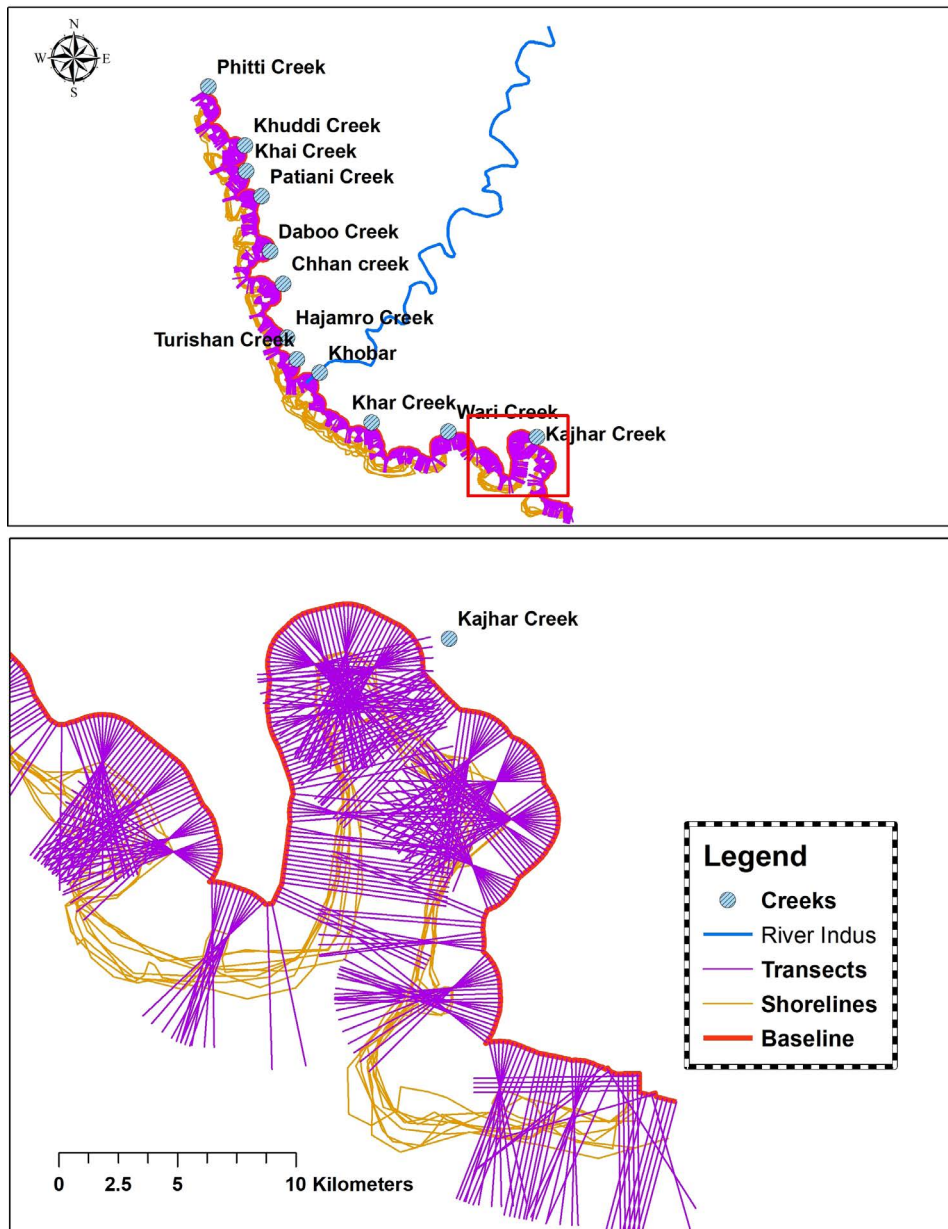


**Fig. 3.35: The position of the shorelines at different times, baseline, transects and the location of major creeks along the entire deltaic coastline**

### **3.5.2 Shoreline change rates (1972-2017)**

The End Point Rate (EPR) of the shoreline of the study area from 1972 to 2017 is shown in Fig. 3.36a while Linear Regression Rate (LRR) is presented in Fig. 3.36b. The graph shows both positive and negative values of EPR which reflects the accretion or erosion of the shoreline, respectively. The figure shows that EPR values are more negative for zones 1 and 2 on the left side of the river compared to zones 3 and 4 on the right side of the river. The erosion was recorded at 237, 245, 198 and 202 transects for zones 1, 2, 3 and 4, respectively. While, accretion occurred at 130, 76, 127 and 167 transects for the respective zones. Mean erosion rates on river left

bank for zones 1 and 2 were 45.69 and 52.1 m/year, respectively while mean accretion rates were 9.86 and 24.21 m/year, respectively (Fig 3.37). Similarly, on river right bank mean erosion and accretion rates were 27.21 and 26.36 m/year, respectively for zone 3 and 31.43 and 24.1 m/year, respectively for zone 4. The net shoreline change rate was higher, i.e.,  $-30.12 \pm 3.13$  m/year on the left side of the river Indus compared to that of on the right side, i.e.,  $-6.34 \pm 2.85$  m/year.

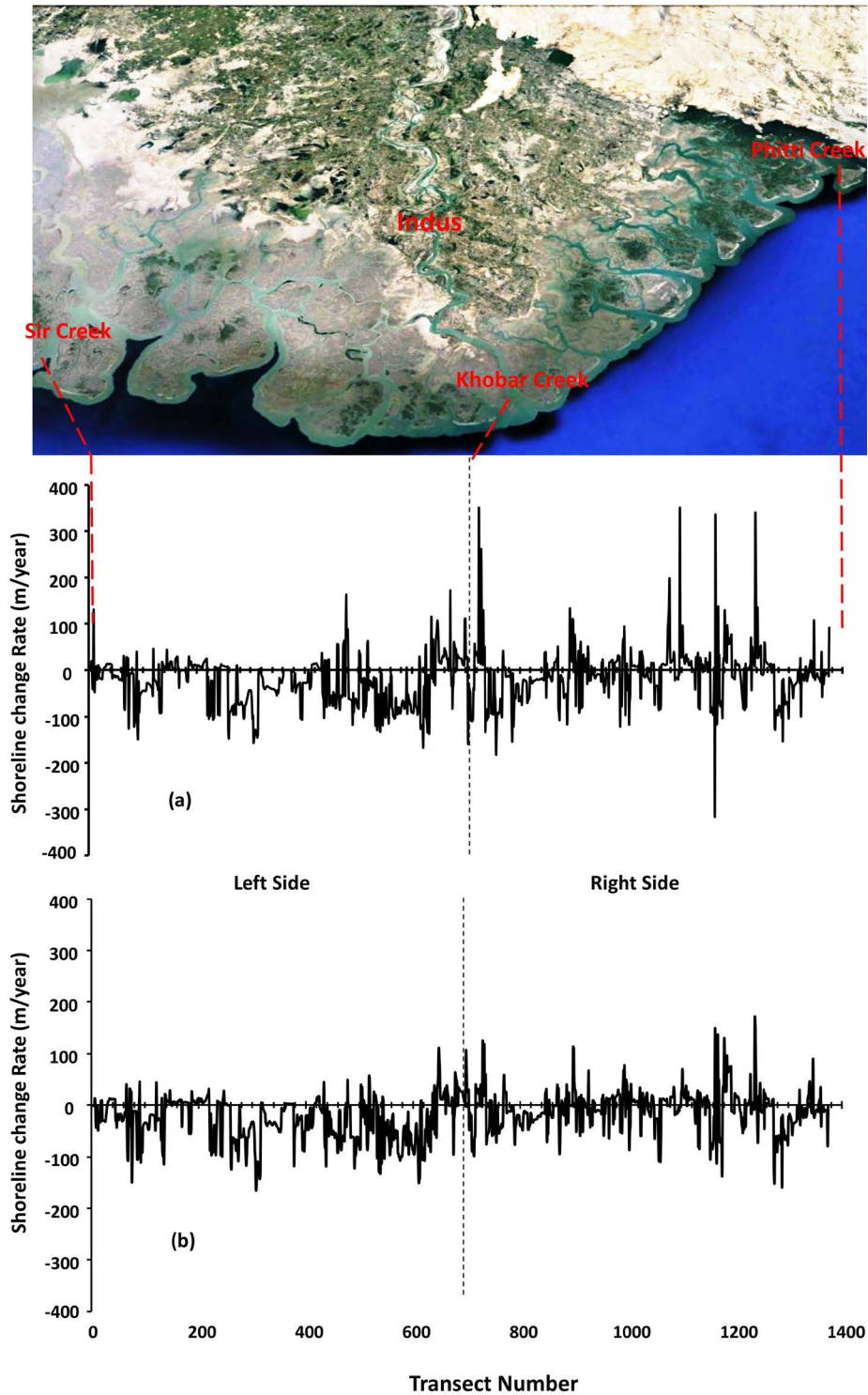


**Fig. 3.36: Shoreline change rate at different transects along coastline estimated by (a) EPR and (b) LRR**

This suggests that erosion rates were higher for the left side (zones 1 and 2) compared to the right side (zones 3 and 4); while accretion rates were higher for the right-side zones than on the left side zones as shown in Fig. 3.37

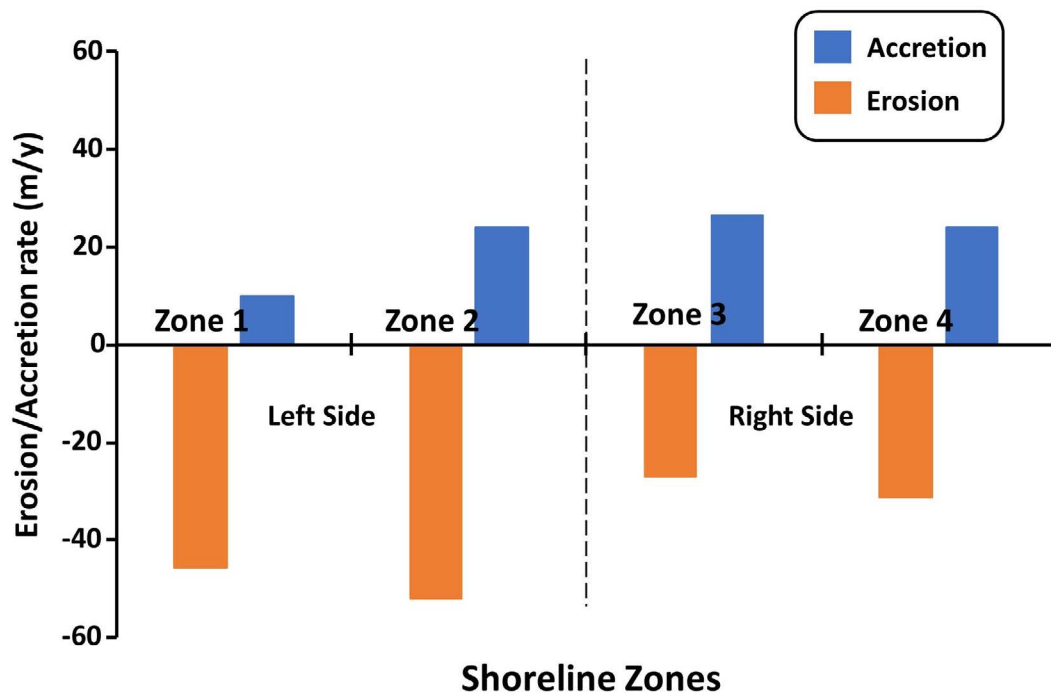


**Fig. 3.37: Shoreline change rate in different zones along the coastline**

It revealed during a thorough investigation of the zones 3 and 4 that there exist densely populated mangrove forests which provide defense-line against highest average sea wave energy (Wells and Coleman, 1984; Mountjoy, 2004), compared to other major deltas in the world. Less erosion of tidal floodplain on the right side of the Indus delta was also reported by Ijaz *et al.* (2018) who associated it to the presence of thick mangrove forests. Also, the topography of the right side of Indus delta is not favorable for the erosion compared to the left side of the delta.

The spatial variation in shoreline change rates estimated through EPR at different transects along the shoreline is shown in Fig. 3.38a. It shows erosion at majority of the transects in zone 2 and also at a bunch of transects in zones 1, 3 and 4. While, at some isolated transects in zone 1, 3 and 4 accretions along the shoreline were also witnessed. LRR shoreline change rate estimations are identical to EPR at many transects in all four shoreline zones (Fig. 3.38a). However, the magnitude of LRR estimates is smaller than EPR estimates. The positive and negative rates of change in shoreline given in the figure represent the corresponding accretion and erosion of the coastline. Fig. 3.38b portrays the spatial distribution of erosion and accretion along the entire shoreline of the delta. It also confirms that coastline along zone 2 is eroded the most compared to rest of the zones.



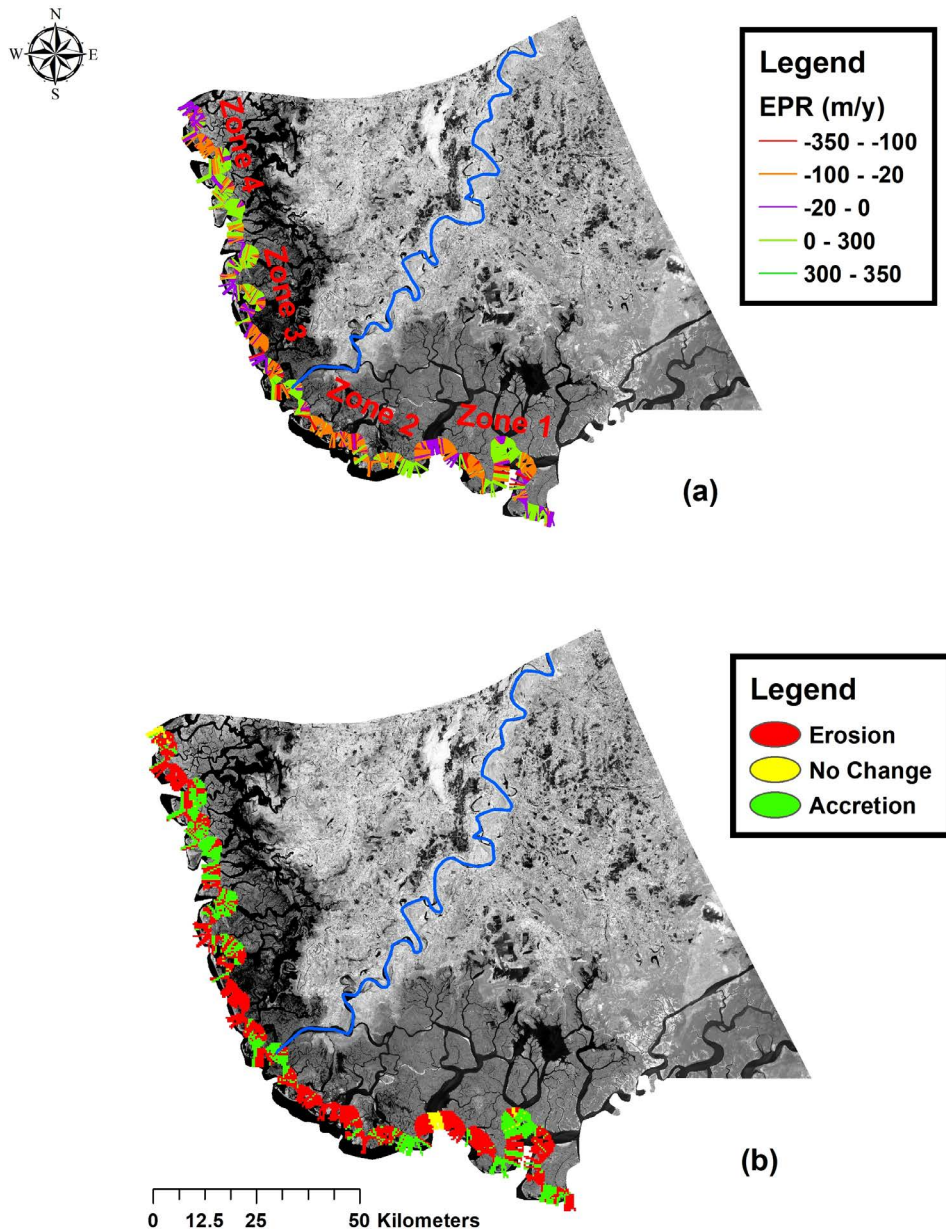


**Fig. 3.38: Spatial variation in shoreline change rates (a) estimated through EPR at different transects along the shoreline and (b) spatial distribution of erosion and accretion along the entire shoreline of the delta**

The net shoreline movement (NSM) evaluates an inward or outward distance of the shoreline at all transects. Thus, it determines the distance between the oldest and the most recent shorelines for each transect. The NSM values at different zones of the shoreline of the delta are portrayed in Fig. 3.39. It highlights that there is a continuous erosion with the passage of time as the distance between the oldest (1972) and youngest shorelines (2017) significantly varies at different transects with a mean value of -1089 meter in zone 1, -1243 m in zone 2, -687m in zone 3 and -411 m in zone 4. Thus, the highest landward NSM was for zone 2, and least NSM was for zone 4.

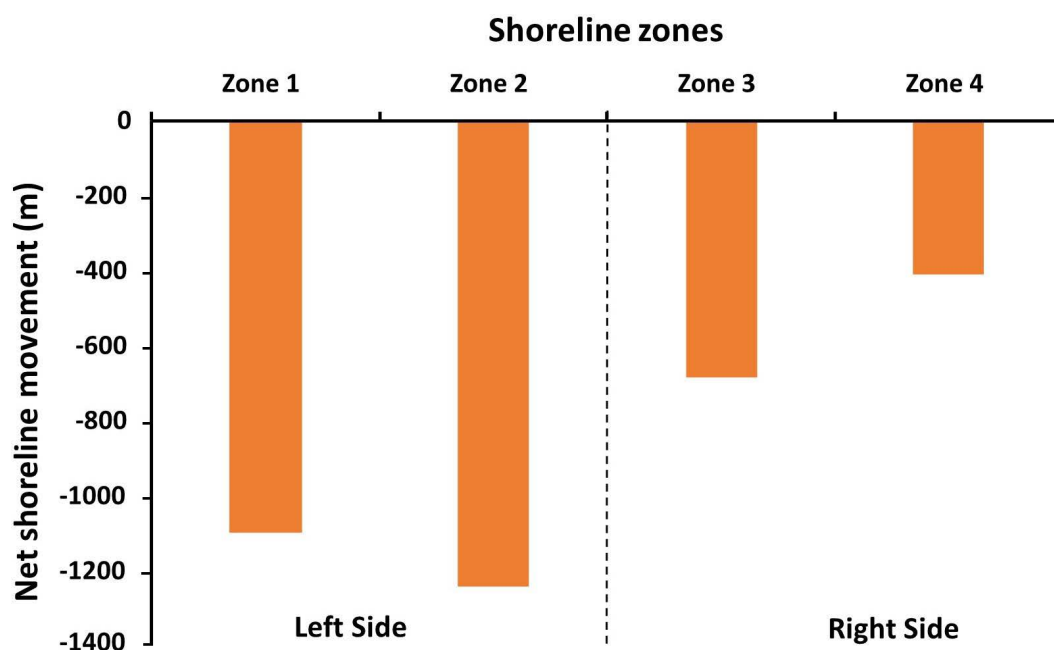


**Fig. 3.39: Net shoreline movement (NSM) at different zones along the Indus delta shoreline (1972-2017)**

Summary of the statistical parameters EPR, NSM and LRR for the Indus delta shoreline for the period 1972 to 2017 (Table 3.11) depicts erosion along the shoreline of all 4 zones. The mean erosion rate was highest for zone 2 followed by zone 1, zone 4 and zone 3. Mean accretion rate was highest for zone 3 followed by zone 4, zone 2 and zone 1. Thus, zones 1 and 2 on the left side of the river Indus were more susceptible to coastal erosion. It may be due to fewer mangrove forests and flat topography of these zones which makes the shoreline vulnerable to withstand the wind and wave power.

**Table 3.11: Summary of shoreline change rate based on NSM, EPR, and LRR for the period 1972-2017**

S #	Parameter	Left Bank Side		Right Bank Side		Total shoreline
		Zone 1 (Sir-Wari Creek)	Zone 2 (Wari-Kho-bar Creek)	Zone 3 (Kho-bar-Daboo Creek)	Zone 4 (Da-boo-Phitti Creek)	
1	Shoreline Length (km)	74	62	65	75.6	276.60
2	Mean shoreline change rate (m/y)	-26.23	-32.53	-14.12	-2.63	-18.87±2.2
3	Mean erosion rate (m/y)	45.69	52.10	27.21	31.43	39.11±2.08

4	Mean accretion rate (m/y)	9.86	24.21	26.36	24.3	21.13±2.06
5	Maximum accretion rate (m/y)	44.46	109.73	125.50	170.00	170.00
6	Maximum erosion rate (m/y)	164.0	150.36	97.36	159.40	159.40
7	Total transect that record (Erosion)	237	245	198	202	882
8	Total transect that record (Accretion)	130	76	127	167	500
9	Net shoreline movement (m)	-1098	-1243	-687	-411	-860±92
10	Trend (erosion/ accretion)	Erosion	Erosion	Erosion	Erosion	Erosion

± Confidence Interval @ 5%

### 3.5.3 Shoreline change rates during 1972-1990 and 1990-2017 periods

Fig. 3.40a shows that the mean shoreline change rate for both the periods (1972-1990 and 1990-2017) was landward with the highest rate for zone 2 followed by zones 1, 3 and 4. However, it illustrates that the shoreline change rates were significantly higher in all zones during the period 1990-2017 compared to those in 1972-1990 ( $p < 0.5$ ). This may be attributed to the factors like strong wave action (Ellison, 1994), decrease in the freshwater flows in the river Indus below Kotri barrage (last barrage on the river Indus), resulting 80% reduction in sediment load after the late 1950s (Kravtsova, 2009; Mahar and Zaigham, 2015), offshore slope (Wells and Coleman, 1984) and also decline in mangrove forests (Ellison, 1994; Memon, 2012) in the tidal floodplains during the period 1990-2017.

The NSM data in Fig. 3.40b showed that maximum NSM was 1162 m for zone 2 followed by -776 m for zone 1 for the period 1990-2017; while it was -578 and -141 m for zones 3 and 4, respectively for the same period. It was also noted that NSM was higher (about double) for zones 1 and 2 on the left side compared to zones 3 and 4 on the right side of the river for the period 1972-1990. For the period 1990-2017, magnitude of the difference between left and right side of the river was even higher. The net inward shift in the shoreline of the delta for all zones from 1972 -1990 was calculated as  $323.97 \pm 40$  m and for the period 1990-2017 it was  $646 \pm 60$  m. The NSM

at all zones was 2 to 4 times more for the period 1990-2017 compared to the period 1972-1990. One of the main reasons for more NSM is higher shoreline change rate during the period 1990-2017 (Fig. 3.40a) and the more total duration of the study period, i.e., 27 years. Also, the low river flows and a decrease in mangrove population might have the synergic impact on the higher NSM during period 1990-2017.

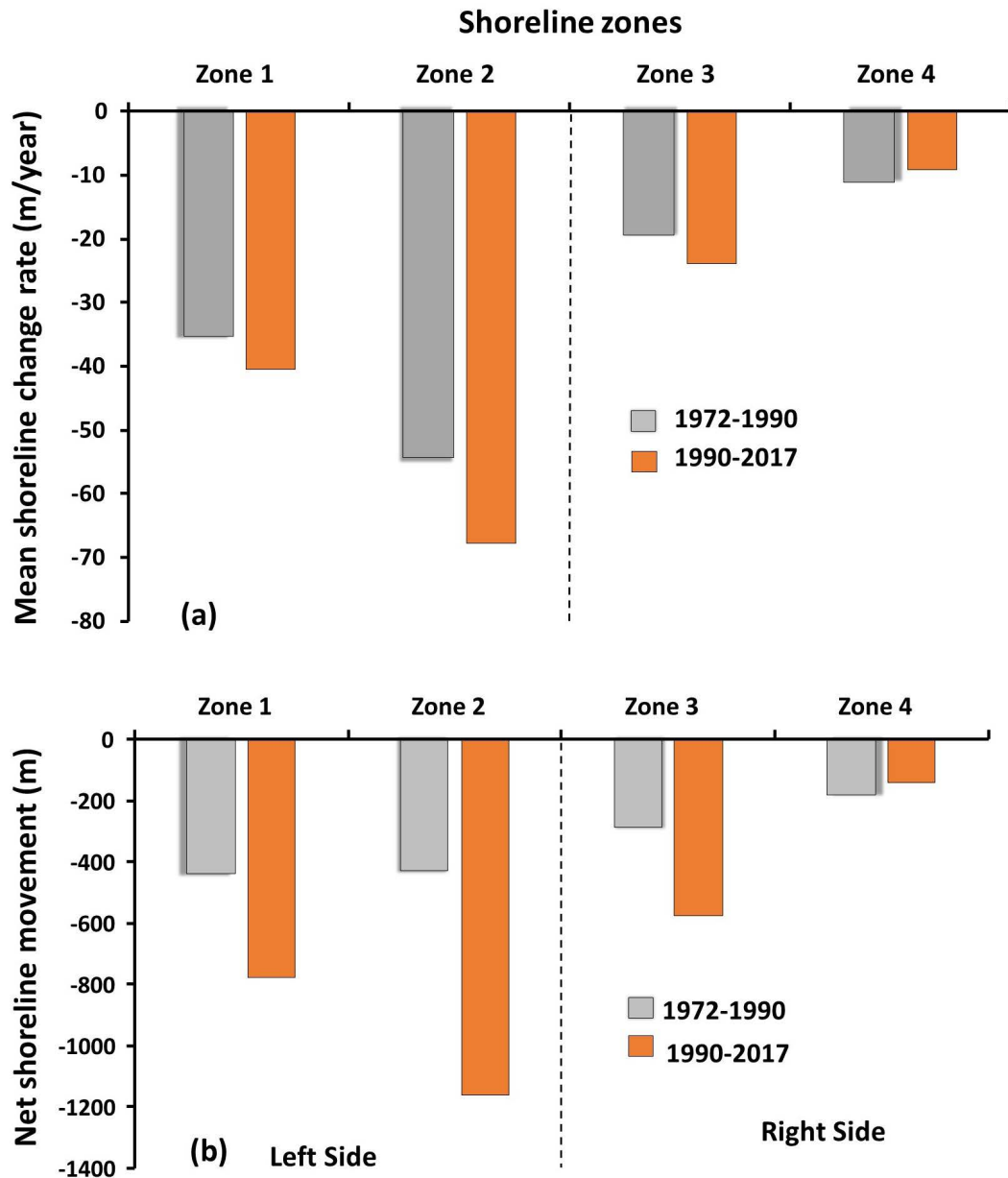


**Fig. 3.40: Mean shoreline change rates and NSM at different zones along Indus delta shoreline for the periods 1972-1990 and 1990-2017 (a) Mean shoreline change rates and (b) NSM**

### 3.5.4 Manual quantification of change in shoreline

The manually calculated data for NSM along the entire shoreline for the period 1972-2017 (Fig. 3.41) demonstrates that the highest landward shift in the shoreline was in zone 2 on the left bank side of the river. Accretion at some transects in zones 1 and 4

was also observed. The NSM for 45 years (1972-2017) was quantified as  $1295 \pm 260$  m, which is nearly 50% more than that calculated with DSAS software (as appraised in the previous section). The higher values of NSM obtained with manual calculations compared to those obtained with DSAS might be due to human error during drawing transects along the baseline and using the ruler for determining the distance between two shorelines. Also, the distance between transects was higher, i.e., 1000 m compared to 200 m used in DSAS software.

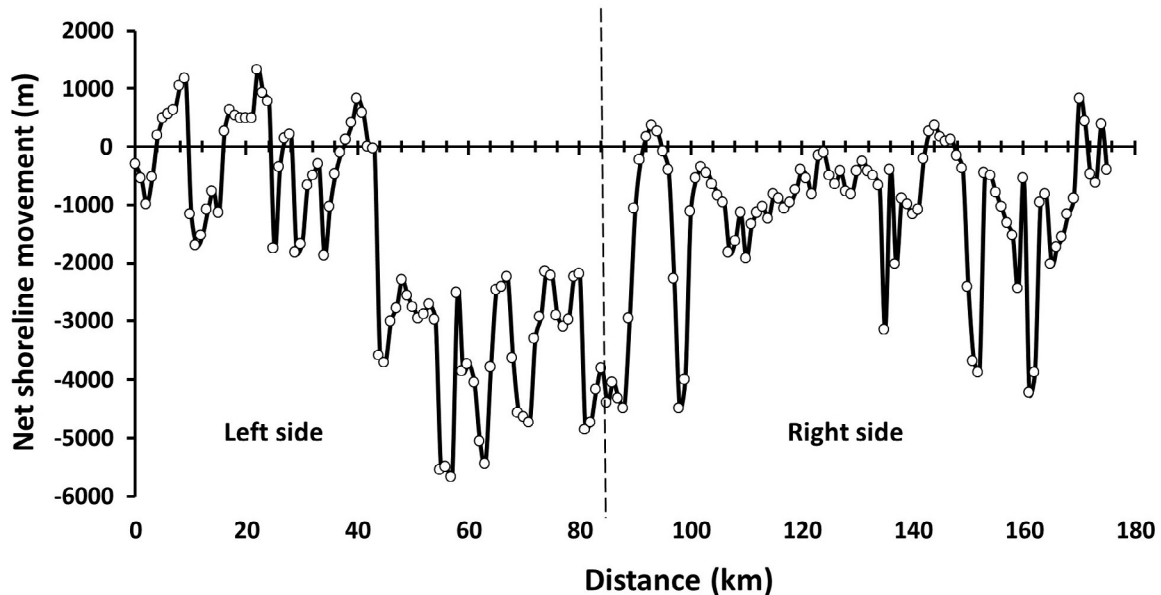


**Fig. 3.41: NSM calculated manually at different zones along the Indus delta shoreline (1972 to 2017)**

### 3.5.5 Variation in tidal floodplain area and the area taken away by the sea

Referring to the unclassified and classified satellite images of tidal floodplain area of the Indus delta in 1972 and after 45 years in 2017 (Fig. 3.42), it is noted that shoreline has moved landward at many places and vast areas of the floodplains are under water during 2017. To get a clear picture of gravity of the problem, only shoreline positions during 1972 and 2017 are plotted (Fig. 3.43) which show only those areas that are taken away by the sea during the last 45 years. The area taken away by the sea and the increase in the tidal floodplain area are quantified and summarized in Tables 3.12 a and b. It depicts that about 42607 ha are degraded due to surface seawater intrusion in the last 45 years which corresponds to a 7.1% increase in the tidal floodplains of the delta. Out of total degraded land of 42607 ha (426 sq, km), 31656 ha (316.6 sq, km) of land are now completely submerged in the seawater while 10951 ha of new land is converted into tidal floodplain area. It was further noted that tidal floodplain area on the left bank of Indus is about 4208 km<sup>2</sup> or about two times larger than that on the right bank side (2220 km<sup>2</sup>).

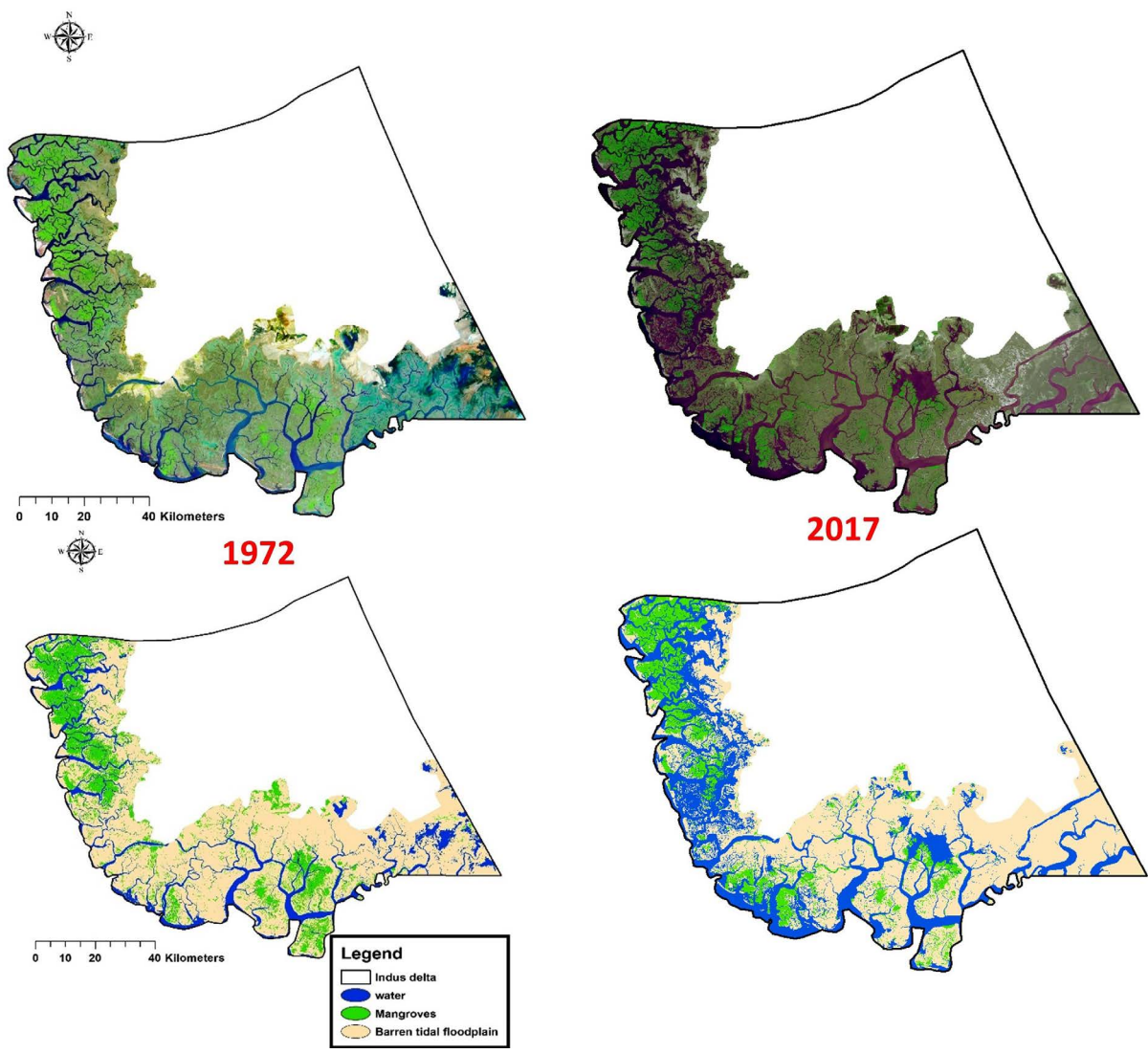


**Fig. 3.42: Unclassified and classified satellite images of tidal floodplain area of Indus delta in 1972 and after 45 years in 2017**

**Table 3.12 (a): Increase in tidal floodplain area in 45 years (1972-2017)**

Year	Area		% of entire delta	Increase km <sup>2</sup> (ha)	% increase
	km <sup>2</sup>	ha			
Oct, 1972	6002.17	600217	45.9	426.07 (42607)	7.1
Oct, 2017	6428.24	642824	49.2		

**Table 3.12 (b): Area of Indus delta degraded and taken away by the sea in 45 years (1972-2017)**

Total degraded area		Taken away by the sea		Converted into tidal floodplains	
ha	acres	ha	acres	ha	acres
42607	105285	31656	78224	10951	27061

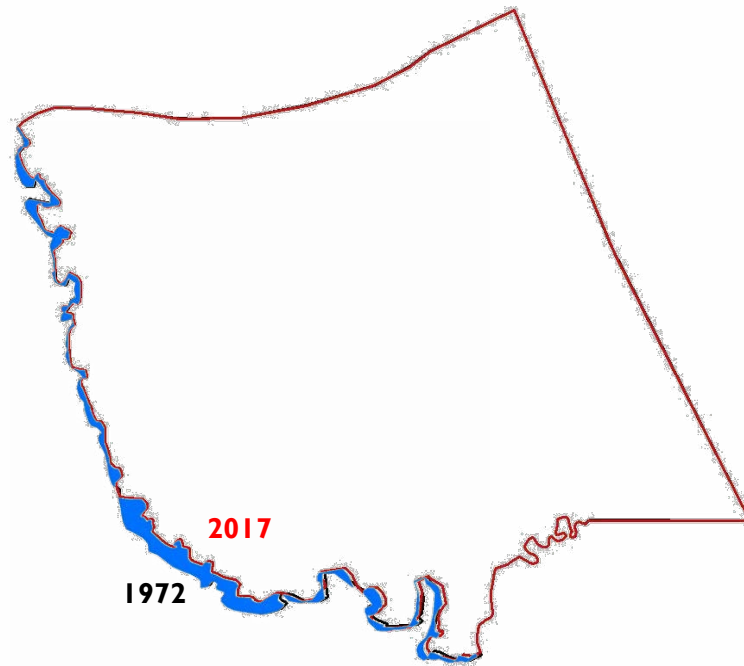


**Fig. 3.43: Shoreline positions of Indus delta in 1972 and 2017 and the area taken away by the sea**

### 3.5.6 Temporal variation in the area underwater in tidal floodplains

The increase in the area underwater in tidal floodplains was also quantified for the last 45 years (1972-2017) and is presented in Fig. 3.44. It portrays that the area underwater increases linearly with time such that it increased from 924 km<sup>2</sup> (14% of the tidal floodplain) in 1972 to 2361 km<sup>2</sup> which are 36.5% of the tidal floodplain. Thus, the area underwater in 2017 has increased more than twice the area underwater in 1972. The surface seawater intrusion has a significant impact on the geomorphology and environment of the delta.

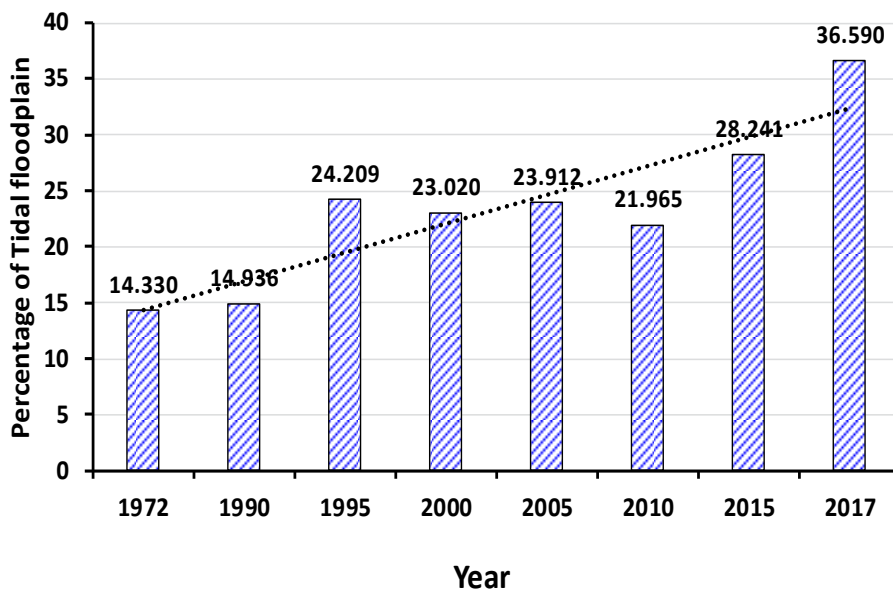


**Fig. 3.44: Temporal variation in area underwater in the tidal floodplain area**

### 3.5.7 Vulnerability of the Indus delta due to coastal flooding

Intergovernmental Panel on Climate Change (IPCC) has projected that sea level is likely to rise by 21 to 71 cm by the year 2070 with the best estimate of 44 cm. Globally deltas are rapidly sinking, often to below local sea level because of reduced river flows and the lack of sediment reaching to delta floodplains and also because of anthropogenic activities that are largely responsible for the present vulnerability of deltas.

The risk prone areas of Indus delta due to coastal flooding are delineated in Fig. 3.45. When a tsunami wave of 5 m height or a cyclone capable of raising sea level up to 5 m comes in the coastal belt of Indus delta, then vast areas of the delta will be inundated, and it will put lives of thousands of coastal communities at risk. The total vulnerable area with 5 m rise is about 9376 km<sup>2</sup> which is 71% of the total area of the delta. It illustrates the vulnerability of delta to coastal flooding and the risk of the life of coastal communities of the delta.

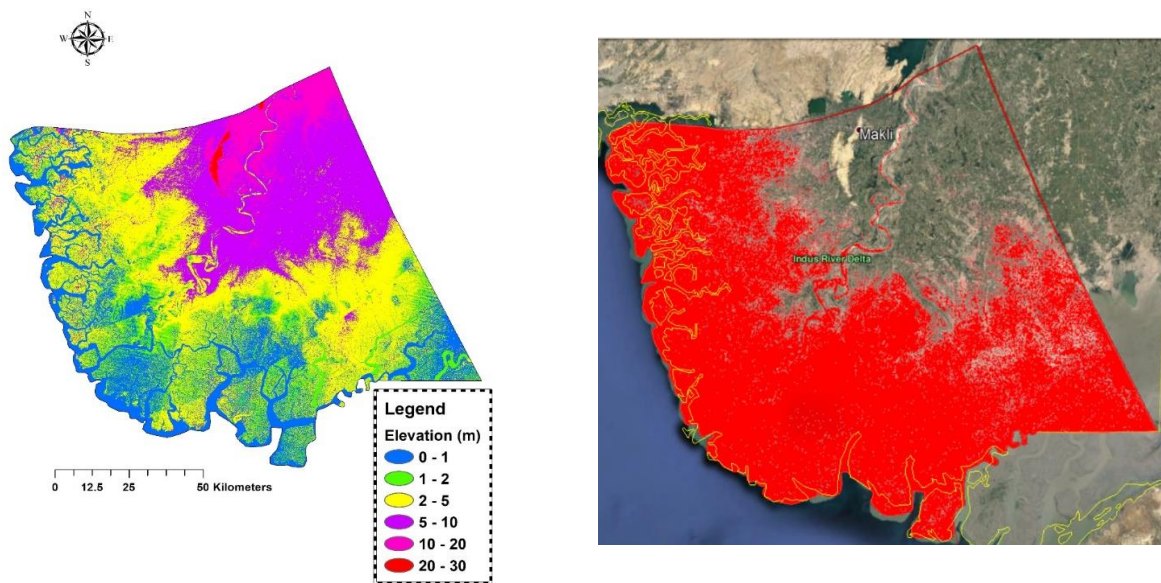


**Fig. 3.45: Risk prone areas of Indus delta due to coastal flooding**



### 3.6 Impacts of Seawater Intrusion on Socio-economic Conditions of the People Living in the Delta

The vulnerability of the coastal socio-ecological system is an indication of climatic stresses, sensitivity to damage, and lack of ability to adapt and adjust (Rahman and Miah 2013; Jongman *et al.*, 2014). Rasul *et al.* (2012) reported that climate change, poverty, lack of resources and low adaptive capacity of the local population are exaggerating the vulnerabilities and posing challenges to sustainable food production in the coastal areas. The socio-economic survey is the process by which the quantitative facts are gathered about the social, economic and demographic aspects of a particular area. Keeping these facts in the background a questionnaire was developed for key Informant Interviews (KII) of the residents of Indus delta.

An important aim of this study was to observe and document the impacts of seawater intrusion on socio-economic conditions of the community living in the Indus deltaic area. This study hypothesized that seawater intrusion has an adverse impact on the socio-economic conditions of people living in the Indus delta. One of the objectives of the present study was to get baseline data about adverse impacts of the seawater intrusion in the Indus delta and its impact on the socio-economic conditions of the people living in the area.

#### 3.6.1 Socioeconomic characteristics of the respondents

The study results revealed that the average age of the respondents was 43.8 years, with minimum 20 and maximum 87 years (Fig. 3.46). Respondents having age between 30 to 40 y were 28%, followed by the 40 to 50 y age group which were 27% of the total respondents of the survey; while 10% of the respondents were senior citizens of the delta.

On average, each family consisted of 11 family members (Table 3.13), most people (78.5%) were living in katcha houses. People living along the coast had houses made of wood and mud while most houses in towns were pakka houses. On average, 4.7 family members were residing in a single room, which was a shocking finding of the study. Similar results are reported by Magsi and Sheikh (2017) for district Badin, Sindh, Pakistan. About 50% respondents were educated, of which only the 8.7% were graduates.

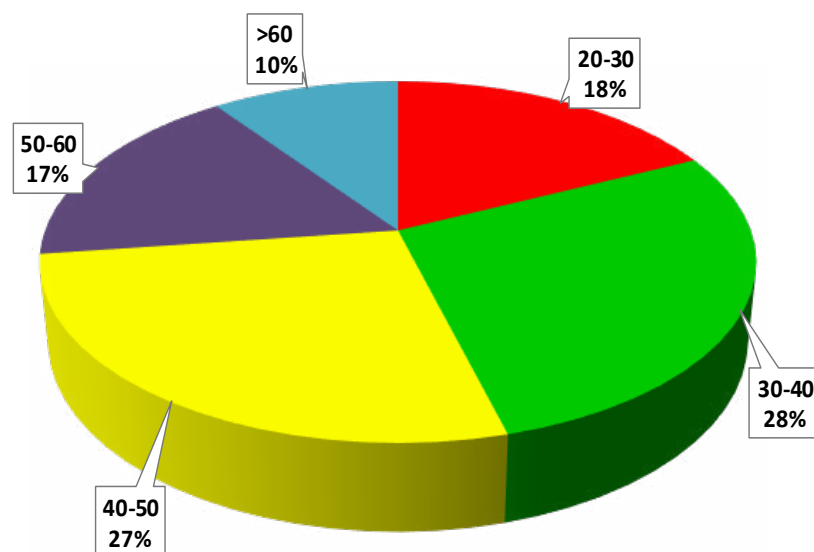


**Fig. 3.46: Age group distribution of the respondents of the survey**

**Table 3.13: Survey response regarding housing/accommodation**

Description	Statistics
Average family size (Male + Female)	11
Katcha houses (wooden made, Jhopra)	78.57%
Pucca houses (cemented)	21.43%
1-2 rooms per house	69.44%
2-4 rooms per house	21.83%
4-6 rooms per house	6.35%
More than 6 rooms per house	2.38%
Average no. of rooms per house	2.3
Average no. of family members per room	4.7

### 3.6.2. Income, expenditure, and source of income

Almost 40% of the respondents were engaged in agriculture and livestock and 17% were engaged in fishing. Only 15.0% of people had govt. /private jobs, 6% were landlords, and 13% were daily wage labors (Fig.3.47) with acute financial problems due to limited job opportunities. Rest of the population was engaged in small-scale self-generated businesses.

Most of the respondents complained about the prolonged outages (12-20 hours), lack of health facilities, schools, potable drinking water, poor condition of roads, etc. The study also revealed that about two-thirds of the population take/eat food only two times a day while only 36% of the respondents/population can eat three meals a day.

About 55% population had livestock, out of which 43% kept animals for their personal milk needs, while rest earned their living from animals. Wood is a major source of firing material for cooking as 89% of the population used wood while only 11% have gas connections and portable gas cylinders to fulfill their cooking fuel requirements. About 45% respondents were without electricity (Table 3.14) while nearly 12% of the respondents (population) used the solar system as a source of energy. More than 50% of the respondents played cricket during free/leisure time. Majority of the respondents also narrated that their income was insufficient to meet their basic needs and they usually borrow loan from various sources to support their families.

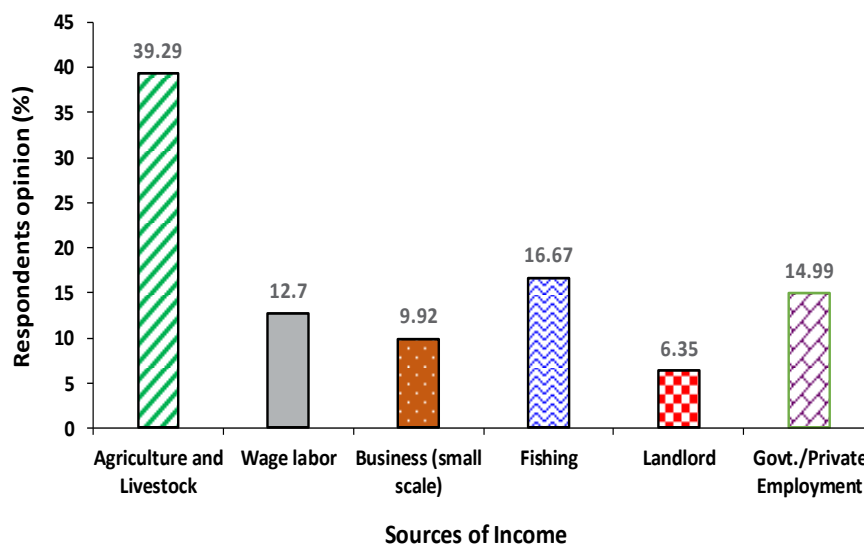


**Fig. 3.47: Main sources of income of the respondents of the Indus Delta**

Seventeen percent respondents had monthly income less than Rs. 10000; 62% had income between Rs. 10000 to Rs. 30000 while only 3% had income more than Rs. 70000 (Fig. 3.48).

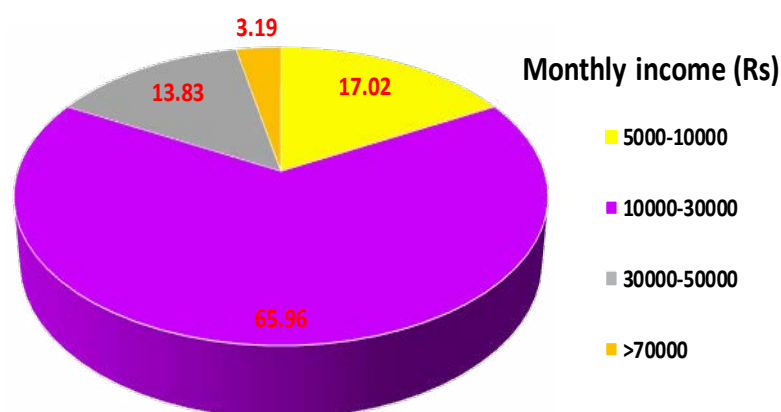


**Fig. 3.48: Monthly income of the respondents**

**Table 3.14: Sources of energy, roads, vehicle, agricultural lands, and livestock in the Indus delta.**

Description	Statistics
<b>Sources of Energy</b>	
Electricity	55.55%
Solar	11.91%
No any source of energy	32.54%
<b>Roads</b>	
Katcha Roads	44.44%
Pucca Roads	50.0%
No, any road facility	5.56%
<b>Vehicle</b>	
Yes	50.0%
No	50.0%
<b>Agricultural Lands</b>	
Yes	48.8%
No	51.2%
<b>Livestock</b>	
Yes	55.16%
No	44.84%
<b>Games</b>	
Cricket	52.4%
Wanjhwati	9.13%
Foot/Volleyball	5.55%
No game	32.92%

### 3.6.3 Climate change Impacts

Climate change impacts on the Indus delta during the last 25 years as perceived by the community are presented in Fig 3.49. Majority of respondents (76.5%) reported an increase in the temperature in last 25 years, 97% reported a decrease in rainfall, 92.5% reported an increase in wind blowing/velocity during summer season in the delta, while 89% reported an increase in humidity in the delta (Fig. 3.49). Mahar (2010) reported that temperature and humidity are increased, precipitation is decreased and socio-economic conditions of the community are badly affected due to climate change and seawater intrusion into the Indus delta. Alamgir *et al.* (2015) reported that some severe meteorological events have not only affected the physical and biological environment of the coast of Sindh, but it has also seriously affected socioeconomic conditions of the community.

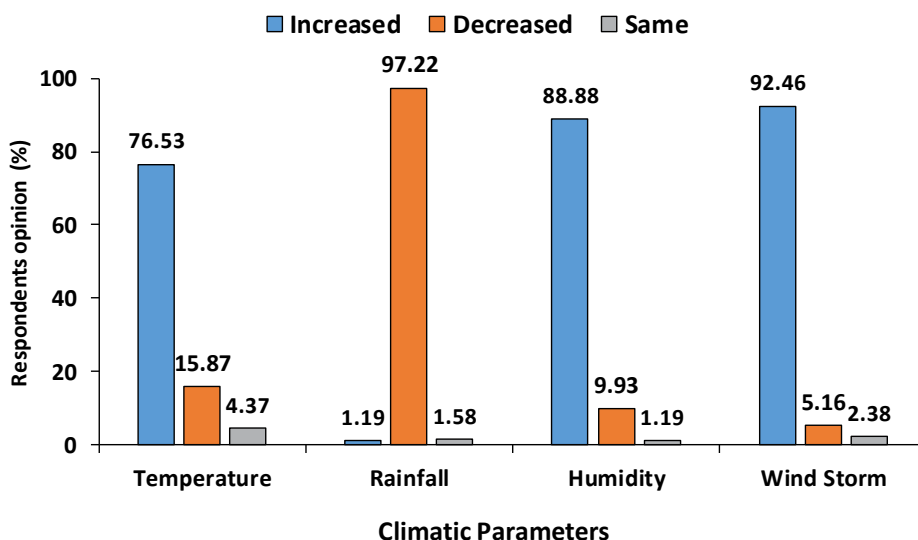


**Fig. 3.49: Variations in climatic parameters of the Indus delta during the last 25 years from the respondents' perspective**

The relationship between changes in temperature and decrease in fish catch (Table 3.15) shows that 92.4% respondents of the study area expressed that there is a change in temperature and in this category 83.2% respondents also reported decrease in the fish catchment, however, 9.2% respondents reported no decrease/change in fish catchment due to the variation of the temperature of the delta. The value of Pearson Chi-square value for relationship between change in temperature and decrease in fish catchment in the study area was 9.13 ( $p = 0.58$ ) similarly which tells that there is statistically weak relation between these two variables. Which Goodman and Kruskal's value of gamma ( $\gamma$ ) was 1.91 at  $p = 0.58$  also shows a weak relationship. Similar results are reported by Imran *et al.* (2013) for the relationship between temperature and fish catchment for Indus River Belt.

**Table 3.15: Relation between change in temperature and decrease in the fish catchment**

Temperature	The decrease in the fish catchment		Total	Percentage
	Yes	No		
Yes	416 (83.2%)	46 (9.2%)	462	92.4
No	28 (5.6%)	10 (2.0%)	38	7.6
Total	444	56	500	100

$\chi^2 = 9.134$  ( $p = 0.58$ ),  $\gamma = 1.91$  ( $p = 0.58$ )

### 3.6.4 Impact of seawater intrusion

Seawater intrusion impacts on water resources, vegetation, crop yield, soil salinity, fishing, mangrove cover in the Indus delta as perceived through the survey are described in this section. The groundwater is the major source of drinking water in the study area as three-fourths of the respondents utilize groundwater extracted through hand pumps and boreholes penetrated at shallow depths, for domestic use. While 14% use surface water, 3.2% use water supplied through water supply schemes, and another 7.5% of the population utilize water supplied through tankers. Most male and female respondents reported that once the fresh water was available near their villages at the shallow depths, but now they collect drinking water 5-10 kilometers away from their villages, which is time-consuming and not economically feasible (Rahman *et al.*, 2017). About 40% respondents told that groundwater has turned saline due to the entry of saline water into the aquifers of the delta, while about 79% respondents reported that groundwater taste keeps changing with the passage of time. Based on the survey, the common diseases prevailing in the study area are plotted in Fig. 3.50. It shows that 20.4% people suffered from gastro, diarrhea, and chest and stomach problem, 14.8% affected by skin diseases, 16.4% by hepatitis, 9.2% by cancer, and 8.4% by sugar, blood pressure, heart, and kidney problems. Most respondents were of the view that the contaminated water, less food availability and absence of healthcare facilities are main reasons for these diseases. Memon *et al.* (2011) reported that common human diseases such as gastro, vomiting, diarrhea, skin and kidney problems might be linked to poor quality drinking water used in the study area.

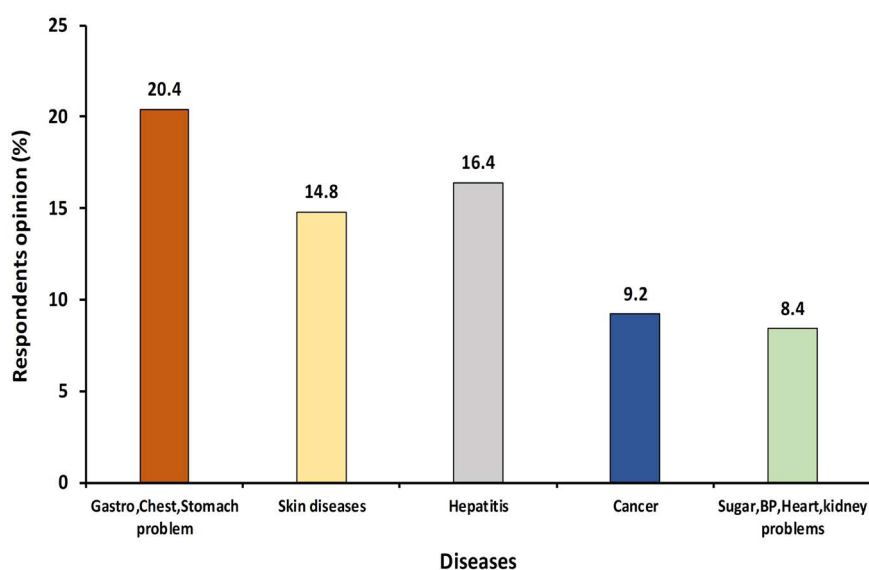


**Fig. 3.50: Some of the common diseases prevailing in the Indus delta as reported by the people**

Almost all respondents (96%) reported that entry of highly saline water from the Arabian sea puts adverse impacts on water resources, agricultural lands, crop yields and ultimately damaged the livelihood of the community living in the coastal areas of Sindh. Most of the people realized such loss since last 5-30 years. For these reasons, about 15% of respondents had migrated from their ancestral towns to the safe places of surrounding cities/towns in search for food, fiber, and shelter.

Responding to question about main causes of seawater intrusion, 47.4% of the respondents viewed it as a result of reduction of freshwater flow in the Indus River, while 4% reported rising sea level, 25.5% reported non existence of flood protection bund (levee), and 18% reported deforestation of mangrove forests in the tidal floodplains, construction of Tidal link Canal (Left Bank Outfall Drain) as main causes of seawater intrusion; thus degradation of the the delta.

Furthermore, 95% respondents (Table 3.16) reported that seawater had adversely affected the income of the community of the delta, while 99.9% respondents reported no change in the cropping pattern. Nearly 97% of respondents said soil salinity in the delta has increased, and that their agricultural lands are facing difficulties due to higher levels of salinity. Besides, 79% respondents viewed that quality of the drinking water has degraded with time.

The data in Table 3.17 depicts that 96% respondents acknowledge the increase in seawater intrusion, 92% of respondents reported the decrease in vegetation during the past 25 years. The value of Pearson Chi-square analysis for the relationship between the seawater intrusion and vegetation was calculated as 14.2 ( $p = 0.08$ ) which tells that there is a strong association between these two variables, while the value of gamma ( $\gamma = 0.238$ ) also shows that this association was strong ( $p = 0.03$ ). Hopkinson *et al.* (2008) reported that during recent years, the impact of sea level rise and wind storms on forests is quite high.

**Table 3.16: Main issues faced by the people of the Indus delta due to seawater intrusion**

Description	Percentage
<b>Impact on Income of the Respondents</b>	
Increased	3.18
Decreased	94.84
Same	1.98
<b>Impact on Quality of Drinking Water</b>	
Improved	0.40
Degraded	78.97
Same	20.63
<b>Impact on Soil</b>	
Soil Salinity Increased	96.82
Soil Salinity Decreased	0.79
Soil Salinity Same	2.39
<b>Impact on Agriculture/Vegetation</b>	
Increased	1.22
Decreased	95.88
Same	2.9
<b>Impact Over Mangrove Cover</b>	
Yes	9.92
No	89.29
Less as compared to past	0.79
<b>Impact on Crop Yield</b>	
Increased	6.4
Decreased	87.22
Same	6.38
<b>Cropping Pattern</b>	
Change in cropping pattern	99.9
No change in cropping pattern	0.01

**Source:** Fieldwork conducted during July 2016-August 2017

**Table 3.17: Relation between seawater intrusion and vegetation**

Seawater intrusion	Decrease in vegetation		Total	Percentage
	Yes	No		
Yes	462 (92.4%)	18 (3.6%)	480	96.0
No	6 (1.2%)	14 (2.8%)	20	4.0
Total	468	32	500	100

$\chi^2 = 14.205$  ( $p = 0.03$ ),  $\gamma = 0.238$  ( $p = 0.03$ )



The relationship between seawater intrusion and soil salinity is presented in Table 3.18. The data shows that 94% respondents reported the increase in soil salinity while only 2% respondents witnessed no increase in soil salinity in the delta. The Pearson Chi-square analysis for the relationship between the two variables was highly significant ( $X^2 = 112.83$ ) which tells that there is a statistically strong association between these two variables. Also the value of gamma ( $\gamma = 0.672$ ) confirms that this relation was very strong.

**Table 3.18: Relation between seawater intrusion and soil salinity**

Seawater intrusion	Increase in soil salinity		Total	Percentage
	Yes	No		
Yes	470 (94.0%)	10 (2.0%)	480	96.0
No	12 (2.4%)	8 (1.6%)	20	4.0
Total	482	18	500	100

$\chi^2 = 112.833$  ( $p = 0.00$ ),  $\gamma = 0.672$  ( $p = 0.00$ )

For the relationship between seawater intrusion and the quality of the ground and surface water (Table 3.19) shows that 93.6% reported adverse impact of seawater intrusion and 2.4% reported no adverse impact on quality of the ground and surface water due to the seawater intrusion in the delta. The value of Pearson Chi-square analysis for the relationship between seawater intrusion and quality of the ground and surface water was calculated as 70.6 ( $p = 0.00$ ) indicating strong significant association between these two variables which is also evident from the gamma value (0.53).

**Table 3.19: Relation between the seawater intrusion and the quality of the ground and surface water**

seawater intrusion	Degradation of quality of ground and surface water		Total	Percentage
	Yes	No		
Yes	468 (93.6%)	12 (2.4%)	480	96.0
No	8 (1.6%)	12 (2.4%)	20	4.0
Total	476	24	500	100

$\chi^2 = 70.604$  ( $p = 0.00$ ),  $\gamma = 0.531$  ( $p = 0.00$ )

Similarly 95% respondents held the view that there is adverse impact of seawater intrusion on their income while only 1.2% respondents reported no adverse impact on their income due to seawater intrusion in the Indus delta (Table 3.20). The value of Pearson Chi-squared test for relationship between seawater intrusion and income of community was highly significant (171.98) which provides the evidence of very strong association between these two variables; while the value of gamma (1.91) at significance level of ( $p = 0.00$ ) also shows that this association was very strong.

**Table 3.20: Relation between seawater intrusion and the income of the respondents**

Seawater intrusion	Impact on the income of the people		Total	Percentage
	Yes	No		
Yes	474 (94.8%)	6 (1.2%)	480	96.0
No	6 (1.2%)	14 (2.8%)	20	4.0
Total	480	20	500	100

$\chi^2 = 171.985$  ( $p = 0.00$ ),  $\gamma = 0.829$  ( $p = 0.00$ )

### 3.6.5 Magnitude of poverty in the delta

Foster Greer Thorbeck (FGT) method, which is a most reliable and widely used method for calculating poverty, was used to determine the gravity of poverty in the study area. Based on FGT technique (Table 3.21), 88% people of the Indus delta suffered from poverty.

**Table 3.21: Measurement of poverty headcount, poverty gap, and severity of poverty in the Indus delta community**

S. No.	Measures of poverty	Foster Greer Thorbeck technique	Poverty Index	Percentage
1.	Headcount poverty	$\frac{1}{n} \sum_{i=1}^q \left( \frac{z - y_i}{z} \right)^0$	442	88.4
2.	Poverty Gap	$\frac{1}{n} \sum_{i=1}^q \left( \frac{z - y_i}{z} \right)^1$	0.586243	58.6
3.	Severity of poverty	$\frac{1}{n} \sum_{i=1}^q \left( \frac{z - y_i}{z} \right)^2$	0.454750	45.5

Based on the international poverty line of 2 dollars respondents of the study area were classified into four categories viz. very poor, moderate poor, poor, and non-poor as in

Table 3.22 and Fig. 3.15 (Imran *et al.*, 2013). First class (very poor) was taken as the one-third of the poverty line, second class (moderate poor) between one-third and two-thirds of the poverty line, third class (poor) between two-thirds of the poverty line and fourth class included the people who were not poor (Imran *et al.*, 2013). It could hamper the growth trend and could create social unrest if due attention is not paid to the poor community (Morrison *et al.*, 2007) of the Indus delta. Results showed that coastal communities of the delta focal server poverty.

**Table 3.22: Distribution of respondents based on their level of poverty**

S. No.	Level of poverty	Frequency	Percentage
1	Very poor	157	31.4
2	Moderate poor	139	27.8
3	Poor	146	29.2
4	Non-poor	58	11.6
Total		500	100

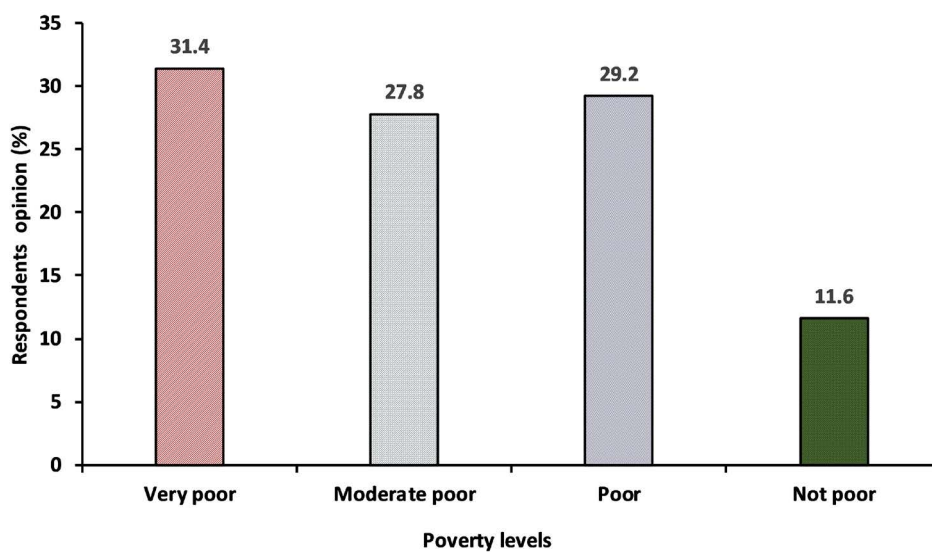


**Fig. 3.51: Variations in the level of poverty in the Indus delta from the respondents' perspective**

### **3.7 Dissemination of Research Results**

The research results were disseminated by publishing articles in different newspapers (Appendix 2) and by organizing a National Seminar titled “Shrinking Indus delta: Status and Way forward” at the Center in March 2018. The seminar was attended by stakeholders from different government and non-government organizations, academia, research scientists, civil society activists and students and chaired by Dr. Muhammad Aslam Uqaili, Vice Chancellor, MUET, Jamshoro. The seminar advertisement and media coverage are given in Appendix 3 and 4.

### **3.8 Research Output**

The details of research output are given in Appendix 5 in terms of research papers published, accepted and under review (Appendix 5a), Ph.D. and M.Sc. thesis completed as a part of this project (Appendix 5b) and the presentations made in national and international conferences (Appendix 5c).

## 4. RECOMMENDATIONS

Based on the present study, the following measures are recommended to the policymakers for mitigation of the adverse impacts of seawater intrusion and revival of the Indus delta:

- Expand already constructed 38 km long coastal highways up to 200 km on the left bank of Indus by putting a bridge over the river Indus at Kharo Chhan (Fig. 4). It will not only provide coastal communities with quick and easy access to the markets of Karachi but will also attract the tourists and flourish tourism in the delta. Hence, socio-economic conditions of poor communities of the delta will be improved.

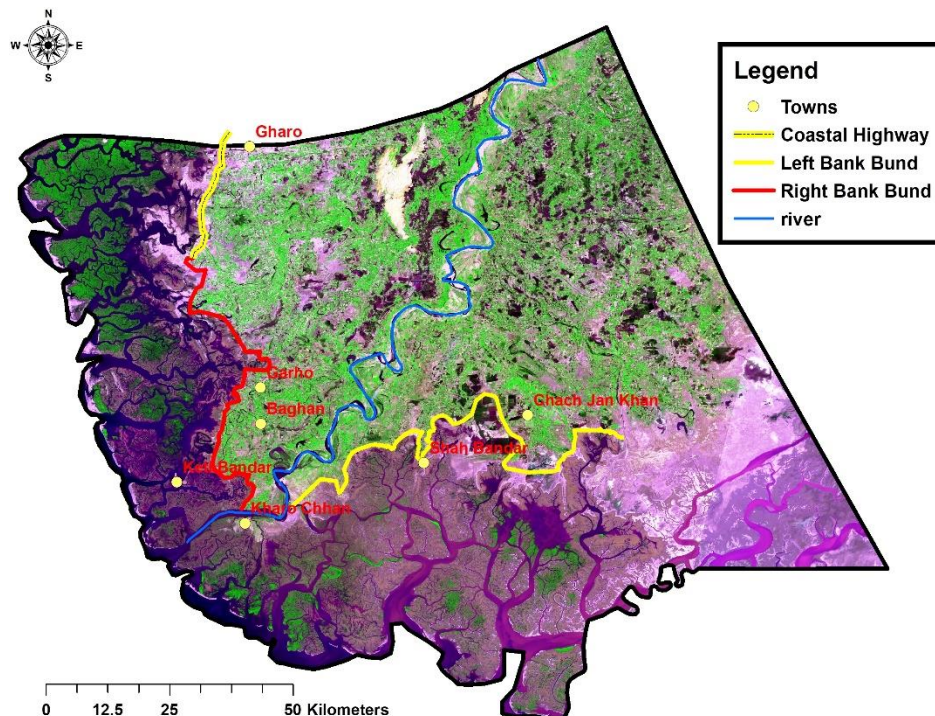


**Fig. 4.1: The layout of proposed coastal highway cum levee**

- The proposed coastal highway will also function as a defense-line against the surface seawater intrusion, thus will impede further swallowing of the delta by sea.
- An escape of 5000 cusecs of water throughout the year below Kotri Barrage should be insured to check seawater intrusion, accommodate the needs for fisheries, environmental sustainability, and to maintain the river channel as recommended by International Experts (IPOE) in 2004. Also, the total volume of 25 MAF in five-year period (an annual equivalent amount of 5 MAF) be released below Kotri as flood flows (Kharif period).

- The environmental river flow is useful in controlling seawater intrusion only in the active delta, while for minimizing surface and subsurface seawater intrusion in the entire delta, enough water flow in the river Indus as well as in canals, originating from Kotri Barrage, should be ensured to minimize subsurface seawater intrusion, provide drinking water to coastal communities, fulfill freshwater needs of flora and fauna and thus mitigate adverse impacts on the ecosystem of the delta. During field survey & satellite images, it is observed that irrigation channels in the delta have a significant impact on the control of seawater intrusion in areas far from the river Indus.
- For this, purpose, if possible relic river channels, such as Ochito and Old Pinyari should be restored. These channels will carry extra flood water to the sea during peak flood to shun the flood pressure on the main river and thus minimize the possibility of the levee breach. This will also supply fresh water to the coastal communities living far away from the main river course. These channels will carry silt-laden water during floods and discharge into the sea away from the main river estuary. It will be supportive in silt deposition in areas where river water and silt usually do not reach. Thus, it will be supportive in revitalizing the delta.
- Plantation of mangroves on the tidal floodplains especially on the left bank of river Indus should be initiated, encouraged and promoted on an emergency basis. For this, community-based natural resource management committees should be established. Thick mangrove forests provide defense-line against natural calamities such as extreme tides, cyclones, and tsunamis; trap river silt to support accretion process along the coast; provide natural breeding ground for fish, shrimps and other marine life; provide wood, fodder, and livelihood to the coastal communities.
- Biosaline agriculture should be encouraged, especially in tidal floodplains and over the vast barren salt-affected soils lying between tidal floodplains and the canal irrigated areas of the delta. Cultivation of Pal grass, Quinoa, Salicornia, Sea Aster, *Spartina alterniflora*, etc. should be introduced and encouraged by the Government. Biosaline agriculture will undoubtedly be a source of food and fodder for the coastal communities and livestock and have a positive impact on the coastal environment.

- Most of the natural lakes in the delta are saline, which should be revived by adding fresh water during the monsoon period. Freshwater lakes can play a vital role in providing drinking water to the communities and will work as groundwater recharge hotspots
- Shrimp and crab farming in natural water bodies, lakes and ponds of the delta should be encouraged.
- The Government should ban on overgrazing and cutting of mangroves for wood, and on the use of fine mesh nets for catching small size fish and shrimps.
- Tourism Industry should be encouraged, especially boat cruising in the mangrove laden creeks in the Delta to improve socioeconomic conditions of poor local communities.

## References

- Abbas, A., and Khan, S. (2007). Remote sensing-based modeling applications in land and water management: Using remote sensing techniques for appraisal of irrigated soil salinity. International Congress on Modelling and Simulation (MODSIM), Modelling and Simulation Society of Australia and New Zealand Brighton 2632-2638.
- Adamu, G.K. (2013). Quality of irrigation water and soil characteristics of Watari Irrigation Project. American Journal of Engineering Research (AJER), 2(3):59-68.
- ADB. (2005). Sindh coastal and inland community development project, interim report, Vol. II, TA 4525-PAK, Asian Development Bank, 1-253.
- Addo, K.A. (2015). Assessment of the Volta delta shoreline change. J. Coast Zone Manag., 18(3): 1-6
- Ahmed, W., and Shaukat, S.S. (2015). Status of mangroves of north-western part of Indus delta: Environmental characteristics and population structure. Pakistan Journal of Marine Sciences, 24(1&2): 61-85.
- Ahuja, S. (2003). Monitoring water quality pollution assessment, analysis, and remediation. Elsevier, Amsterdam, Netherlands, pp. 37.
- Ajayi, F., Nduru, A., and Oningue. (1990). Halting the salt that kills crops. African Farmer No .4, pp 10-12.
- Al-Ahmadi, M.E., and El-Fiky, A.A. (2009). Hydrogeochemical evaluation of shallow alluvial aquifer of Wadi Marwani, Western Saudi Arabia. J. King Saud Univ. (Science), 21, 179.
- Allison, E.H., Perry, A.L., Badjeck, M.C., Neil Adger, W., Brown, K., Conway, D., ... an Dulvy, N. K. (2009). Vulnerability of national economies to the impacts of climate change on fisheries. Fish and Fisheries, 10(2): 173-196.
- Alamgir, A., Khan M.A., Shaukat S.S., Kazmi S.J., Qureshi S., and Khanum F. (2015). Appraisal of climate change impacts on the coastal areas of Sindh using remote sensing techniques. American-Eurasian J. Agric. & Environ. Sci., 15 (6): 1102-1112.



- Alobaidy, A.H.M.J., Abid, H.S. and Maulood, B.K. (2010). Application of water quality index for assessment of Dokan lake ecosystem, Kurdistan Region, Iraq. *Journal of Water Resource and Protection*, 2, 792-798. doi:10.4236/jwarp.2010.29093.
- APHA, AWWA and WEF, D.E. (1992). *Standard Methods for the Examination of Water and Wastewater*. American Public Health Association, American Water Works Association and Water Environment Federation, 18th Edition, Washington, DC.
- Amanullah, M., Ahmed, A., and Ali, G. (2014). Ecological impacts of altered environmental flow on Indus Deltaic ecosystem, Pakistan: A review. *Journal of Environmental Professionals, Sri Lanka*, 3(1): 11-21.
- Amjad, A.S., Kasawani, I., Kamar-u-zaman, J. (2007). Degradation of Indus delta mangroves in Pakistan. *Int. J. Geol.* 3: 27–34.
- Arnell A. and Browne A. (2007). *Revise KS3 Geography*. Letts and Lonsdale.
- Asfaw, E., Suryabhagavan, K.V., and Argaw, M. (2016). Soil salinity modeling and mapping using remote sensing and GIS: the case of Wonji sugar cane irrigation farm, Ethiopia. *Journal of the Saudi Society of Agricultural Sciences*. <http://dx.doi.org/10.1016/j.jssas.2016.05.003>.
- Aziz, I., and Khan, M.A. (2001). Experimental assessment of salinity tolerance of *Ceriops tagal* seedlings and saplings from the Indus delta, Pakistan. *Aquatic Botany*, 70(3): 259-268.
- Bablani, S.A., and Soomro, S.A., (2006). Evaluation of seawater intrusions in left bank sediments of coastal district Thatta, Sindh, Pakistan. Paper presented at the 1st SWIM-SWICA Joint Saltwater Intrusion Conference, 24-29 September 2006.
- Baig, M.A., Sultan, M., Khan, M.R., Zhang, L., Kozlova, M., Malik, N.A., and Wang, S. (2017). Wetland change detection in protected and unprotected Indus coastal and inland delta. *The International Archives of Photogrammetry, Remote Sensing and Spatial Information Sciences*, 42: 1495.
- Bianchi, T.S., and Allison, M.A. (2009). Large-river delta-front estuaries as natural “recorders” of global environmental change. *Proceedings of the National Academy of Sciences*, 106 (20): 8085-8092.

- Balakrishnan, P., Saleem, A., and Mallikarjun, N.D. (2011). Groundwater quality mapping using geographic information system (GIS): A case study of Gulbarga city, Karnataka, India. *African Journal of Environmental Science and Technology*, 5(12): 1069-1084.
- Bokhari, A. (2015). Advancing sea swallows fertile farmlands. *Daily DAWN*. Oct. 19, 2015. <https://www.dawn.com/news/1214108/advancing-sea-swallows-fertile-farmlands>. (visited on Feb. 9, 2018).
- Boon, P., and Raven, P. (Eds.). (2012). *River Conservation and Management*. John Wiley & Sons.
- Bouyoucos, G.J. 1936. Directions for making mechanical analysis of soils by the hydrometer method. *Soil Science* 4: 225 – 228.
- Callaghan, L. (2014). Working together to protect the Indus River delta. [https://www.koreannewsletter.org/uploads/7/0/4/0/7040474/working\\_together\\_to\\_protect\\_the\\_indus\\_river\\_delta\\_liam\\_o'callaghan.pdf](https://www.koreannewsletter.org/uploads/7/0/4/0/7040474/working_together_to_protect_the_indus_river_delta_liam_o'callaghan.pdf) (visited on March 10, 2018).
- Chander, G., Markham, B.L., and Helder, D.L. (2009). Summary of current radiometric calibration coefficients for Landsat MSS, TM, ETM+, and EO-1 ALI sensors. *Remote Sensing of Environment*, 113(5): 893-903.
- Chandio, N.H., Anwar, M.M., and Chandio, A.A. (2011). Degradation of Indus delta, Removal of mangroves fores and its causes: A Case study of Indus River delta. *Sindh Univ. Res. Jour. (Sci. Ser.)*. 43(1): 67-72.
- Chaudhry, Q.U.Z. (2017). *Climate Change Profile of Pakistan*. Asian Development Bank. <http://dx.doi.org/10.22617/TCS178761>
- Cochran, W.G. (1977). *Sampling Techniques* (3<sup>rd</sup> edition). New York: John Wiley & Sons.
- Daily Times. (2018). Sindh government sets to make a record of mangrove plantation on February 15. *Daily Times*. Jan. 13, 2018. <https://dailytimes.com.pk/179993/sindh-government-sets-make-record-mangrove-plantation-february-15/> (visited on April 5, 2018).
- Danko, M.M. (1997). Comparative analysis of variables of irrigation water quality along River Rima. B. The agricultural project, Department of Soil Science and Agricultural Engineering, Usman Danfodio Sokoto. pp.45.

- DasGupta, R. and Shaw, R. (2013). Cumulative impacts of human interventions and climate change on mangrove ecosystems of South and Southeast Asia: An overview. *J. Ecosyst.* 2013, 15.
- Das, N., Paul, S., Chatterjee, D., Banerjee, N., Majumder, N.S., Sarma, N., Sau, T.J., Basu, S., Banerjee, S., Majumder, P., Bandyopadhyay, A.K., States, J.C. and Giri, A.K. (2012). Arsenic exposure through drinking water increases the risk of liver and cardiovascular diseases in the population of West Bengal, India. *BMC Public Health Journal*, 12:639. <http://www.biomedcentral.com/1471-2458/12/639>.
- Davis, A.P., Shokouhian, M., Sharma, H., Minami, C., and Winogradoff, D. (2003). Water quality improvement through bioretention: Lead, copper, and zinc removal. *Water Environment Research*, 75(1), 73-82.
- DAWN. 2008a. Climate change and the Indus delta. *Daily Dawn* (Dec. 15, 2008). <https://www.dawn.com/news/334207>. (Visited on Feb. 09, 2018).
- DAWN. 2008b. Indus delta mangrove ecosystem close to death. *Daily Dawn* (Nov. 24, 2008). <https://www.dawn.com/news/917397>. (Visited on Feb. 11, 2018)
- Dixon W., and Chiwell, B. (1992). The use of hydro-chemical sections to identify recharge areas and saline intrusions in alluvial aquifers, Southeast Queensland, Australia. *J. Hydrol*, 135: 259-274.
- Dong, F., Chen, J., and Yang, F. (2018). A study of land surface temperature retrieval and thermal environment distribution based on landsat-8 in Jinan City. In *IOP Conference Series: Earth and Environmental Science*, 108(4):042008. IOP Publishing.
- Dyoulgerov, M., Bucher, A., Zermoglio, F., & Forner, C. (2011). *Vulnerability, Risk Reduction, and Adaptation to Climate Change: Lao PDR*. The World Bank Group, Washington, DC.
- El-Hoz, M., Mohsen, A., and Iaaly, A. (2014). Assessing groundwater quality in a coastal area using the GIS technique. *Desalination, and Water Treatment*, 52, 10-12, 1967-1979, DOI: 10.1080/19443994.2013.797368.

- Ellison, J.C. (1994). Climate change and sea-level rise impacts on mangrove ecosystems. In: Pernetta J, Leemans R, Elder D, Humphrey S (eds) Impacts of Climate Change on Ecosystems and Species: Marine and Coastal Ecosystems. IUCN, Gland, pp 11–3.
- Ewaid, S.H. (2016). Water quality evaluation of Al-Gharraf river south of Iraq by two water quality indices, Springer. Appl. Water. Sci. (2016). DOI.org/10.1007/s13201-016-0523-z.
- Ewaid, S.H., and Abed, S.A. (2017). Water quality index for Al-Gharraf River, southern Iraq. Egyptian Journal of Aquatic Research, <http://dx.doi.org/10.1016/j.ejar.2017.03.001>.
- FAO. (1985) Guidelines. Land Evaluation for Irrigated Agriculture. Soil Bull. No 55, FAO Rome, Italy.
- FFC. (2005). Study on water escapages below Kotri barrage to check seawater intrusion (Study-I). Final Report. Ministry of Water and Power. Government of Pakistan.
- Fourati, H.T., Bouaziz M., Benzina, M., and Bouaziz, S. (2015). Modeling of soil salinity within a semi-arid region using spectral analysis, Arab J Geosci. DOI 10.1007/s12517-015-2004-3.
- Ghabour, T.K., and Daels, L. (1993). Mapping and monitoring of soil salinity of ISSN. Egyptian Journal of Soil Science 33 (4): 355-370.
- Gimenez E. and Morell, I. (1997). Hydrogeochemical analysis of salinization processes in the coastal aquifer of Oropesa (Castellon, Spain). Environ Geology, 29:118-131.
- Giosan, L., Constantinescu, S., Clift, P.D., Tabrez, A.R., Danish, M., and Inam, A. (2006). Recent morpho-dynamics of the Indus delta shore and shelf. Cont. Shelf Res. 26, 1668–1684; Syvitski, J.P.
- Giri, C., Long, J., Abbas, S., Murali, R. M., Qamer, F. M., Pengra, B., & Thau, D. (2015). Distribution and dynamics of mangrove forests of South Asia. Journal of Environmental Management, 148: 101-111.
- GoP. (2001). Economic Survey. Ministry of Finance, Islamabad.

- Gupta, A. (2008). Large rivers: Geomorphology and Management. John Wiley & Sons.
- Haig, M.R. (1894). The Indus Delta Country: A Memoir, Chiefly on Its Ancient Geography and History. K. Paul, Trench, Trübner & Company, Limited.
- Hamid, G., Khan, N.A., Mohsin, S.I., and Meynell, P. J. (2000). Impact of sedimentological processes on the mangrove ecosystem of the Indus Delta. *Pakistan Journal of Marine Sciences*, 9(1-2): 1-15.
- Hecht, J.E. (Ed.). (1999). The economic value of the environment: Cases from South Asia. IUCN--The World Conservation Union.
- Hillel, D. (2000). Salinity management for sustainable irrigation: Integrating science, environment, and economics. The World Bank: Washington D.C.
- Hopkinson, C.S., Lugo, A.E., Alber, M., Covich, A.P., and Bloem, S.J.V., (2008). Forecasting effects of sea level rise and wind storms on coastal and inland ecosystems. *Front. Ecol. Environ.* 6: 255-263.
- Hudson, P.F. (2005). Deltas. *Encyclopedia of Water Science*. Taylor & Francis. CRC Press Book.
- Huang, C., and Ye, X. (2015). Spatial modeling of urban vegetation and land surface temperature: A case study of Beijing. *Sustainability*, 7(7): 9478-9504.
- Husain, V., Nizam, H. and Arain, G.M. (2012). Arsenic and Fluoride Mobilization Mechanism in Groundwater of Indus Delta and the Thar Desert, Sindh, Pakistan, *International Journal of Econ. Env. Geology*, 3(1): 15-23.
- Ijaz M.W, Mahar, R.B., Siyal, A.A, and Anjum, M.N. (2017). Geospatial analysis of creeks evolution in the Indus Delta, Pakistan using multi-sensor satellite data. *Estuarine, Coastal and Shelf Science*. doi.org/10.1016/j.ecss.2017.11.025.
- Imran, M., Bano, S., Dawood, M., Tarar, M.A., and Ali, A. (2013). Climate change, poverty, and agricultural resource degradation: A case study of district D.G. Khan. *Pak. J. Agri. Sci.*, 50(1): 163-167.
- Inam A., Cliff P.D., Giosan L., Tabrez A.R., Tahir M., Rabbani M.M. and Danish M. (2007). The geographic, geological and oceanographic setting of the Indus River. In *Large Rivers: Geomorphology and management*, edited by A. Gupta, John Wiley & Sons, Ltd. 333-346.

- IRIN. (2001). Pakistan: Intruding seawater threatens Indus river, UN Office for the Co-ordination of Humanitarian Affairs, Integrated Regional Information Networks article: December 31.
- Ismail, S., Saifullah, S. M., and Khan, S. H. (2014). Bio-geochemical studies of Indus Delta mangrove ecosystem through heavy metal assessment. *Pak. J. Bot.* 46(4): 1277-1285.
- IUCN. (2002). regional technical assistance for coastal and marine resources management and poverty reduction in South Asia: Situation analysis report, RETA 5974- PAK, Asian Development Bank and the International Union for Conservation of Nature.
- IUCN. (2003). Environmental degradation and impacts on livelihoods sea intrusion, – A case study, IUCN Pakistan, 1-77.
- IUCN. (2005). Mangroves of Pakistan: Status and management. International Union for Conservation of Nature. <http://www.iucn.org>.
- Jamshid, Z., and Mirbagheri, S.A. (2011). Evaluation of groundwater quantity and quality in the Kashan Basin, Central Iran. *Desalination* 270 (1-3): 23-30.
- Jongman, B., Hochrainer-Stigler, S., Feyen, L., Aerts, J.C.J.H., Mechler, R., Botzen, W.J.W., Bouwer, L.M., Pflug, G., Rojas, R., and Ward, P.J. (2014). Increasing stress on disaster-risk finance due to large floods. *Nat. Clim. Change*, 4: 264-268.
- Kaliraj, S., Chandrasekar, N., and Magesh, N.S. (2014). Impacts of wave energy and littoral currents on shoreline erosion/accretion along the south-west coast of Kanyakumari, Tamil Nadu using DSAS and geospatial technology. *Environ Earth Sci.* doi:10.1007/ s12665-013-2845-6.
- Karanth, K.R. (2014). Groundwater Assessment Development and Management. Handbook, McGraw Hill Education (India) Private Limited New Delhi.
- Ketata-Rokbani, M., Gueddari, M., and Bouhlila, R. (2011). Use of geographical information system and water quality index to assess groundwater quality in El Khairat Deep Aquifer (Enfidha, Tunisian Sahel), *Iranica, J. Energy Environ.*, 2: 133–144.

- Khan, N.M., Rastoskuev, V.V., Sato, Y., and Shiozawa, S. (2005). Assessment of hydro saline land degradation by using a simple approach of remote sensing indicators. *Agric. Water Manage.*, 77(1-3): 96-109.
- Khan, M.Z., and Akbar, G. (2012). In the Indus delta, it is no more the mighty Indus. *River Conservation and Management*, 69-78.
- Khan, M.H. (2015). Unrestrained sea intrusion. *Daily DAWN*. Dec. 28, 2015. <https://www.dawn.com/news/1228964>. (Visited on Feb. 9, 2018).
- Khan, N.M., Rastoskuev, V.V., Shalina, E.V., and Y. Sato (2001). Mapping salt-affected soils using remote sensing indicators-a simple approach with the use of GIS IDRISI. *22nd Asian Conference on Remote Sensing*, 5, p9.
- Kravtsova, V.I., Mikhailov, V.N., and Efremova, N.A. (2009). Variations of the hydrological regime, morphological structure, and landscapes of the Indus River delta (Pakistan) under the effect of large-scale water management measures. *Water Resources*, 36(4): 365-379.
- Kriegler, F.J., Malila, W.A., Nalepka, R.F., and Richardson, W. (1969). Preprocessing transformations and their effects on multispectral recognition. In *Proceedings of the Sixth International Symposium on Remote Sensing of Environment*, pp. 97–131, Univ. of Mich., Ann Arbor.
- Kusky, T. M. (2003). *Geological Hazards: A Sourcebook*. Greenwood Publishing Group.
- Laghari A., Abbasi, H., Aziz, A., and Kanasro, N. (2015). Impact analyses of upstream water infrastructure development schemes on downstream flow and sediment discharge and subsequent effect on deltaic region. *Sindh University Research Journal-SURJ (Science Series)*, 47(4): 805-808.
- Leichenko, R.M., and Wescoat Jr, J.L. (1993). Environmental impacts of climate change and water development in the Indus delta region. *International Journal of Water Resources Development*, 9(3): 247-261.
- Ma, J., Ding, Z., Wei, G., Zhao, H., and Huang, T. (2009). Sources of water pollution and evolution of water quality in the Wuwei basin of Shiyang river, Northwest China. *J. Environ. Manag.* 90(2): 1168-1177.
- Magsi, H., and Sheikh, M.J. (2017). *Seawater Intrusion, Land Degradation and Flood Insecurity among coastal communities of Sindh, Pakistan*.

Springer International Publishing AG 2017. S. Bandyopadhyay *et al.* (eds.), Regional Cooperation in South Asia, Contemporary South Asian Studies, DOI 10.1007/978-3-319-56747-1\_12.

- Mahar, G.A. (2010). Geomorphic degradation of Indus Delta and its demographic impact (Doctoral dissertation, University of Karachi. <http://eprints.hec.gov.pk/6578/> Last access on 12/11/2016).
- Mahar, G.A., and Zaigham, N.A. (2015). Examining spatiotemporal change detection in the Indus river delta with the help of satellite data. *Arabian Journal of Science and Engineering*, 40(7): 1933-1946.
- Majeed, Z., Ul-Hasan, Z., and Piracha, A. (2008). Developing hydropower schemes on existing irrigation network: A case study of upper Chenab Canal System. In the International River Basin Management Congress Book (No. 70, p. 884).
- Majeed, S., Zaman, S.B., Ali, I., and Ahmed, S. (2010). Situational analysis of Sindh coast: Issues and Options. *Managing National Resources for future Agriculture, Research Briefings*, 2(11).
- Memon, A.A. (2005). Devastation of the Indus river delta. In impacts of global climate change (pp. 1-12).
- Memon, M., Soomro, M.S., Akhtar, M.S. and Memon, K.S. (2011). Drinking water quality assessment in Southern Sindh (Pakistan), *Environmental Monitoring and Assessment*, 177: 39-50.
- Meynell, P. and Qureshi, T. (1993). Sustainable management of mangroves in the Indus Delta, Pakistan, in David, T. (ed) *Towards the Wise Use of Wetlands*, Ramsar Bureau, Gland.
- Mimura, N. (2008). *Asia-Pacific coasts and their management: States of Environment* (Vol. 11). Springer Science & Business Media. Springer, The Netherlands.
- Morrison, A., Raju, D., and Sinha, A. (2007). Gender equality, poverty and economic growth. Policy research working paper no. 4349, The World Bank, gender and development group, poverty reduction and economic management network.



- Mountjoy, S. (2004). *The Indus River (Rivers in World History)*. Infobase Publishing.
- Mtoni, Y., Mjemah, I.C., Bakundukize, C., Camp, M.V., Martens, K., and Walraevens, K., (2013). Saltwater intrusion and nitrate pollution in the coastal aquifer of Dar-es-Salaam, Tanzania. *Environ Earth Sciences*, 70:1091-1111.
- Mujabar, P.S., and Chandrasekar, N. (2013). Shoreline change analysis along the coast between Kanyakumari and Tuticorin of India using remote sensing and GIS. *Arabian Journal of Geosciences*, 6(3): 647-664.
- Nasir, S.M. and Akbar, G. (2012). Effect of river Indus flow on low riparian ecosystems of Sindh, a review paper, *Rec. Zool. Surv. Pakistan*, 21: 86-89.
- Nickson, R.T, McArthur, J.M., Shrestha, B., Kyaw-Nyint, T.O., and Lowry, D. (2005). Arsenic and other drinking water quality issues, Muzaffargarh District, Pakistan. *J. Appl Geochem*, 20: 55-68.
- Oyedotun, T.D. (2014). Shoreline geometry: DSAS as a tool for historical trend analysis. *British Society for Geomorphology, Geomorphological Techniques*. ISSN, 2047-0371.
- Patil, P.N., Sawant, D.V., and Deshmukh, R.N. (2012). Physico-chemical parameters for testing of water-A Review. *International Journal of Environmental Sciences*, 3(3): 1194-1207.
- Peracha, M.A., Hussain, M., Khan, N., Ali, M.L., and Khan, M. (2015). Degradation of Mangroves Ecosystem of Indus Delta. *International Journal of Scientific & Technology Research*, 4(8): 106-108.
- Peracha, M. A., Khan, N., Shahid, M., Hussain, M., Ali, M. L., & Mansoor, A. (2017). Mathematical model to quantify the mass of mangroves forest of Indus delta to study the economic recession. *Journal of Multidisciplinary Engineering Science and Technology*. 4(5): 1698-1702.
- Pessoa, L.G.M., Maria, B.G.D.S.F., Freire, D.S., Wilcox, B.P., Green, C.H.M., Araujo, R.J.T.D., and Filho, J.C.D.A., (2016). Spectral reflectance characteristics of soils in northeastern Brazil as influenced by salinity levels. *Environmental Monitoring and Assessment*, 188:616.
- Popovic, N.Z., Duknic, J.A., Atlagic, J.Z., Rakovic, M.J., Marinkovic, N.S., Tubic, B.P., and Paunovic, M.A. (2016). Application of the water pollution index in the

assessment of the ecological status of rivers: A case study of the Sava River, Serbia, *Acta Zool. Bulg.*, 68: 97–102.

- Postel, S. (1999). *Pillar of Sand: Can the Irrigation Miracle Last?* W.W. Norton and Company, New York, 313 pp.
- Quraishee, G.S. (1988). Global warming and rise in sea level in the South Asian Seas Region. In: *The Implication of Climatic Changes and the Impact of Rise in Sea Level in the South Asian Seas Region*, pp. 1-21.
- Raghunath, H.M., (1990). *Groundwater*. Wiley Eastern Ltd., New Delhi.
- Rahman, M.T., Rasheduzzaman, M., Habib, M.A., Ahmed, A., Tareq, S.M., and Muniruzzaman, S.M. (2017). Assessment of fresh water security in coastal Bangladesh: An insight from salinity, community perception and adaptation. *Ocean and Coastal Management*, 137: 68-81.
- Rahman, A. and Miah, G. (2013). Causes of coastal ecosystem degradation in Bangladesh. In: *Proceedings of the 10th Global Congress on ICM: Lessons Learned to Address New Challenges, EMECS 2013-MEDCOAST 2013 Joint Conference*, Marmaris, Turkey; Middle East Technical University: Ankara, Turkey, 2: 853-862.
- Rasul, G., Mahmood, A., Sadiq, A., and Khan, S. I. (2012). Vulnerability of the Indus delta to climate change in Pakistan. *Pakistan Journal of Meteorology*, 8(16): 89-107.
- Rehman, Z.U., Kazmi, S. J. H., Khanum, F., and Samoon, Z. A. (2015). Analysis of land surface temperature and NDVI using geo-spatial technique: A case study of Keti Bunder, Sindh, Pakistan. *Journal of Basic and Applied Sciences*, 11: 514-527.
- Renaud, F. G., Syvitski, J. P., Sebesvari, Z., Werners, S. E., Kremer, H., Kuenzer, C., ... and Friedrich, J. (2013). Tipping from the holocene to the anthropocene: How threatened are major world deltas? *Current Opinion in Environmental Sustainability*, 5(6): 644-654.
- Saboor, A., Tanwir, F., Ali, I. and Maan, A. A. (2006). Demographic dimensions of rural poverty in Pakistan. *Pak. J. Agri. Sci.* 43: 69-72.

- Sahu, P. and Sikdar, P.K. (2008). Hydrochemical framework of the aquifer in and around East Kolkata Wetlands, West Bengal. *India Environ. Geol.*, 55: 23-835.
- Sappa, G., Ergul, S., Ferranti, F., Sweya, L.N., and Luciani, G. (2015). Effects of seasonal change and seawater intrusion on water quality for drinking and irrigation purposes, In: Coastal aquifers of Dar es Salaam, Tanzania, *Journal of African Earth Sciences*, 105: 64-84.
- Sargaonkar, A., and Deshpande, V. (2003). Development of an overall index of pollution for surface water based on a general classification scheme in the Indian context. *Environmental Monitoring and Assessment*, 89, 43-67.
- Shabbir, R., and Ahmed, S.S. (2015). Use of geographic information system and water quality index to assess groundwater quality in Rawalpindi and Islamabad. *Arab J. of Sci. Eng.*, 40: 2033-2047.
- Sherif, M., Kacimov, A., Javadi, A., and Ebraheem, A.Z. (2012). Modeling groundwater flow and seawater intrusion in the coastal aquifer of Wadi Ham UAE. *Water Resources Management*, 26: 751-774.
- Sidra, M., Zaman, S.B., Ali. I., and Ahmad, S. (2010). Situational analysis of Sindh coast-issues and Options. *Managing Natural Resources for Sustaining Future Agriculture. Research Briefings PARC*. 2(11), 2-23.
- Sivakumar, S., Ponnambalam, K. and Chokkalingam, L. (2011) Estimation of Carbon Stock in above Ground Biomass. In: Muthupet Mangrove, Southeast Coast of India. *International Journal of Intellectual Advancements and Research in Engineering Computations (IJIAREC)*, Volume 2, 139-150
- Siyal, A. A., Siyal, A. G., & Abro, Z. A. (2002). Salt affected soils their identification and reclamation. *Pak. J. Appl. Sci*, 2(5), 537-540.
- Siyal, A. A., Dempewolf, J., & Becker-Reshef, I. (2015). Rice yield estimation using Landsat ETM+ Data. *Journal of Applied Remote Sensing*, 9(1), 095986-1 - 095986-16.
- Smitha, A.D., and Shivashankar, P. (2013) Physicochemical analysis of the freshwater at river Kapila, Nanjangudu industrial area, Mysore, India. *J. Environ. Sci.*, 2(8):59-65.

- Sohl, M.A., Mehmood, A., Saeed, U., and Rafique, H. M. (2006). Temporal mapping and prediction of coastal biomass for Keti Bundar. *Terra*, 2: 5-192.
- Spalding, M., Kainuma, M., and Collins, L. (2010). *World Atlas of Mangroves*. Earthscan
- Stewart, R.W. (1989). Sea-level rise or coastal subsidence? *Atmosphere-Ocean*, 27(3): 461-477.
- Sultana, J., Syed, J.H., Mahmood, A., Ali, U., Rehman, M.Y.A., Malik, R.N., and Zhang, G. (2014). Investigation of organochlorine pesticides from the Indus Basin, Pakistan: Sources, air–soil exchange fluxes and risk assessment. *Science of the Total Environment*, 497: 113-122.
- Supriyadi, K. and Putro, A.S.P. (2017). Geophysical and hydro-chemical Approach for Seawater Intrusion in North Semarang, Central Java, Indonesia, *International Journal of Geomate*, 12(31):134-140.
- Syvitski, J.P., Kettner, A.J., Overeem, I., Giosan, L., Brakenridge, G.R., Hannon, M., and Bilham, R. (2013). Anthropocene metamorphosis of the Indus Delta and lower floodplain. *Anthropocene*, 3: 24-35.
- Tejedor, A., Longjas, A., Edmonds, D. A., Zaliapin, I., Georgiou, T. T., Rinaldo, A., & Foufoula-Georgiou, E. (2017). Entropy and optimality in river deltas. *Proceedings of the National Academy of Sciences*, 114(44): 11651-11656.
- Thieler, E.R., Himmelstoss, E.A., Zichichi, J.L., and Ergul, A. (2009). *The Digital Shoreline Analysis System (DSAS) Version 4.0 - An ArcGIS Extension for Calculating Shoreline Change*. Open-File Report. US Geological Survey Report No. 2008- 1278: <http://woodshole.er.usgs.gov/projectpages/dsas/version4/>.
- Tiwari, T., and Mishra, M. (1985). Preliminary assignment of water quality index of major Indian rivers, *Indian J. of Environ. Prot.*, 5(4): 276-279.
- USDA (1954). *Diagnosis and improvement of saline and alkaline soils*: USDA Agriculture Handbook. No. 60. 160 pp.
- Van Vuuren, D.P., Meinshausen, M., Plattner, G.K., Joos, F., Strassmann, K.M., Smith, S.J., ... and Den Elzen, M.G.J. (2008). Temperature increase of 21st-century mitigation scenarios. *Proceedings of the National Academy of Sciences*, 105(40): 15258-15262.

- Wells, J.T., and Coleman, M. (1984). Deltaic morphology and sedimentology, with special reference to the Indus River delta. In: Haq. B.U., Milliman. J.D. (eds.), *Marine Geology and Oceanography of the Arabian Sea and Coastal Pakistan*. von Nostrand Reinhold Company, New York, pp 85–100.
- Werner, A.D., Bakker, M., Post, V.E.A., Vandenbohede, A., Lu, C., Asthiani, B.A., Simmons, C.T., and Barry, D.A., (2013). Seawater intrusion processes, investigation, and management: Recent advances and future challenges. *Advances in Water Resources*, 51: 3-26.
- WHO. (2011). *Guidelines for Drinking Water Quality*, (4<sup>th</sup> ed.). Geneva: World Health Organization. <http://www.who.int/water>
- Wood, A., Pamela, S., and Johanna, M. (2013). The root causes of biodiversity loss Pakistan Mangroves. pp. 257–261.
- Wright, L.D. (1978). River deltas. In *Coastal Sedimentary Environments* (pp. 5-68). Springer, New York, NY.
- Wright, L.D.; Nittrouer, C.A. (1995). Dispersal of river sediments in coastal seas: Six contrasting cases. *Estuaries*, 18 (3): 494-508.
- WWF. (2007). *Indus delta: A vanishing ecosystem*. Indus for All Program, WWF – Pakistan, Regional Office, Karachi.
- WWF- Pakistan. (2008). *Detailed ecological assessment of fauna, including limnology studies at Keti Bunder 2007–2008*. Indus for All Program, WWF – Pakistan, Regional Office, Karachi.
- Yue, W., Xu, J., Tan, W., and Xu, L. (2007). The relationship between land surface temperature and NDVI with remote sensing: Application to Shanghai Landsat 7 ETM+ data. *International Journal of Remote Sensing*, 28(15): 3205-3226.
- Yu, J., Li, Y., Han, G., Zhou, D., Fu, Y., Guan, B., ... and Wang, J. (2014). The spatial distribution characteristics of soil salinity in the coastal zone of the Yellow River Delta. *Environmental earth sciences*, 72(2), 589-599.

## Appendix 1 Socio-Economic Survey Questionnaire (Indus delta)

Sample No.		Date:	
Interviewer		Altitude	
Longitude		Latitude	
Village/Town		Union Council	
Taluka		District	
Name of Respondent		Age	
Gender	Male/Female	Language	Sindhi/Urdu/Siraiki/other
Current Occupation		Previous Occupation (if any)	
Other source of income		Income Increase/Decrease in last 10 years	Increased/Decreased
Per Month income (Rs.)		Per Month Expenditure	
Family Size (Male+Female)		Education Level	Illiterate/Primary/Matric/Inter/Graduate/.....
Education Level of children	Illiterate/Primary/Matric/Inter/Graduate/.....	Religion	Islam/Hindu/Christian/Sikh
Name in voter list	Yes/No	Possess NIC	Yes/No
House	Own/rented	House	Katcha/Paka
No. of Rooms	1/ 2/ 3/ 4/ more	Source of drinking water	pond/canal/groundwater
Quality of drinking water	sweat/salty	Quality of water same/improved/degraded with time	
If source is groundwater, then depth of bore		If fetch then how much time and distance spends?	
If fetch then how much do you pay for it?		Source of Energy	Electricity/ Solar System /Other
Vehecal	Yes/No	If Yes, type of vehical	Cycle/Motorcycle/Car/-----
Eating 1, 2, 3 times		Condition of road	Katcha/pakka
Livestock: If yes then Number	Yes/No.	Per annum earnings from Livestock (Rs.)	
Source of firing material		How much pay per month for firing material	
Do you have any agricultural Land	Yes/ No	If yes then how much?	
Crop yield		How many days freshwater is available for drinking/irrigation	
Opinion about sea water intrusion	Increas/Decrease	If increase, then cause of seawater intrusion	
Since when you felt adverse effect of seawater intusion		Which game is most common in the area	
Any signficiant change in cropping pattern in last 20 years	Yes/ No	If Yes, then what is change	
Since when you felt adverse effect of seawater intusion		Vegetation in area Increase/decreased	
Any Adverse/positive impact of seawater intrusion on source of income		Increase/Decrease in soil salinity	
Does mangrove exist in the area		Any special disease not experieneecd before? If Yes, its name?	
Is Govt./NGOs doing enough for mitigation of seawater intrusion effects	Yes/No	Your opinion about how to tackle with seawater intrusion	
Seawater impact on quality of sgroundwater		The number of fishermen in area increased/decreased	
Do you feel any change in temperature in delta	Increase/ Decrease	Is there any change in rainfall pattern	Increase/ Decrease
Any Change in Wind direction & Intensity		Any change in any humidity	

# Appendix 2 Newspaper Articles



## How we can revive the shrinking Indus delta

The active delta has shrunk 92pc to 1,000 sq km in the last almost two centuries

By Altaf Ali Syal

**T**HE ecosystem of the Indus delta is under threat owing to a drastic fall in river flows below the Kotri barrage.

As a result, the mangrove population in tidal floodplains and fish and shrimp production have decreased, agricultural land and riverine forestry have dwindled, surface and subsurface seawater intrusion has increased, soil has become more saline, surface and groundwater bodies stand polluted and irrigation water for agriculture has significantly dropped.

This hydrological, geomorphological and environmental degradation of the delta poses a risk to the livelihood of people living alongside it. It also makes them more vulnerable to cyclones, floods and droughts.

But the extent to which the delta has been damaged and its revival have always been a burning issue for environmentalists, civil society, agriculturalists, local communities, non-governmental organisations, policymakers and government officials for the last few decades.

The Indus delta, a designated Ramsar wetland, is the fifth largest delta in the world and spreads from Sir Creek in the east to Phitti Creek in the west with the apex at Banoo town (where once the Pinyaree river originated from the Indus to 3,000 sq km in the last 26 years. During the Rabi season, the vegetation region and discharged into the sea via Sir the creek) from 3,100 sq km in 1990 to 2,600 sq km last year.

Before the construction of diversion hydraulic structures over the Indus river, there were 13 active creeks in the delta. 1972, 1979, 1990, 2000, 2010 and 2017 which have now decreased to only two showed that the inland shift of coastline active creeks, namely Khobar and Khar, varied from 10 to 150 metres per year with the active delta has shrunk by 92 per cent on an average of 19 metres annually. The cent from 13,000 square kilometres in total inland shift during the 45-year period 1833 AD to only 1,000 sq km now.



This fan-shaped delta supports the seventh largest mangrove forest system of the world in vast tidal mud floodplains.

But it is shrinking rapidly owing to decreasing river flows to the delta, land subsidence, a rise in sea level, low rainfall because of climate change, and surface and subsurface seawater intrusion.

The US-Pakistan Centre for Advanced Studies in Water at the Mehran University of Engineering and Technology, Jamshoro, recently conducted a study to gauge the impact of seawater intrusion on the Indus delta, using remote sensing and geospatial tools.

The study found that mangrove swamps have decreased to only 80,000 hectares. The area under water bodies in

the delta has increased from 1,600 sq km in 1972 to 3,000 sq km in the last 26 years. During the Rabi season, the vegetation region shrunk 19pc from 3,100 sq km in 1990 to 2,600 sq km last year.

The analysis of coastline positions in 1972, 1979, 1990, 2000, 2010 and 2017 showed that the inland shift of coastline active creeks, namely Khobar and Khar, varied from 10 to 150 metres per year with the active delta has shrunk by 92 per cent on an average of 19 metres annually. The cent from 13,000 square kilometres in total inland shift during the 45-year period was estimated at 1.3km.

The Indus delta shoreline is exposed to the highest average sea wave energy compared to other major deltas in the world. However, small accretion was also observed at some places.

The inward shift in the coastline was 22 metres per year on the left bank of the Indus river and 16 metres on the right bank.

The shoreline of the delta on the left bank is more vulnerable to coastal erosion because of less mangrove population and more and flat tidal floodplains as compared to that of the right bank of the delta.

The total tidal floodplain area has increased from 6,000 sq km in 1972 to 6,500 sq km at present.

The impact of sub-surface seawater intrusion was estimated over an area of about 600,000 hectares, spoiling not only fertile alluvial agricultural lands of Sujawal and Thatta districts, but also having a devastating environmental and social impact on the rich ecosystem of the Indus delta.

Policymakers can take the following measures to revive the Indus delta:

- A protective levee — about 200km long and two to three metres high — should be constructed along the periphery of the tidal flood on an emergency basis to mitigate the adverse impact of surface seawater intrusion on the delta.
- At least 10 million acre feet of water should be allowed every year as an environmental flow below the Kotri barrage.
- The environmental river flow might be useful in controlling seawater intrusion

only in the active delta. Therefore, for minimising surface and subsurface seawater intrusion in the entire delta, irrigation canals off-taking from the Kotri barrage should be supplied enough water so that irrigation water should reach the tail end of the delta. Field surveys and satellite images showed that irrigation channels in the delta have a significant impact in controlling seawater intrusion in areas far from the Indus river.

If possible, relic river channels such as Ochito and Old Pinyari should be restored. These channels should be used to carry extra flood water during peak flood in the sea to shun the flood pressure on the main river and thus minimise the possibility of a breach in the levee. This will help supply freshwater to coastal communities living far from the main river.

Mangrove plantation on the tidal floodplains along coastline should be encouraged by establishing community-based natural resource management committees. Thick mangrove forests provide defence-line against natural calamities such as extreme tides, cyclones and tsunamis; trap river silt to support accretion along the coast; provide natural breeding ground for fish, shrimps and other marine life, and provide people living along the coast with wood, fodder and livelihood.

The government should introduce and encourage the cultivation of value-added halophytes such as Salicornia, Sea Aster, Spartina alterniflora, Suaeda, etc. in the tidal flood plains.

The government should ban over-grazing and cutting of mangroves for wood, and the use of fine mesh nets for catching small size fish and shrimps.

The tourism industry, especially boat cruising, should be encouraged in the mangrove-laden creeks in the delta to improve socio-economic conditions of poor local communities.

The writer teaches at the Mehran University of Engineering and Technology, Jamshoro



میں صورتحال تي مختلف فردن، ادارن ۽ گورنمنٽ جي ليول تي ٻارها بحث مباحثا ٿيا آهن. جيئرا وات اوتريون ڳالهون آهن پر جري جئين ويران وير ڌڙ وانگر مسئلو ڏينهن ڏينهن وڃي ٿو ڊيڪٽ خراب ٿيندو. انڊس ڊيلٽا هجي يا ايل بي ايل هجي، منجر ڏيندو هجي يا آر سي ايل هجي سڀ گورنمنٽ جي سنجيده قابل ۽ ساڪر رکندڙ ادارن جي هنگامي توجھ جا معاملا آهن ڇاڪاڻ ته انڊس ڊيلٽا اڄ سڪڙهي پئي پر پوءِ لاڙ سڄو ڪارڊ ڇاڻ بڻجي ويندو. ظاهر آهي ته هن هيٺي ساري معاملي تي هڪ نشست پر نٿو لکي سگهجي. بحث ڪي اڳتي وڌائيندي انڊس ڊيلٽا ۽ سامونڊي پاڻي جي مداخلت سبب خراب اثرات کي گهٽائڻ لاءِ ڪم ترويجين هيٺ ڏهن ٿيون آهن:

1. سنڌ جي زمين جي معياري ڏانهن گهڙي اچڻ کي گهٽائڻ لاءِ تقريبن 200 ڪلوميٽر ڊيگهه 5 ميٽر ويڪر ۽ 2 کان 3 ميٽر جي اوچائي وارو هڪ حفاظتي بند سامونڊي ويران واري حد تي هنگامي بنيادن تي تعمير ڪيو وڃي.
2. گهٽ ۾ گهٽ 10 ملين ايڪڙ فوٽ (MAF) پاڻي کي ڪوٺڙي بيراج کان هيٺ ماحولياتي رهڪري طور ڇڏيو وڃي انهي سان گڏ ڪوٺڙي بيراج کان نڪرندڙ ڍانڍن ۾ پڻ ڊيڪٽ پاڻي ڇڏيو وڃي ته جيئن پاڻي ڊيلٽا جي پيڙاڙ تائين پهچي ۽ سامونڊي پاڻي جي مداخلت تي ضابطو آڻي زميني پٽڙاڙ ٿوري سيٽلائيٽ وسيلي ورتل تصويرون ۾ اهو واضح آهي ته ڊيلٽا ۽ آبپاشي جا راهه ۽ شاخن سنڌوندي کان پري وري علائقن ۽ سامونڊي مداخلتي ضابطو آڻڻ ۽ ڊيڪٽ اتراندا ۽ ڪارناما ۽ مفيد آهن

(Intrusion) جي ڪري دنيا جي هن ڊيلٽا جو فطرتي، قدرتي حسن ۽ ماحولياتي نظار سنگين خطري ۾ آهي جنهن ڪري ڊيلٽا جي زمين، نباتات، چرند ۽ پرند جو وجود خطري هيٺ آهي ۽ هر گز رنڊڙ ڏينهن سان ان ۾ ابتري اچي رهي آهي. انڊس ڊيلٽا ۾ وڌيڪي پاڻي جو ضرورت کان گهٽ پهچڻ، ماحولياتي تبديلين ۽ نتيجي ۾ ڊيلٽا جي ساحلي ڪناري ۽ تبديلي تي بيراجن پاڪستان سينٽر فار ايڊوانسڊ اسٽيڊيز ان واٽر، مهراڻ يونيورسٽي آف انجنيئرنگ ۽ ٽيڪنالاجي ڄامشورو ۾ انڊس ڊيلٽا جي مصونتي سيارن وسيلي 1972ع کان 2017ع تائين ورتل تصويرون جي تجزيي وسيلي هڪ ڪوڻا ڪئي وئي آهي. جنهن ۾ جديد خاص زميني اوزار (Geospatial tools) ۽ ماڊل استعمال ڪيا ويا ته جيئن خبر پئي ته ٽنر جا پيلا گهڻي ايراضي تي پاڻي بچيا آهن ۽ اصل ۾ سنڌو خشڪي طرف ڪلا ڪري سراسري طور گهڻو اٿڙ ڏکي آهي. تحقيق مان خبر پئي ته هاڻي ٽنر جا پيلا تقريبن 80 هزار هيڪٽرن تي پاڻي بچي بچيا آهن. ڊيلٽا ۾ پاڻي هيٺ ايراضي گڏريل 26 سالن ۾ 1600 چورس ڪلوميٽرن مان وڌي 3000 چورس ڪلوميٽرن تائين پهتي آهي. جڏهن ته ربيع جي مند ۾ ساڙڪ (Vegetation) سڪڙو گهٽجي وئي آهي. تحقيق مان اها به خبر پئي آهي ته زمين جي معياري تي سنڌو 10 کان 150 ميٽر ساليانو مطلب ته سراسري طور 19 ميٽر ساليانو خشڪي طرف وڌي رهيو آهي. 1972 کان وٺي 2017 تائين انڊس ڊيلٽا جو سامونڊي ڪنارو تقريبن 1.30 ڪلوميٽر تائين سنڌو پاڻي چڪو آهي. سنڌو درياءَ جي کاٻي پاسي (ساحل ضلعو) کي سنڌو ڊيڪٽ تيزي سان يعني سراسري طور 22 ميٽر ساليانو جي حساب پاڻي رهيو آهي جڏهن ته ساڄي پاسي ان کي پاڻي جي رفتار سراسري طور 16 ميٽر ساليانو آهي. درياءَ جو کاٻو پاسو ڊيڪٽ غير محفوظ ان ڪري آهي جو ٺٽي ضلعي واري پاسي جي مقابلي ۾ ساحل ضلعي واري طرف ٽنر جا پيلا تيار ڪيا آهن ۽ سامونڊي ويران جي ڪري بيل سبب سبب سبب علائقو (Tidal flood plain) (تقريبن بيهر) ۾ هيٺاهن آهي. انڊس ڊيلٽا ۾ سن 1972ع ۾ ويران هيٺ سبب سبب علائقو (Tidal flood plain) تقريبن 6000 چورس ڪلوميٽر پکيڙو هو، جيڪو سال 2017ع ۾



ڊاڪٽر ا Altaf Ali Syal  
syal1990@gmail.com  
سنڌو جو سڪڙندڙ ڊيلٽا

نوعي سيار ليد سبب (Landsat) وسيلي ورتل تصويرون جو تجزيو ٿي سان ظاهر ٿيو آهي ته انڊس ڊيلٽا جي تقريباً 276 ڪلوميٽر ڊگهي لاري کي سنڌو تيزي سان پاڻي رهيو آهي ۽ هر سال سامونڊي ڪنارو سري طور تقريبن 19 ميٽر خشڪي طرف وڌي رهيو آهي. سنڌو 1972ع ۾، هن وقت تائين سراسري طور تقريبن 1.3 ڪلوميٽر تائين سنڌو زمين پاڻي آيو آهي، جنهن ڪري ٺٽي ۽ ساحل ضلعي جي هزارين ايڪڙ بيز زرعي زمين سنڌو هيٺ اچي وئي آهي.

1. درياءَ جي پيڙاڙ ۾ هڪ هموار ۽ هيٺائين وارو علائقو آهي جيڪو ٺٽي لٽ مان وجود ۾ آيو آهي ۽ جتي درياءَ مختلف ڇاڙون ۾ ورهائجي ٻي ۾ داخل ٿئي ٿو ڊيلٽا جو ٽن صدين جو عمل آهي جيڪو درياءَ وهڪري جي رفتار ۾ گهٽتائي جي نتيجي ۾ لٽ جمع ٿيڻ سان ۽ 2. پاڻي مختلف ڇاڙون وسيلي سنڌو ۾ داخل ٿيڻ سان ٺهيس انڊس 1. جنهن کي رامسر لڊلي علائقو پڻ قرار ڏنو ويو آهي، دنيا جو پنجون وڏو ڊيلٽا آهي، جيڪو اوڀر ۾ سرڪرڪ کان اولهه ۾ ٺٽي ڪريڪ ن پکڙيل آهي. سن 1833ع ۾ وان ڊيلٽا جي شروع ٿيڻ وارو هنڌ بڻيو. جيو وڻو جتان ڪنهن وقت ۾ پيڇاري درياءَ (Creek) سنڌو مان نڪري سرڪرڪ وسيلي سنڌو ۾ ڇوڙ ڪندو هو. سنڌو ندي مختلف هنڌن تي بيراج ۽ ڊيم تعمير ٿيڻ کان اڳ، انڊس ڊيلٽا ۾ ٺهڻ وهندڙ ڇاڙون هنين جيڪي گهٽجي هاڻي صرف ٻه ڪور ۽ ڪار وڻ آهن. سال 1833ع ۾ انڊس ڊيلٽا 13000 چورس ڪلوميٽرن پکيڙو هو، جيڪو گهٽجي هاڻي صرف 1000 چورس ڪلوميٽرن ن محدود ٿي ويو آهي يعني ان جي ايراضي ٻه تقريبن 92 سيڪڙو تائي ٿي آهي. انڊس ڊيلٽا جي شڪل جيتي هٿ واري پکي وانگر جنهن ۾ دنيا جا سٽين نمبر تي وڏا ٽنر جا پيلا آهن. پر سنڌو ندي

## Appendix 3 Seminar Advertisement



Center for Advanced Studies in Water  
Mehran University of Engineering and Technology, Jamshoro

**NATIONAL SEMINAR**

ON  
"SHRINKING INDUS DELTA:  
STATUS AND WAY FORWARD"

Friday; March 02, 2018

**Mr. Muhammad Ali Malkani**  
Minister for Climate Change, Environment, Livestock,  
Fisheries and Coastal Development, Government of Sindh,  
has consented to grace the occasion as **Chief Guest**

Venue: USPCAS-W Auditorium  
Time: 9:30am to 1:00pm

For further information contact:  
**Prof. Dr. Altaf Ali Siyal (Principal Investigator / Focal Person)**  
Email: aasiyal.uspcasw@faculty.muett.edu.pk  
Cell# 0335-334-0405



سینئر فار ایڈوانسڊ اسٽڊيز ان واٽر  
مهراڻ يونيورسٽي آف انجنيئرنگ اينڊ ٽيڪنالاجي، ڄامشورو

**قومي سيمينار**

موضوع: انڊس ڊيلٽا جو سُڪڻو ڇڻو: موجوده صورتحال ۽ اڳتي وڌڻ جي راه

سيمينار پر سنڌ حڪومت جي ماحولياتي تبديلي، موسميات، مال موٽي، ماهيگيري ۽ ساحلي ترقي وارن کاتن جو صوبائي وزير جناب محمد علي ملڪاڻي جن مهمان خاص جي حيثيت ۾ شرڪت هوندا.

سيمينار جو هنڌ: آڊيٽوريم مهراڻ يونيورسٽي واٽر سينٽر  
ڏينهن: جمع 2 مارچ 2018 تائين: 9:30 صبح کان 1:00 منجھند  
وڌيڪ رابطي ۽ معلومات جي لاء:

پروفيسر ڊاڪٽر الطاف علي سيال (پرنسپل انويسٽيگيٽر / فوڪل پرسن)  
اي ميل: aasiyal.uspcasw@faculty.muett.edu.pk فون نمبر: 0335-334-0405



Center for Advanced Studies in Water  
Mehran University of Engineering and Technology, Jamshoro

**NATIONAL SEMINAR**

ON  
"SHRINKING INDUS DELTA:  
STATUS AND WAY FORWARD"

Friday; March 02, 2018

**Mr. Muhammad Ali Malkani**  
Minister for Climate Change, Environment, Livestock,  
Fisheries and Coastal Development, Government of Sindh,  
has consented to grace the occasion as **Chief Guest**

Venue: USPCAS-W Auditorium  
Time: 9:30am to 1:00pm

For further information contact:  
**Prof. Dr. Altaf Ali Siyal (Principal Investigator / Focal Person)**  
Email: aasiyal.uspcasw@faculty.muett.edu.pk  
Cell# 0335-334-0405







## Appendix 5 Research Output

### Appendix 5a Research Papers

#### (a) *Published*

- i. Solangi, G.S.; **Siyal, A.A.**; Babar, M. and Siyal, P. 2018. Evaluation of surface water quality using the Water Quality Index (WQI), and the Synthetic Pollution Index (SPI): A case study of the Indus Delta region of Pakistan. *Desalination and Water Treatment*. 118: 39-48. doi: 10.5004/dwt.2018.22407 [**Impact factor = 1.383**]
- ii. Solangi, G.S.; **Siyal, A.A.**; Babar, M; and Siyal, P. 2017. Groundwater Quality Mapping using Geographic Information System: A Case Study of District Thatta, Sindh. *Mehran University Research Journal of Engineering and Technology*. 36(4): 1059-1072 [**HEC Recognized in X Category**]

#### (b) *Accepted*

- i. Solangi, G.S.; Siyal, A.A.; Babar, M; and Siyal, P. 2019. Use of Water Quality Index and Geospatial tools for Evaluation of Groundwater Quality in the Indus Delta of Pakistan. *Desalination and Water Treatment*. (Accepted) [**Impact factor = 1.383**].
- ii. Solangi, G.S.; Siyal, A.A.; Babar, M; and Siyal, P. 2019. Temporal Dynamics of Vegetative Cover and Surface Water Water Bodies in the Indus Delta, Pakistan. *Mehran University Research Journal of Engineering and Technology*. (Accepted) [**HEC Recognised in X Category**].
- iii. Solangi, G.S.; Siyal, A.A.; Babar, M; and Siyal, P. 2019. Spatiotemporal Dynamics of Land Surface Temperature and its impact on the Vegetation of the Indus Delta, Pakistan. *Civil Engineering Journal*. 5(1), 153-164. [In ISI Master List-Equivalent to **X Category** in HEC recognized journals].

### Appendix 5b Thesis

#### *Ph.D.*

- i. Solangi, G.S. 2018. Impact Assessment of seawater intrusion on Soil, Water, and Vegetation of Indus delta using Field and Satellite Data. Ph.D. Thesis.

#### *M.E.*

- i. Raza, M. 2017. Mapping of Soil Salinity in District Thatta Using GIS and Remote Sensing Tools. M.E. Thesis (Completed).

- ii. Solangi, K. 2017. Assessment of Spatial and Temporal Distribution of Soil Salinity in District Sujawal using Field and Satellite data. M.E. Thesis (Completed).

#### **Appendix 5c Conference/Seminar Presentations**

- i. Siyal, A. A. (2016). Soil, Water, Environment and Socio-economic conditions of Indus Delta under seawater intrusion and climatic change scenario. WEF National Conference on “Water and Environment: Sustainable Development in Changing Climate” held at Marriot Hotel, Islamabad from 17-19th October 2016.
- ii. Siyal, A. A. (2017). Environmental issues of Indus Delta. Paper presented in a Public Awareness Seminar on “Environmental Issues of Sindh and their solutions”. Held at Indus Hotel, Hyderabad on Nov. 21, 2017 organized by Environment, Climate Change and Coastal Development (Sindh).
- iii. Siyal, A.A.; Solangi, G.S.; Ansari, K.; Babar, M.M. 2017. Assessment of the shoreline changes and erosion risk assessment along Indus Delta using GIS-DSAS technique. Science-Policy Conference on Climate Change (SP3C), Islamabad. December 18-20, 2017
- iv. Solangi, G.S.; Siyal, A.A.; and Babar, M.M. (2018). Use of Geospatial tools for assessment of Soil Salinity in the Indus River Delta, Pakistan. 17th International Congress of Soil Science, organized by Soil Science Society of Pakistan. March 13-15, 2018 at Serena Hotel, Faisalabad.
- v. Solangi, G.S.; Siyal, A.A.; Babar, M.M; and Siyal, P. (2018). Use of Water Quality Indices and Geospatial tools for assessment of Groundwater Quality in Thatta District, Pakistan. 2nd International Conference on Chemical Engineering, organized by Department of Chemical Engineering, MUET, Jamshoro. January 22-23, 2018 at Movenpick Hotel, Karachi.
- vi. Solangi, G.S.; Siyal, A.A.; and Babar, M.M. (2018). Mapping of Soil Salinity in Coastal areas of Sindh, Pakistan. 2nd National Conference on Water and Environment, organized by USPCAS-W, MUET, Jamshoro. August 2-13, 2018 at USPCAS-W, MUET, Jamshoro.

## About Author

Dr. Altaf Ali Siyal is currently working as a Professor and Head of Integrated Water Resources Management Department (IWRM) in U.S.-Pakistan Center for Advanced Studies in Water (USPCAS-W) at Mehran University of Engineering & Technology Jamshoro. Before joining Mehran University of Engineering & Technology Jamshoro, he worked as Incharge Dean of Faculty of Agricultural Engineering and the Chairman of the Department of Land & Water Management, at Sindh Agriculture University Tandojam, Pakistan. In 2011, he got Endeavour







Research Fellowship sponsored by the Australian Government for conducting Postdoctoral Research on 'Soil, Water and Crop Environment' at CSIRO-ATSIP, Townsville, Australia. During 2007-8, Dr. Siyal was also awarded Fulbright Scholar Award to conduct Post-Doctoral Research on 'Subsurface Irrigation Simulations' at University of California and the USDA-ARS Salinity Laboratory in Riverside, USA. He got his Ph.D. Degree in 2001 from the Cranfield University, the United Kingdom on 'Maximising salt leaching efficiency of aggregated clay saline soils' under Quaid-e-Azam Merit Scholarship sponsored by Ministry of Education, Government of Pakistan. He earned his Master's degree in Irrigation & Drainage in 1998 and Bachelor's degree in Agricultural Engineering in 1990 from the Sindh Agriculture University Tandojam, Sindh, Pakistan. Dr. Siyal received training on 'GIS and Remote Sensing Applications for the Water Sector' from UNESCO-IHE, Delft, Netherlands under the Netherlands Fellowship Program (NFP). He also got different trainings in GIS and Remote Sensing Applications in Monitoring & Management of natural resources from the University of Maryland, USA, under Borlaug Fellowship and from SUPARCO, Pakistan. He has written many articles on water, agriculture and environment related issues published in local and national newspapers. He has published more than 50 research articles, related to soil, water, and irrigation related issues, published in national and international Journals with a total ISI impact factor of 25. His field of interest is Water Resources Engineering & Management, Irrigation and Drainage, Soil Salinity and Land Reclamation, and GIS & Remote Sensing Applications in the Management of Water and other Natural Resources.

Main thrust of Applied Research component of the Water Center is to stimulate an environment that promotes multi-disciplinary research within the broader context of water-development nexus to support evidence-based policy making in the water sector. This is pursued using the framework provided by the six targets of the Sustainable Development Goal on Water i.e. SDG-6.

## Contact:

**U.S.-Pakistan Centers for Advanced Studies in Water**

Mehran University of Engineering and Technology, Jamshoro-76062, Sindh - Pakistan

 92 22 210 9145  [water.muett.edu.pk](http://water.muett.edu.pk)  /USPCASW  /USPCASW